Journal of Thermal Analysis and Calorimetry (2023) 148:8697–8745
https://doi.org/10.1007/s10973-023-12292-0

A review of numerical investigation on pool boiling

Hantao Jiang[1] · Yingwen Liu[1] · Huaqiang Chu[2]

Received: 2 December 2022 / Accepted: 23 May 2023 / Published online: 4 July 2023

Abstract
The rapid development of industrial technology and the increasing computational power have provided the possibility to improve the accuracy of multiphase flow field simulation studies. In addition, the chaotic nature of boiling phenomena increases the difficulty of experimental studies, and there is an urgent need to improve the computational methods to meet the needs of industrial applications. This paper presents a comprehensive review of the published literatures on the study of pool boiling using computational methods in the last two decades, including macroscopic-scale computational methods based on continuous medium theory, mesoscopic-scale methods based on lattice Boltzmann method (LBM), and nanoscale molecular dynamics. The advantages and disadvantages of different approaches to study bubble dynamics, including nucleation mechanisms, bubble growth, bubble detachment, and nucleation sites density, are evaluated based on different modeling features and phase change mechanisms. After considering micro-layer evaporation, wall convection, and transient conduction in the macroscopic scale model, the shape diffraction of isolated bubbles and departure diameters obtained by the macroscopic approach agree well with experimental data, and the Rensselaer Polytechnic Institute model achieves promising results for the simulation of low concentration nanofluids as well. The coupling of Shan–Chen model (S–C model) and Peng–Robinson (P–R) equation of state and considering the thermal lattice Boltzmann approach can effectively solve the phase separation problem, and the simulation results can match the theoretical analysis with the highest accuracy. In addition to the above results, a complete boiling heat transfer curve was successfully simulated for the first time using the LBM method. Molecular dynamics provides an in-depth mechanistic explanation of nucleation of nanobubbles in microstructures and on different wettability surfaces in terms of free energy and pressure fluctuations. Although different methods have achieved different degrees of success in pool boiling simulations, problems of boundary capture and heat and mass transfer near macroscopic methods, mesh accuracy in mesoscopic methods, treatment of density ratios and error terms, and accuracy of gas–liquid interfaces in molecular dynamics methods still limit the development of numerical computation. Therefore, this review also presents the challenges and future directions of simulation methods for modeling at different scales from the authors' perspective. Multi-scale coupling methods will be highlighted as an important goal to accommodate the development of advanced pool boiling simulations.

Keywords Simulation scheme · Multi-scale modelling · Nucleate boiling · Bubble dynamics · Heat flux

List of symbols

c_s	Lattice sound velocity
D	Bubble departure diameter
E	Specific internal energy
E_{ik}	Kinetic energy time average value
$\boldsymbol{e}_i$	Lattice velocities
F	Fraction of phase in computational cell
$\vec{F}_s$	Force
f_i	Discrete density distribution function
$f_i^{(eq)}$	Equilibrium distribution function
H	Heaviside function
h	Cell width
g	Gravitational acceleration
k	Effective thermal conductivity

✉ Yingwen Liu
ywliu@xjtu.edu.cn

✉ Huaqiang Chu
hqchust@163.com

[1] Key Laboratory of Thermo-Fluid Science and Engineering of MOE, School of Energy and Power Engineering, Xi'an Jiaotong University, Xi'an 710049, Shaanxi, People's Republic of China

[2] School of Energy and Environment, Anhui University of Technology, Ma'anshan 2423002, People's Republic of China

k_B	Boltzmann constant
M	Orthogonal transformation matrix
p	Pressure
Q	Energy source term for energy equation
S	Source term in thermal LB equation
T	Temperature
t	Time
$\vec{u}$	Velocity vector
w_i	Weights

Greek symbols

α	Non-dimensional parameter
β	Weighting factor
ε	Energy of interaction
δ_t	Time step
ρ	Density
σ	Equilibrium distance
τ_f	Relaxation time
μ	Dynamic viscosity
φ	Chemical potential
ψ	Level-set function; effective mass
Λ	Diagonal matrix

Abbreviations

ALE	Arbitrary Lagrange–Eulerian method
BGK	Bhatnagar–Gross–Krook
CFD	Computational fluid dynamics
CHF	Critical heat flux
CML	Coupled map lattice method
CLSVOF	Coupled level-set and volume of fluid
CHARMM	Chemistry at Harvard macromolecular mechanics
DVDWT	The dynamic van der Waals theory
DnQm	N Dimensional m velocity
EOS	The equation of state
FTM	Front tracking method
FLAIR	Flux line-segment model for advection and interface reconstruction
GROMACS	GROningen MAchine for Chemical Simulations
GROMOS	GROningen MOlecular Simulation
HFP	Heat flux partitioning
Kn	Knudsen number
LAMMPS	The large-scale atomic/molecular massively parallel simulator
LBM	Lattice Boltzmann method
LS	Level set
LJ	Lennard–Jones
MAC	Marker and cell method
MCMP	Multiphase multicomponent
MD	Molecular dynamic
MRT	Multi-relaxation time
N–S	Navier–Stokes
NVT	Canonical ensemble
NVE	Microcanonical ensemble
P–R	Peng–Robinson
PFM	Phase field method
PLIC	Piecewise linear interface construction
RPI	Rensselaer Polytechnic Institute
S–C	Shan–Chen
SLIC	Simple line interface calculation
SRT	Single relaxation time
VOF	Volume of fluid
VOSET	Coupled volume of fluid and level set
2D	Two dimensional
3D	Three dimensional

Introduction

Pool boiling background

In the period before the twenty-first century, the issue of thermal management of equipment has not been prominently yet. The problem of cooling encountered in engineering was usually rendered by the traditional single-phase convective heat dissipation technology. However, the equipment in various state-of-the-art fields has gradually developed in the direction of miniaturization, compactness and high power in the past 20 years. The generation of relatively high heat flux in equipment applications such as computing, energy, aerospace, and medical fields coupled with the badly in need of enhancing heat transfer capacity has necessitated people to find new mode in steading single-phase methods with low efficiency [1–3]. Boiling, a typical type of two-phase heat transfer method, has attracted the extensive attention due to the high coefficient which generates from the evaporation process from liquid to vapor. The original experiments of pool boiling from Nukiyama [4] have shown that there were three regions existed by analyzing the curve between the heat flux and surface temperature, also the boiling phenomena. The nucleate boiling, one of the three situations, has shown the best performance in heat transfer coefficient, and this method has the potential to be the mainstream heat dissipation in the future.

Figure 1 shows the classical pool boiling curve, which consists of four main regions: (1) natural convection region: no bubbles appear on the superheated wall, and the heat flux is low; (2) nucleation boiling region: after the wall temperature exceeds the onset nucleation of boiling temperature, bubbles begin to appear and become progressively more intense as the wall temperature increases; (3) transition boiling stage: beyond the critical heat flux, the heated surface starts to be covered by gas film and the heat flux drops sharply; (4) film boiling stage: after reaching the minimum heat flow flux, the heat flux increases again, but the wall temperature is higher at this time. The desired boiling region

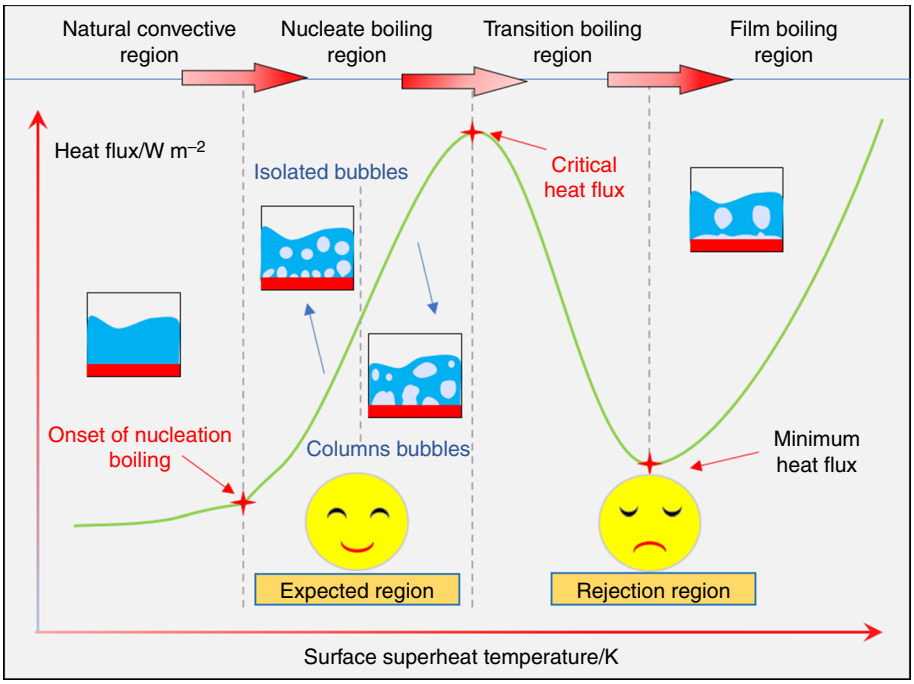

Fig. 1 Pool boiling curve

in industrial applications is in nucleation boiling, which has a high boiling heat transfer coefficient, while the transition region after the critical heat flow flux and the film boiling region need to be completely avoided.

Despite the excellent heat removal capacity, the limitation of the pool boiling heat transfer is still unfathomed, that are, the high temperature of the onset of nucleation boiling and low critical heat flux (CHF). The heating surface will be in the convective heat transfer with poor heat transfer performance for a long time if nucleate boiling is not activated. Entering the nucleate boiling regime, the heat flux on the heating surface will increase sharply until the critical heat flux occurs. At this moment, the film vapor blanket on wall will make local heat transfer performance deteriorate, and the dramatic increase temperature will damage the heating surface seriously. The existence of this situation will cause safety hazards to the chemical industry, nuclear energy and other industrial fields. How to solve these problems reasonably has become an urgent problem for now.

Complexity effect factors of pool boiling

Nucleate boiling is a complicated process that still unable to accurately understanding the heat transfer mechanism. Different interactions of heat transfer mechanism near overheating surface during boiling have led to contradictory findings. The generation of high heat flux in the boiling process is believed to mainly have three heat transfer processes [5]: (1) during bubble growing period, the evaporation of the microlayer, (2) the micro-convection heat transfer formed at the adjacent liquid caused by bubble departure, (3) rewetting the dry spots with the liquid as the bubble departs. The foundation of enhancing heat transfer performance is to optimize these heat transfer progress to the greatest extent.

Effective means that have been proposed to improve the nucleate boiling heat transfer capacity can be divided into two primary method: active and passive [6]. Compared with the active pattern that requires extra control, such as vibration, suction and electrostatic field [7], the passive techniques, that include modifying coolant properties and surface character, do without the external power to enhancing the heat coefficient, which is very convenient for industrial applications in the future. Figure 2 illustrates both the active and passive methods often used and shows several modified surfaces, including micropillars, micropores, and nanowires [8–13]. This is particularly important for enhanced heat transfer under microgravity conditions, especially since CHF is easily triggered under those conditions [14, 15].

The introduction of active and passive methods has challenged the understanding of the boiling heat transfer mechanism while increasing the boiling intensity. This is because the mechanism of bubble nucleation at the solid–liquid interface on the microscopic scale, the transient heat transfer mechanism during bubble different behaviors on the macroscopic scale, and the characteristics of local temperature evolution when the bubble is detached from the disturbed wall will change. The previous conclusions for smooth planes may no longer be well applicable. Despite extensive research efforts in passive methods, the mechanism of the pool boiling phenomena is still unclear and the unified conclusion has not yet been proposed. The response and accuracy of the limited measurement means in the experiment limit the

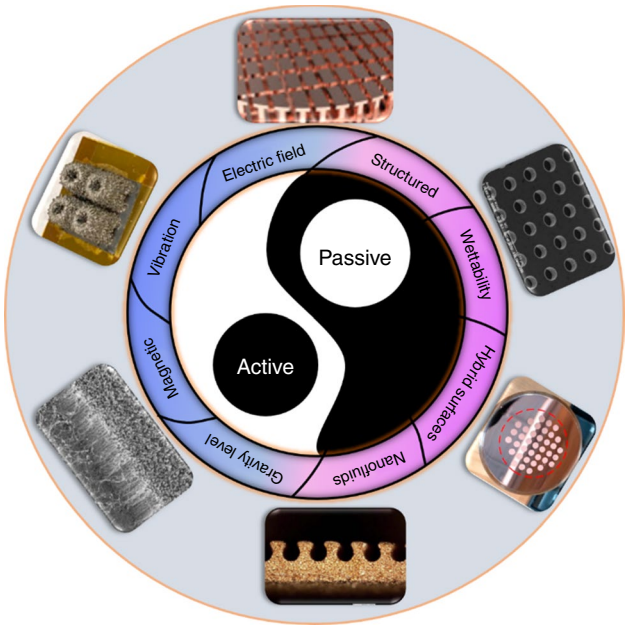

Fig. 2 Pool boiling enhancement technique and typical structure [8–13]

further in-depth analysis of the above boiling mechanism. This has limited the development of industry to some extent.

Advantages of computational fluid dynamics

The heat transfer process of boiling has motivated extensive experimental studies, which have mostly led to positive results based on the visualization [16–19]. Also efforts to analytically model for predicting pool boiling based on the local data have been made [20–24]. But these proposed efforts have always involved inevitable simplifications, and the models have met with merely success in data from other literatures, which due to the empirical constants needed to match the local data from experiments. The flaws were inescapable along with in this manner.

Limited by technology, the researches on the mechanism of boiling heat transfer have mainly focused on theoretical analysis based on experiments and hypotheses for a long period of time in the past. The emergence of high-speed camera technology, infrared temperature measurement technology and phase detection technology has provided enormous contribution for the research of pool boiling mechanism especially the microlayer formed progress [25–28]. This is more conducive to the proposal of the pool boiling theoretical model and the improvement of the data accuracy from the correlation equation predicted. However, the process of pool boiling involved complex coupled heat transfer action of solid and fluid and also existed varies of subprocesses during thermal exchange. Therefore, it is difficult to obtain a common formula for predicting pool boiling based on the limitation of empirical and theoretical analysis. The advent of computational fluid dynamics can provide a new means of refining boiling experiments and theory. In phase change region, the CFD are able to show the transient change details during heat transfer process, including the temperature distribution, phase volume fraction and the rate of the phase change heat transfer, especially. Obviously, compared with the experimental investigations, which are not equipped with these advantages, simulation research is more suitable for the research and application of pool boiling heat transfer mechanism.

Pool boiling heat transfer has typical multi-scale influence features, including surface characteristics (roughness, wettability, microstructure, micro-liquid layer diffraction, etc.) at the microscopic scale, and bubble dynamics (bubble nucleation, growth, detachment, and merging, etc.) at the macroscopic scale. The different modeling characteristics bring about different research attention so that simulations at different scales can analyze the boiling mechanism from different perspectives, but there is no literature to discuss in depth the qualitative and quantitative conclusions obtained.

Many models have been proposed in the early stage of pool boiling simulation solution, due to the problems in the hypothesis stage, the results were naturally not in line with the actual situation [29–31]. But this paved the way for the success of the later simulation. Son et al. [32] were the first to simulate the bubble growth process successfully, in which the results are validated by comparing the data from the literature. The model of Son et al. [32] was extended by Abarajith [33] to numerical pool boiling under low gravity. Not only the first pool boiling curve was obtained in his paper, but also the variation of bubble interaction phenomenon was captured by analyzing the numerical results. Although the results contained some blemishes, in which the temperature was constant, simulation is a method to investigate the phase change that has gradually matured.

Prior reviews on simulation of boiling heat transfer

A considerable amount of literature has been published on numerical of pool boiling. The article published by Dhir [34] in 2003s has summarized some results obtained in the initial stage of pool boiling simulation. Based on the well agreement between the simulation data and the experimental results, that the simulation method can further study the mechanism of pool boiling that have been proposed. Due to the limitations of computer development at this time, this article was mainly aimed at studying pool boiling simulation using the LS method. Kunugi [35] has given a brief systematic summary of the simulation theory used in pool boiling and theoretical applications; however, only very limited simulation results are described in their paper. Dhir et al. [36] have focused on the LS model and summarized the

effects of different parameters on bubble dynamics, including film boiling and nucleate boiling. Furthermore, Dhir [37] also focused on summarizing the influence of gravity level on pool boiling. In the review of Li et al. [38], the lattice Boltzmann method is comprehensively introduced in theories and applications of the phase change, including the boiling. Kharangate and Mudawar [39] published review article addressing the computational schemes and phase change model concerning the condensation and boiling, including the film boiling. Dadhich and Prajapati [40] have dedicated mainly to the simulation research progress of nanofluids in pool boiling and film boiling. In general, the published review articles on pool boiling simulation mainly focus on the influence of the single-scale simulation method or a single influence feature in modeling and simulation results, while this paper compares and evaluates the advantages and disadvantages of different methods from the perspectives of physical model building, bubble dynamics, and boiling curves, thus well compensating for the above problems. In addition, the similarities and differences of research findings on the boiling mechanism based on different-scale simulation means are discussed.

Objective of present review

A review of the above reviews reveals that no article has yet reviewed pool boiling simulation studies at different scales, and a detailed analysis of this area would provide key information for future research developments in pool boiling simulation. Therefore, this paper provides a comprehensive and integrated evaluation of a large number of articles on pool boiling simulation at different scales in the last two decades. This includes (1) the differences between simulation theories at different scales computational schemes, (2) the modeling key issues of different simulation methods in studying the effects of different factors on bubble dynamics, (3) important areas of different simulation methods in predicting boiling heat transfer curves with different capabilities and accuracy, and (4) the key challenges in studying pool boiling using simulation methods and suggestions for future work to be carried out. In conclusion, this review can help relevant researchers to keep abreast of the latest advances in the field and may be useful for related scholars to improve the pool boiling simulation models.

Simulation methods for macroscopy

In order to analyze the liquid–vapor flows on heating surfaces, the classical thermal hydrodynamics that solved by the Navier–Stokes (N–S) equation and various conservation laws of relevant physical quantities can be used, respectively. Numerous models for the liquid–vapor phase change heat transfer have been proposed for decades. It is noticeable that the interface and necessary boundary conditions must be supplemented in the numerical process. The following briefly introduces the common simulation theories.

Governing equation

Boiling is a very complicated process of heat transfer that owning huge thermal remove coefficient. The keys of modeling accurate flow field and the heat transfer are explaining the mechanism of phase change and describing the constantly changing interface between varies phases. Based on the hypothesis of fluid continuity, mass, momentum, and energy conservation equations are often used for macroscopic descriptions, as follows:

$$\frac{\partial}{\partial t}(\rho) + \nabla \cdot \left(\rho \vec{u}\right) = 0 \tag{2-1}$$

$$\frac{\partial}{\partial t}\left(\rho \vec{u}\right) + \nabla \cdot \left(\rho \vec{u}\vec{u}\right) = -\nabla p + \nabla \cdot \left[\mu\left(\nabla \vec{u} + \nabla \vec{u}^{T}\right)\right] + \rho \vec{g} + \vec{F}_{s} \tag{2-2}$$

$$\frac{\partial}{\partial t}(\rho E) + \nabla \cdot \left(\vec{u}(\rho E + \mathrm{p})\right) = \nabla \cdot (k \nabla T) + Q \tag{2-3}$$

It is worth mentioning that different methods for predicting interfacial mass, momentum, and energy transfer have been described in detail in previous papers, so this matter will not be described in detail here [39].

The macroscopic depiction of multiphase flow is solved based on these equations. Different simulation methods will describe in this section, while Sects. 3 and 4 will introduce another two-scale numerical methods, with the lattice Boltzmann method (LBM) and molecular dynamic (MD) computational theory.

Simulation methods

Lagrangian methods

The Lagrangian method is based on the investigation of the movement of individual fluid particles, and the movement of the entire fluid can be grasped by studying the movement of sufficient fluid particles. Having reviewed related work, the main numerical methods that the main body of the Lagrangian methods are presented in the following.

- Marker and Cell method (MAC)

The MAC method was proposed firstly by Harlow and Welch [41]. In the description of this method, the fluid particle is represented by a virtual mark point that only contains spatial coordinate information, and its phase interface is shown

between the marked particle area and the unmarked particle area. But interface orientation and free surface boundary conditions are problematic due to the false regions of void. The first boiling simulation based on the MAC method was done by Madhaven et al. [42] in 1970.

- Moving mesh method

Moving mesh method was used to simulate the rising motion of the unsteady bubble in three dimensions, and the result proved that the method of using the boundary fitting grid has high prediction accuracy [43]. This method is very effective for solving grid densification problems, but additional processing is required when the shape of the gas–liquid interface is more complex or the interface deformation is large, and hence, it has certain limitations on applied scope.

- Arbitrary Lagrange–Eulerian method (ALE) [44, 45]

ALE method was proposed to solve the problem of fluid dynamics firstly. The motion form of the computational grid can be arbitrarily selected, and the object motion interface tracking can be described by different grid motion forms. Some positive role for simulating the interaction between fluid and solid has been obtained from related literatures [46–48]. But according to the feature of this method, the center of the control volume may not coincide with the center of mass, which will compelled to introduce a larger artificial viscosity in the end.

- Front tracking method (FTM)

Front tracking is an adaptive computational method in which the fixed and moving grids are fitted to and follows the dynamical evolution of distinguished waves in a fluid flow [49, 50] as illustrated in Fig. 3d. Marking points are set at the boundary points of different phase states, and the phase interface can be easily described by solving the movement of that by using this method [51, 52]. This method seems similar in principle of the MAC method. The verification of this method has been widely proved in the literature, which confirmed with the rising behavior of bubbles under buoyancy [53–56]. The movement of the finer grid in this method represents the movement of the phase interface. But dealing with interface cracking and interface merging is still a problem.

Euler methods

Different from the Lagrangian method, Euler's method defines fluid properties as a function of space, that is, it focuses on state changes at a fixed position. The main

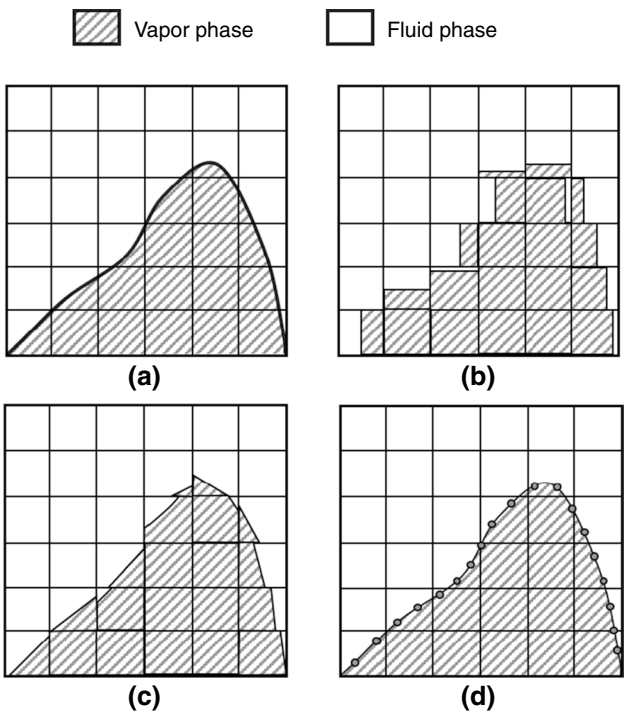

Fig. 3 Comparisons of typical interface techniques for actual interface: **a** actual interface, **b** SLIC, **c** PLIC, **d** Front tracking

numerical methods based on the Euler method are shown in the following:

- Volume of fluid (VOF)

The key mechanism of VOF method is to determine the distribution of each phase through the volume fraction α. The volume fraction refers to the volume ratio of a certain phase in the control unit, where the volume fraction in the unit is 1 that implies that the unit is completely occupied by one phase, and 0 for the other phase while the volume fraction of the interface unit is identified between 0 and 1, respectively. The specific position and shape of the two-phase interface are determined by the spatial distribution of the fluid volume function, and its transport equation is:

$$\frac{\partial F}{\partial t} + \vec{u} \cdot \nabla F = 0 \tag{2-4}$$

where F denotes the fraction of phase in the computational cell and $\vec{u}$ is the velocity vector. However, this method suffers from instability to capture the phase interface smoothly, due to the difference scheme. Two categories were proposed to recover this issue, which was distinguished by usage of the interface reconstruction method.

A multitude of methods with no interface reconstruction has been presented, including donor–acceptor scheme [57], flux corrected transport scheme [58] and compressive

interface capturing scheme for arbitrary meshes [59]. The diffusion of the phase interface to the adjacent multi-grid leads to the formation of smearing thickness, which exacerbated analysis difficulty. In order to improve the accuracy of interface capture technology, new methods with zero thickness are constantly being proposed, such as Simple Line Interface Calculation (SLIC) [60], Piece-wise linear Interface construction (PLIC) [61] and Flux Line-segment Model for Advection and Interface Reconstruction (FLAIR) [62]. If the grid system is fine enough, the surface can be viewed as composed of line segments. Locally, this line segment can be forced at the cell boundary by checking the area fractions of two adjacent cells. In SLIC method, the surface is reoriented in a manner where all the surfaces are considered to be vertical for flux calculations in the x-direction and horizontal in the y-direction, in which the orientation determined by the volume fractions weighting criterion that on adjoining cells [60] as shown in Fig. 3b. Different from the SLIC method, the slope of line segment is fitted inside each cell, that was used in PLIC method as shown in Fig. 3c, which will improve the calculation results accuracy. Same as the boundary processing technique, the line segments are drawn at the cell boundaries in the FLAIR method, with the interface changes; the cell boundary velocity is defined and generated in the trapezoidal fluid inside. Also, some PLIC modified schemes have been derived to figure out the discontinuity problem that produced at the interface [63, 64]. Once dealing with the interface reconstruction process completed, the transport equation is performed to numerical solution.

- Level-set method (LS)

The isosurface function φ is introduced to distinguish between the continuous phase region and the discrete phase region, where $C>0$ means the continuous region, $C<0$ means the discrete phase region, and $C=0$ means the interface. The transport equation is expressed as follows:

$$\frac{\partial \varphi}{\partial t} + \nabla \cdot (\vec{u}\varphi) = 0 \tag{2-5}$$

The more advanced than the VOF method is that the topological changes of the phase interface can be automatically captured, once the isosurface function is solved. Son et al. [32] introduced the calculation of the phase change model on the basis of the level-set method and simulated the bubble growth process on the heating wall. Mukherjee and Dhir [65] used the same method to simulate the polymerization process of bubbles in the nucleate boiling process. However, this method has some shortcomings; the evolution of time may change the smoothness of the function as well as the mass conservation; hence, larger calculation errors will appear. This is due to the fact that φ cannot maintain the property of the signed distance function, thus leading to a larger error in the calculation of the interface curvature, which is the main problem when the gas–liquid interface is nonzero. In order to eliminate the simulation shock caused by the discontinuity of fluid properties, based on the Heaviside function proposed by Sussman et al. [66], Son and Dhir [67] modified the Heaviside function in the calculation of fluid physical properties by solving the following function:

$$H = 1 \quad \psi \geq 1.5h \tag{2-6a}$$

$$H = 0.5 + \frac{\psi}{3h} + \frac{1}{2\pi}\sin\left(2\pi\frac{\psi}{3h}\right) \quad |\psi| \leq 1.5h \tag{2-6b}$$

$$H = 0 \quad \psi \leq -1.5h \tag{2-6c}$$

where h is cell width, ψ is defined to represent the distance from the interface that for 0 at the interface.

- Coupled VOF and LS methods

In order to overcome the respective disadvantages of the LS method and the VOF method, a combination theory of the two methods has been proposed, which can be divided into Coupled Volume of Fluid and Level-set (VOSET) [68] and Coupled Level-set and Volume of Fluid (CLSVOF) [69]. In the VOSET method, the VOF method was used to capture the interfaces, which can conserve the mass and overcome the disadvantage of mass nonconservation in the LS method. An iterative geometric operation was proposed to calculate the ψ in Eqs. (2–6), which can compute the accurate curvature and the discontinuous physical quantities near interfaces. Sussman and Puckett [70] have proposed the CLSVOF method to deal with the curvature issue, in which the just right function will avoid constant curvature or obvious oscillations even for circles. The results also showed that the surface tension-driven flows by CLSVOF method can be achieved in their literature.

- Phase-field method (PFM):

Antanovskii [71] proposed the phase field method for the first time in 1995 and used this method to conduct a series of simulation studies on two-phase flow. The free energy-based phase field method provides a method for simulating a fluid interface with finite thickness, which allows the use of common, easy-to-analyze and easy-to-use central finite volume, finite difference, or finite element convection schemes to calculate the interface movement and deformation on a fixed grid. Jacqmin [72] has defined this method as the theory

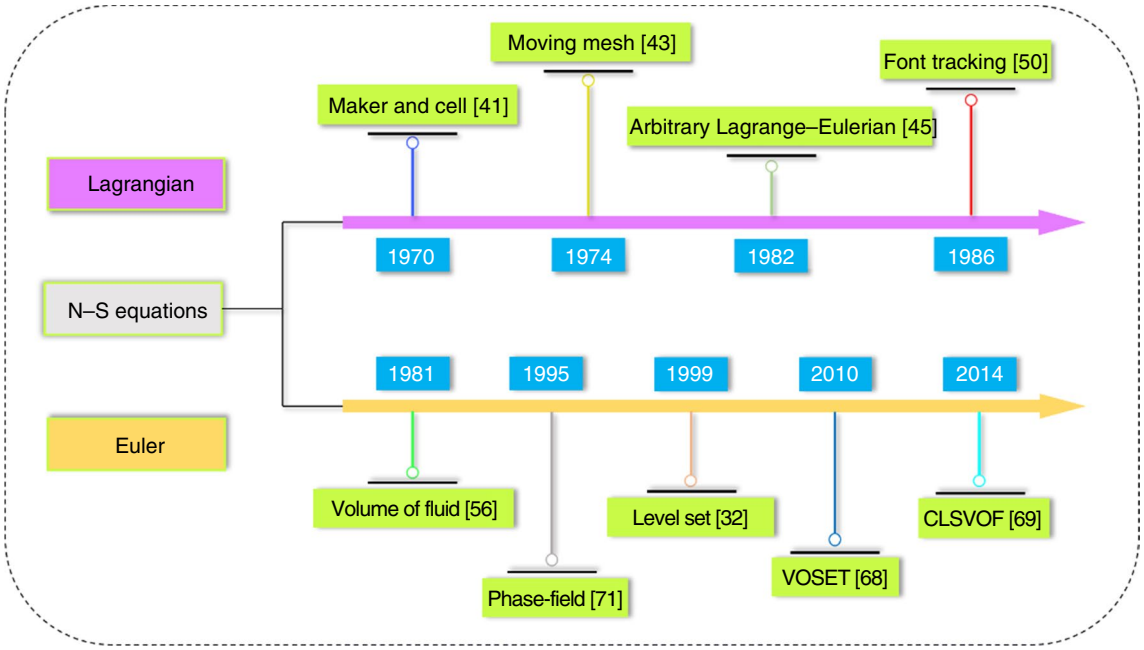

Fig. 4 Typical computational methods based on macroscopic of pool boiling

of diffusion interface with finite thickness. In their article, the interface was traced by solving the advection–diffusion equation.

Other methods

In order to solve the local nonlinear interaction caused by the growing of adjacent bubbles during the pool boiling process, the cellular automata (CA) technique is introduced in the computational fluid dynamic for pool boiling [73]. The bubble nucleation was treated as a random process in this method in which the generation can be represented by Poisson distribution function. This method can be considered as an approach coupling microscopic molecular dynamics and conventional macroscopic fluid dynamics. However, this method is different to represent the bubble population dynamics with the rigid-grid representation. He et al. [74] have developed a model based on a two-phase pattern formed by the macro-thermal layer on the heated surface and the vapor stems. This numerical model is based on the thickness of the macro-layer, which is determined by the evaporation at stem–liquid interface.

Coupled map lattice method (CML) is a dynamical system with discrete-time, discrete-space, and continuous states in which local dynamics propagates in space by diffusion or flow and time is advanced by repeated mapping [75]. This method was proposed to investigate the pool boiling phenomenon firstly by Yanagita [76]. In their model, the piecewise linear function was proposed to replace the hyperbolic tangent, which represents the phase transition.

The dynamic van der Waals theory (DVDWT) has recently been used to investigate the pool boiling of one-component liquid [77]. As a diffuse-interface model formulated for multiphase flows, the DVDWT provides an effective continuum method for investigating the thermal dynamics of boiling process at the contact line scale which adopted from the isothermal Cahn–Hilliard method. In this method, not only the stress and thermal singularities can be solved automatically, but also the phase change rate at the interfaces can be treated as the outcome, which was instead of the prerequisite [78].

The typical numerical method that widely performed to simulate pool boiling based on the N–S equations is listed in Fig. 4.

Lattice Boltzmann method

Briefly introduction of LBM

Knudsen number (Kn) was proposed to distinguish the different dimension, which is defined by the mean free path of fluid molecules (λ) to characteristic length ratio (L). The N–S equation has higher calculation reliability when the Kn number is less than 0.001, and this part of the region is called the continuum region. For the Kn number higher than 10, the main computation method is molecular dynamics (MD), which has the huge computation cost, and this method will discuss in the next section. During the past two decades, the lattice Boltzmann method (LBM) as the mesoscopic

dimension method has been proposed to solve the fluid flow problems, which the Kn number is located at the middle region. The LB equation can be either viewed as a special discrete solver for the Boltzmann equation or a minimal form of the Boltzmann equation in which the microscopic kinetic principles are preserved to recover the hydrodynamic behavior at the macroscopic scale [79]. Therefore, the mesoscopic LBM has many advantages that conventional methods cannot approach. Compared with traditional finite difference, finite element or finite volume methods, LBM can easily add microscopic fluid internal interactions and external macroscopic force forms to the evolution equation and can handle complex boundary conditions. Compared with the microscopic molecular dynamics method, it does not need to pay attention to the details of molecular movement and can simulate a larger area, effectively reducing the amount of calculation.

The basic Lattice Boltzmann method model

The lattice Boltzmann method relies on discrete numbers of the same parameters and uses collisions and evolution on a defined lattice to simulate microflow. The pseudopotential model has been the most popular approach due to its simplicity and high efficiency. Hence, the following will mainly introduce pseudopotential model. According to the related literatures, the collision evolution equation of the distribution function in the commonly used single relaxation time (SRT) of Bhatnagar–Gross–Krook (BGK) model [80, 81] is shown:

$$f_{\mathrm{i}}\left(\mathbf{x}+\mathbf{e}_{\mathrm{i}}\delta_t, t+\delta_t\right)-f_{\mathrm{i}}(\mathbf{x},t)=-\frac{1}{\tau_{\mathrm{f}}}\left(f_{\mathrm{i}}(\mathbf{x},t)-f_{\mathrm{i}}^{(\mathrm{eq})}(\mathbf{x},t)\right)+\Delta f_{\mathrm{i}}(\mathbf{x},t) \tag{3-1}$$

which $f_{\mathrm{i}}(\mathbf{x},t)$ is discrete density distribution function, which represents the distribution of particles evolving in the movement direction $\boldsymbol{e}_{\mathrm{i}}$ on position $\boldsymbol{x}$ at the $\boldsymbol{t}$ moment. δ_{t} is the time step and the $\Delta f_{\mathrm{i}}(\mathbf{x},t)$ is forcing term. τ_{f} is the relaxation time of the velocity field distribution function that related to the kinematic viscosity and can be obtained by following equation:

$$\upsilon=c_{\mathrm{s}}^2(\tau-0.5)\delta_{\mathrm{t}} \tag{3-2}$$

The $f_{\mathrm{i}}^{(\mathrm{eq})}(\mathbf{x},t)$ in Eqs. (3–1) is the equilibrium distribution function, which is expressed as:

$$f_{\mathrm{i}}^{(\mathrm{eq})}=w_{\mathrm{i}}\rho\left[1+\frac{\mathbf{e}_{\mathrm{i}}\cdot\mathbf{u}}{c_{\mathrm{s}}^2}+\frac{\left(\mathbf{e}_{\mathrm{i}}\cdot\mathbf{u}\right)^2}{2c_{\mathrm{s}}^4}-\frac{\mathbf{u}^2}{2c_{\mathrm{s}}^2}\right] \tag{3-3}$$

where the w_{i} is the weights, $\boldsymbol{e}_{\mathbf{i}}$ is the lattice velocities and the c_{s} is the lattice sound velocity, which are all determined by the lattice model. The DnQb lattice model established by Qian et al. [81] in 1992, where n is the number of spatial dimension and b is the number of discrete velocities, has greatly promoted the development of LBM, among which the most commonly used for two-dimensional and three-dimensional spaces are D2Q9 and D3Q19 as shown in Fig. 5.

For the D2Q9 model, the w_{i} and the $\boldsymbol{e}_{\mathrm{i}}$ are given by:

$$w_{\mathrm{i}}=\begin{cases}4/9, & i=0\\ 1/9, & i=1\sim4\\ 1,36 & i=5\sim8\end{cases} \tag{3-4}$$

$$\mathbf{e}_{\mathrm{i}}=\begin{cases}(0,0), & i=0\\ (\pm1,0)c,(0,\pm1)c, & i=1\sim4\\ (\pm1,\pm1)c, & i=5\sim8\end{cases} \tag{3-5}$$

For the D3Q19 model, the w_{i} and the $\boldsymbol{e}_{\mathbf{i}}$ are given by:

$$w_{\mathrm{i}}=\begin{cases}1/3 & i=0\\ 1/18 & i=1\sim6\\ 1/36 & i=7\sim18\end{cases} \tag{3-6}$$

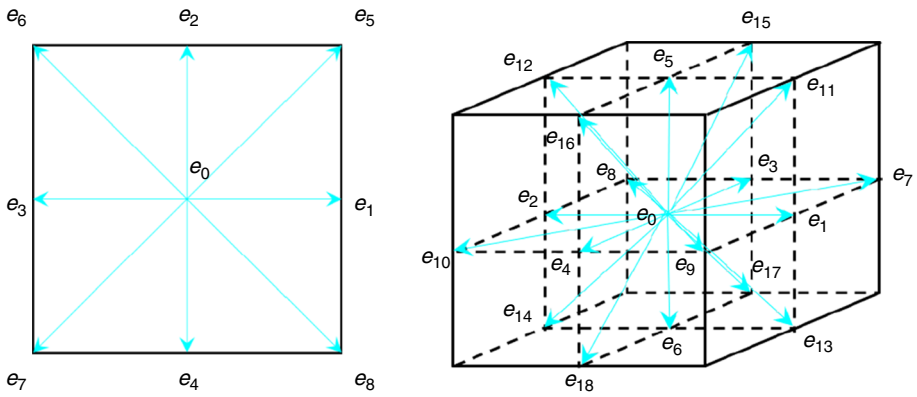

Fig. 5 Typical model (a)D2Q9, (b)D3Q19

$$\mathbf{e}_{\mathrm{i}}=\begin{cases}(0,0,0), & i=0\\ (\pm1,0,0)c,(0,\pm1,0)c,(0,0,\pm1)c, & i=1\sim6\\ (\pm1,\pm1,0)c,(\pm1,0,\pm1)c,(0,\pm1,\pm1)c, & i=7\sim18\end{cases} \tag{3-7}$$

where $c=\delta_{\mathrm{x}}/\delta_{\mathrm{t}}$ is the lattice constant and the δ_{x} is the lattice spacing. In the D2Q9 and D3Q19 model, $c_{\mathrm{s}}=c/\sqrt{3}$. In this model, the density and the velocity can be obtained by following equations:

$$\rho=\sum_{\mathrm{i}} f_{\mathrm{i}} \tag{3-8}$$

$$\rho\mathbf{u}=\sum_{\mathrm{i}} \mathbf{e}_{\mathrm{i}} f_{\mathrm{i}} \tag{3-9}$$

Another more used method is the multi-relaxation-time collision operator lattice Boltzmann method (MRT-LBM), which can increase the stability of the simulation by controlling the multi-relaxation factor, respectively, and more detailed details can be found in Ref. [38].

Interaction forcing

There were many multiphase LBM new models that have been proposed with time elapsing. Several common theories are listed in the following: the free energy LBM [82–84], the phase-field LBM [85–88], the color gradient LBM [89–92], and the pseudopotential LBM [93–97]. In this section, we will briefly introduce the development of the item $\Delta f_{\mathrm{i}}(\mathbf{x},t)$ in Eqs. (3–1) based on the pseudopotential method that widely used in the pool boiling numerical.

The pseudopotential model has received significant attention due to the automatically enables phase separation from a non-monotonic equation of state and naturally generates surface tension, in which this progressive was caused by the introduction of the interaction force to mimic intermolecular interactions [98]. In S–C model [93], the interparticle interaction force is expressed as:

$$\mathbf{F}_{\mathrm{int}}(\mathbf{x},t)=-\psi(\mathbf{x})\sum_{\mathbf{x}'} G(\mathbf{x},\mathbf{x}')\psi(\mathbf{x}')(\mathbf{x}'-\mathbf{x}) \tag{3-10}$$

where $G(\mathbf{x},\mathbf{x}')$ is Green's function and satisfies $G(\mathbf{x},\mathbf{x}')=G(\mathbf{x}',\mathbf{x})$. It reflects the interaction strength between neighboring fluid particles, with $G(\mathbf{x},\mathbf{x}')<0$ representing attractive forces between particles. $\psi(\mathbf{x})$ is the "effective mass" which is determined by the local density, the square root in the original equation limits the maximum density ratio applicable to the modified model. Furthermore, Eqs. (3–10) can be expressed in the following form while simplification [99]:

$$\mathbf{F}_{\mathrm{int}}(\mathbf{x},t)=-c_0\psi(\mathbf{x})g\nabla\psi(\mathbf{x}) \tag{3-11}$$

where c_0 is equal to 6 for the D2Q9 and D3Q19 lattices. g is the interparticle interaction strength. The equation of state (EOS) of the fluid corresponding to Eqs. (3–9) is given as:

$$p=\rho c_{\mathrm{s}}^2+\frac{c_0}{2}g[\psi(\rho)]^2 \tag{3-12}$$

Solving pressure p and substituting it into Eqs. (3–9), then the corresponding "effective mass" will obtain.

Zhang and Chen [100] have expressed the body force as the following form:

$$\mathbf{F}_{\mathrm{int}}(\mathbf{x},t)=-\nabla U(\mathbf{x},t) \tag{3-13}$$

while a straightforward method was used to express an arbitrary equation of state $p=\rho T_0+U$, and then, the corresponding $U(\mathbf{x},t)=p(\rho(\mathbf{x},t),T(\mathbf{x},t))-\rho(\mathbf{x},t)T_0$.

Gong and Cheng [101] have modified the S–C equation and proposed a new force term scheme that combines Eq. (3–9) as shown below:

$$\mathbf{F}_{\mathrm{int}}(\mathbf{x},t)=-\beta c_0\psi(\mathbf{x})g\nabla\psi(\mathbf{x})-(1-\beta)c_0g\nabla\psi^2(\mathbf{x})/2 \tag{3-14}$$

where β is the weighting factor depending on the particular equation of state chosen, in which the value is 0.886 for S–C EOS, 0.55 for van der Waals (VdW) EOS, 1.16 for Peng–Robinson (P–R) EOS. It is worth noting that compared with the other interparticle interaction force terms [93, 100, 102], Eqs. (3–14) have shown the lowest error, which the results were compared based on the Maxwell construction. The more details that different EOS selection effects on LBM simulation are shown in the literature [99, 101]. It is obvious that the selection of EOS is a crucial part while the appropriate EOS will increase the accuracy of the LBM simulation.

Li et al. [97, 103] have given a new formation of interaction force, which caused the phase separation, as follows:

$$\mathbf{F}_{\mathrm{int}}(\mathbf{x},t)=-g\psi(\mathbf{x})\sum_{\alpha=1}^{N}\omega\left(\left|\mathbf{e}_\alpha\right|^2\right)\psi\left(\mathbf{x}+\mathbf{e}_\alpha\right)\mathbf{e}_\alpha \tag{3-15}$$

where $\omega\left(\left|\mathbf{e}_\alpha\right|^2\right)$ are $\omega(1)=1/3$ and $\omega(2)=1/2$ for the case of nearest-neighbor interactions on the D2Q9 lattice. Using the modified pseudopotential LBM model, the simulation multiphase flows at large density ratio and relatively high Reynolds number have been extended. In addition to the above-mentioned formulation, Mukherjee et al. [104] have focused on augmenting the basic algorithm by enhancing the isotropy of the discrete equation and thermodynamic consistency of the overall formulation to expedite simulation of pool boiling at higher-density ratios, in which the modification was proposed in the discrete form of the updated

interparticle interaction term by expanding the discretization to the eighth order.

The wetting condition of the superheated surface is an important factor to be taken into account because the phase change process during pool boiling phenomenon takes place on the superheated surface. Contact angle is usually considered as a measure of the solid surface wettability, which is defined as the angle at the two kinds of fluid interface meets a solid phase. According to the Martys and Chen [105], the force between the fluid and the solid surface can be calculated by the following general form:

$$\mathbf{F}_{\text{ads}}(\mathbf{x},t) = -g_{\text{w}}\psi(\mathbf{x})\sum_{\alpha=1}^{N}\omega\left(\left|\mathbf{e}_{\alpha}\right|^{2}\right)\psi\left(\rho_{\text{w}}\right)s(\mathbf{x}+\mathbf{e}_{\alpha})\mathbf{e}_{\alpha} \tag{3-16}$$

where s is a function that equals 1 for solid and 0 for fluid, g_{w} and ρ_{w} can be tuned separately or jointly to achieve different contact angle. This equation can also modified by Gong and Cheng [106]:

$$\mathbf{F}_{\text{ads}}(\mathbf{x},t) = -(1-e^{-\rho(\mathbf{x})})\sum_{\alpha=1}^{N}g_{\text{w}}\omega\left(\left|\mathbf{e}_{\alpha}\right|^{2}\right)s(\mathbf{x}+\mathbf{e}_{\alpha}\delta_{\text{t}})\mathbf{e}_{\alpha}\delta_{\text{t}} \tag{3-17}$$

The gravity force also plays an important role in multiphase flow such as bubble growth and departure. To calculate the gravity force, the equation is given by:

$$\mathbf{F}_{\text{g}}(\mathbf{x},t) = G(\rho(\mathbf{x})-\rho_{\text{ave}}) \tag{3-18}$$

where $\mathbf{G}$ is the acceleration of gravity and ρ_{ave} is the average density of the whole computation domain. This equation can ensure a zero external force averaged in the entire domain, thus keeping the mass-average velocity of the system constant [107].

So, the total force acting on a fluid particle in multiphase flow can be expressed as following:

$$\mathbf{F}(\mathbf{x},t) = \mathbf{F}_{\text{ads}}(\mathbf{x},t) + \mathbf{F}_{\text{int}}(\mathbf{x},t) + \mathbf{F}_{\text{g}}(\mathbf{x},t) \tag{3-19}$$

It is worth noting that if there has another physical fields action together, additional field force needs to be added to the right side of Eqs. (3–19), such as the electrical field [108].

LBM thermal model

The change of thermal field must be considered in the simulation of pool boiling phase change process. Zhang and Chen [100] have proposed the thermal pseudopotential LB model firstly to solve the energy change problem during nucleate boiling. Since then, the thermal pseudopotential LB model has been continuously improved [106, 109–114], and its temperature-based expression is as follows:

$$g_{\text{i}}(\mathbf{x}+\mathbf{e}_{\text{i}}\delta_{\text{i}},t+\delta_{\text{t}}) - g_{\text{i}}(\mathbf{x},t) = -\frac{1}{\tau_{\text{f}}}(g_{\text{i}}(\mathbf{x},t) - g_{\text{i}}^{\text{eq}}(\mathbf{x},t)) + S \tag{3-20}$$

where $g_{\text{i}}^{(\text{eq})}$ is the equilibrium temperature distribution function, S is source term and the more details are shown in Ref. [38]. The fourth-order Runge–Kutta algorithm coupled with finite difference method is often used to solve the temperature distribution problem as well. The next section will introduce the last numerical method that named molecular dynamics simulation.

Molecular dynamics simulation

Background and feasibility

Molecular dynamics simulation method is based on the classical Newton's second law to accurately solve the motion trajectory of atoms or molecules in the simulation system after reasonably selecting the field potential energy function of the simulation system, while constructing the simulation model in accordance with the real physical system. By means of statistical thermodynamics, the macroscopic physical properties of the simulated system reflected by the atomic or molecular trajectory can be obtained accurately. This simulation method has been deeply used to analyze and discover the physical phenomena and internal mechanism at atomic or molecular level, which are difficult to be revealed by ordinary simulation methods. Therefore, in the past few decades, the numerical simulation method has been widely promoted and applied in different fields [115–120].

Pool boiling is a typical heterogeneous nucleation, which the bubbles nucleation occurs on solid surfaces. A serious complex phenomenon involving bubble dynamics is always occurred on the superheating surface, such as the bubble nucleation, bubble growth, bubble coalescence and bubble departure. A large number of documents have proved that the bubble dynamics of the superheated surface will be affected by the state of the surface condition, such as roughness [121–124], porous materials [125–128] and multi-dimensional structure [129–133]. The molecular dynamics theory can effectively capture the nonequilibrium properties of boiling and the interactions between molecules in local regions at the nanoscale. In addition, surface properties can also be effectively reflected in the model, which provides new possibilities for understanding key mechanisms in the boiling process.

Molecular dynamics method

For molecular dynamics simulation methods, it is crucial to calculate the interaction potential between molecules or

atoms, which determines the accuracy of particle motion characteristics. The widely used calculation method is the Lennard–Jones (LJ) potential function [134], and its mathematical expression is as following:

$$\phi(r) = 4\varepsilon\left[\left(\frac{\sigma}{r}\right)^{12} - \left(\frac{\sigma}{r}\right)^{6}\right] \tag{4-1}$$

where ε is the energy of interaction, σ is the equilibrium distance, and these two parameters depend on the type of atoms.

For interactions between two atoms i and j, the parameters ε and σ can be calculated by:

$$\varepsilon_{ij} = \sqrt{\varepsilon_i \varepsilon_j} \tag{4-2}$$

$$\sigma_{ij} = \frac{\sigma_i + \sigma_j}{2} \tag{4-3}$$

After calculating the potential energy, it is necessary to integrate the time of Newton's law of motion to calculate the force and acceleration of each molecule in the system during a continuous moment, so as to obtain the position and velocity. The Verlet algorithm is the earliest method used to solve the Newtonian equation of motion, and the core is Taylor expansion of position function [135]. However, in the execution process, it must be obtained through two large differences in position, so the accuracy is inevitably reduced. Velocity-Verlet algorithm with higher accuracy is developed based on Verlet algorithm [136]. The positions, velocities and accelerations at time t + Δt were obtained from the same quantities at time t by the integrated using the velocity-Verlet as shown in the following:

$$r(r + \Delta t) = r(t) + v(t)\Delta t + (1/2)a(t)\Delta t^2 \tag{4-4a}$$

$$v(r + \Delta t/2) = v(t) + (1/2)a(t)\Delta t^2 \tag{4-4b}$$

$$a(t + \Delta t) = 9(1/m)\nabla V(r(t + \Delta t)) \tag{4-4c}$$

$$v(r + \Delta t) = v(t + \Delta t/2) + (1/2)a(t + \Delta t)\Delta t \tag{4-4d}$$

In order to introduce the evolution of thermodynamic systems into statistical mechanics, the ensemble was proposed, which is composed of a series of fixed and known thermodynamic variables related to physical quantity systems. There are two main ensembles in equilibrium statistics theory, that are, the canonical ensemble (NVT) suitable for large heat source energy exchange which the number of molecules and temperature are fixed, and the microcanonical ensemble (NVE) with fixed energy and particle number. In the canonical ensemble, in order to keep the temperature constant, the system needs to be kept to the thermostat and be in thermal equilibrium. For the ith region, the temperature calculation formula obtained based on the principle of statistical mechanics in MD is as follows:

$$T_i = \frac{2E_{ik}}{(3N_i - N_{ic})k_B} \tag{4-5}$$

where E_{ik} is kinetic energy time average value, N_i is the number of atoms in the ith region, N_{ic} is the number of degrees of freedom, k_B is the Boltzmann constant. Equations (4–5) also reflect the relationship between temperature and velocity. The most widely used thermostats to maintain temperature including Nose–Hoover thermostats [137], Berendsen thermostats [138] and Langevin thermostats [139]. The Nose–Hover method realizes the constant temperature of the simulation system by adjusting the Hamiltonian of the particle motion equation in the simulation system. The critical idea of other temperature control methods Berendsen [138] and Langevin [139] is to connect the middle layer atoms with a virtual thermostats system, and each step is to scale the speed of the atoms in the system.

In the MD method, the heat flux vector is always evaluated from MD trajectories as following [140]:

$$\mathbf{J} = \frac{1}{V}\left[\sum_i (e_i \mathbf{v}_i) + \frac{1}{2}\sum_{i<j} (\mathbf{F}_{ij}(\mathbf{v}_i + \mathbf{v}_j))\mathbf{r}_{ij}\right] \tag{4-6}$$

where V is the volume of the region, e_i is the total energy of each atom i, $\mathbf{v}_i$ is the per-atom velocity vector and $\mathbf{F}_{ij}$ is the force acting on atom i due to the pairwise interaction with an atom j. It is worth noting that the second term on the right side of the formula corresponds to the virial contribution of each atom's stress tensor. Among the various existing MD software packages, popular options involve LAMMPS [141], AMBER [142], GROMACS [143], CHARMM [144] and GROMOS [145]. The large-scale Atomic/Molecular Massively Parallel Simulator (LAMMPS) has been widely used to simulate the processes of bubble nucleation. Compared with the previous simulation methods, MD method provides insights and available information that can be investigated by focusing on the atomistic nature of phase change, and this is a method with broad research prospects.

Bubble dynamics in pool boiling

Once the average temperature on the superheated surface exceeds the onset of nucleation boiling temperature, the bubble will appear at the activated nucleation site and the number of bubbles on the surface will increase with the increase of temperature, which accompanied by different bubble behaviors. The bubbles from nucleation to detachment are invariably isolated bubbles with moderate heat flux.

However, when the heat flux is higher enough, violent bubble merge will appear on the superheated surface. Therefore, the heat transfer mechanism in the two states is very complicated and nonlinear, which adds inevitable difficulties to the successful simulation of the pool boiling process. Dhir et al. [36] have discussed the previous simulation models and results of isolated bubbles and merged bubbles, etc., which was mainly obtained by macroscopic simulation methods. However, with the rapid development of molecular dynamics and lattice Boltzmann methods in the past ten years, many new research results have emerged. Therefore, this section provides a detailed and in-depth discussion on the boiling bubbles obtained by different simulation methods.

As introduction before, the complex mechanism of pool boiling has made the numerical hard to realize. Many scholars have made a lot of efforts for this, but the simulation results have not been able to meet the actual situation due to the limitation of the model, such as not to consider the micro-region [29, 31, 146, 147]. Until the boiling region it was divided into two parts as shown in Fig. 6, that are micro-region and macro-region; Son et al. [32] have successfully simulated the complete bubble nucleate process firstly. A finite difference scheme was used to solve the equation governing conservation and the level set was appropriated to capture the vapor–liquid interface. They introduced lubrication theory in solving for the micro-layer and used the Clausius–Clapeyron equation to calculate the evaporative heat flux. The bubble shape at the moment before departure was compared, and the results were shown at the high accuracy of consistency. Besides, they also simulated the effect of static contact angle on bubble diameter. It was noticed that the microlayer contribution to be about 20% during bubble growth has reported in their result.

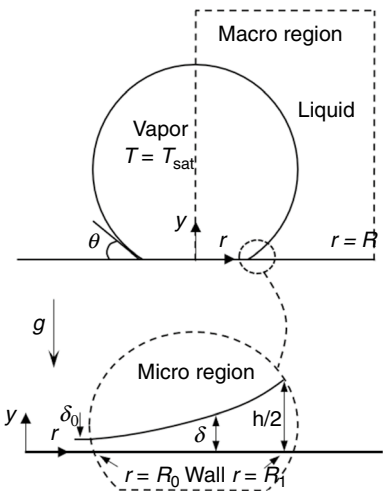

Fig. 6 Different computational domain in pool boiling with micro- and macro-regions [32]

Furthermore, they used the previous theory [32] to successfully simulate the vertical bubble merger and it was consistent with the experimental results [148]. They also quantified the effect of bubble merging on the vapor removal rate, flow field and heat transfer. The vapor removal rate has shown a larger error when the superheat degree is high, about 30%, due to the horizontal direction as they explained. It should be noted that since the lubrication theory assumes that the liquid film is in laminar flow and homogeneous, there may be some error in the prediction of the contribution of the micro-layer to evaporation. Mukherjee and Dhir [65] have also introduced this method [32] to investigate the multiple bubble mergers with different nucleation sites location. The results have shown that the merger of bubbles significantly increased the overall wall heat transfer due to the cooler liquid that was draw towards the heated surface at the base of bubble merger region. By introducing the color function, Sato and Niceno [149] have investigated the bubble nucleation in 3D domain using mass conservative constrained interpolation profile scheme coupled in the PSI-BOIL code that developed by themselves, which the fine grid resolutions that under the half μm showed the excellent ability to capture the microlayer formation and depletion. They use the energy jump model at the interface to solve the phase transition problem. The microlayer was considered in their following research, and the numerical results of bubble growth have manifested well consistent with experiment as shown in Fig. 7 [150].

Jia et al. [151] introduced an improved height function algorithm coupling monotonic variation and the contact angle methods in the VOF method, where the phase change model uses Hardt and Wondra simplified Schrage model with accommodation coefficient $\gamma = 1$. The advantage of this method is that it can obviously reduce the unavoidable spurious speed of the VOF method. However, the departure time of the single bubble is longer than the experimental results, and the neck reduction phenomenon is not captured during the detachment process of the bubble. The latest article by Mobli et al. [152] on the pool boiling simulation by using the CLSVOF method solves the above problems very well, where the phase change model is the same as Jia et al. [151], but in addition they use a flux-corrected transport method of multidimensional universal limiter with explicit solution and an arbitrary mesh compressive interface capturing scheme coupling method to solve the parasitic current problem. In addition, the micro-layer depletion model proposed by Sato et al. [149] was used to calculate the bubble bottom evaporation effect and the evaporation stops when the microfluidic layer thickness is 10 nm. The simulation results show a satisfactory agreement with the experimental results, especially the evolution of bubble shapes and micro-layer thickness. A new temperature interpolation method was coupled into the VOSET theory by Ling et al. [69] to obtain the gas phase

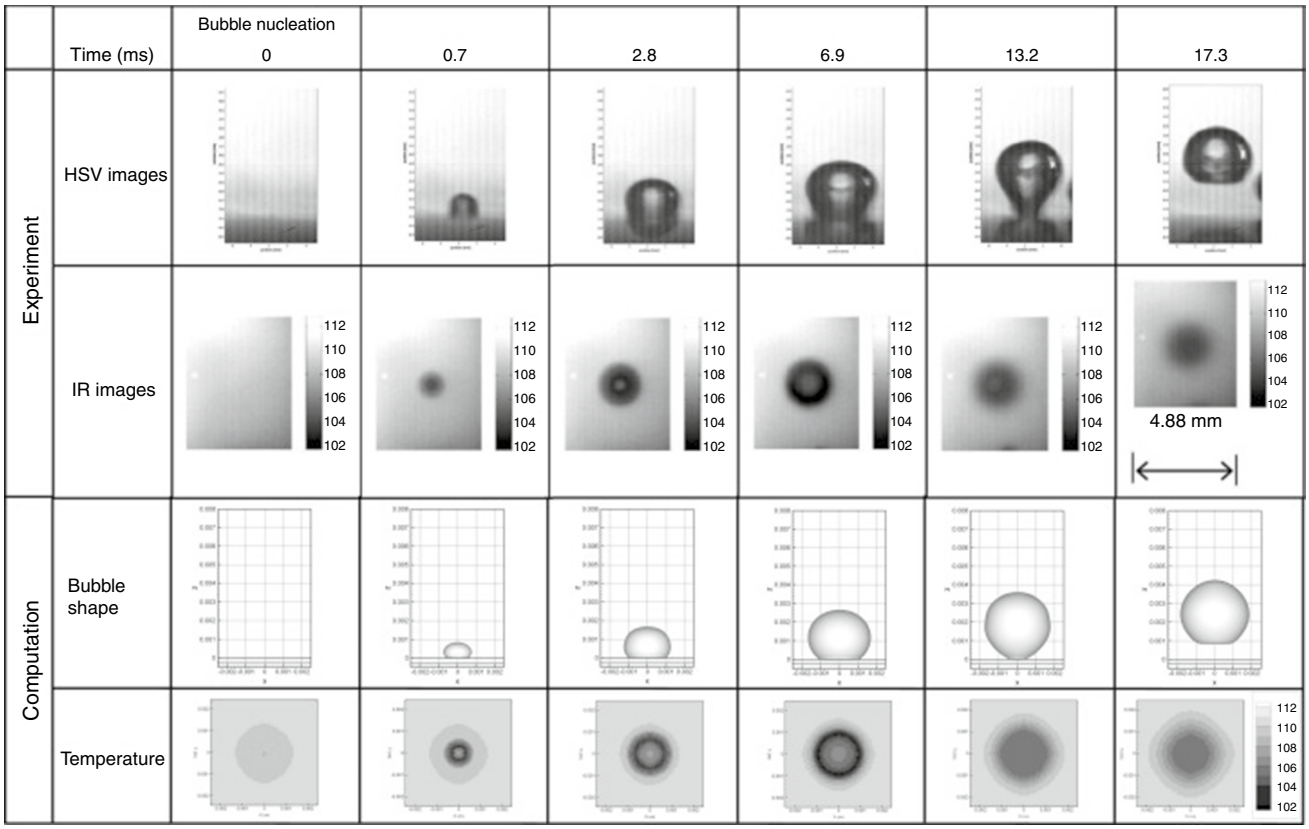

Fig. 7 Comparisons of bubble shape and temperature distribution between experimental measurement and CFD computation [149]

temperature, and the two-region model was also considered by them. Based on this model, the phenomena of bubble detachment, growth and merging are studied.

The Lagrangian-based front tracking method is significantly different from the Euler-based VOF or LS methods and is more suitable for complex two-phase flow simulations due to the explicitly tracking the interface as a moving boundary without requiring any additional approximations. Salehi et al. [153] used the front tracking method to study the growth and detachment of bubbles in the boiling range of saturated pools, focusing on the influence of different dimensionless numbers on the overall and average heat transfer rate. The normal component of the velocity of the interface in the model controlled by fluid advection and phase change is determined by Peskin interpolation method and first-order finite difference approximation, respectively. It is worth mentioning that the overall heat transfer rate is different from existing, in which the maximum error of the comparison of correlation is 25%.

In addition to the continuous medium model, mesoscopic methods have led to a series of outstanding results in simulating bubble dynamics. In order to solve the instability problem caused by the large density ratio in the LBM two-phase model, Inamuro et al. [154] derived a free-energy model applicable to high-density-ratio two-phase flow that can track the interface by applying a diffuse equation analogy to the Cahn–Hilliard equation and performed a series of simulations based on it [155–157]. Safari and Rahimian [160] proposed a phase-field LBM large density ratio model by incorporating equations describing the finite divergence of the velocity field in the interface region and based on this model to study the bubble dynamics. Dong et al. [158] used the proposed modified free energy model combined with the large density ratio model of Zheng et al. [159] to quantitatively investigate the effect of bubble aggregation on bubble growth and departure. Figure 8 shows the variation of the temperature field during the bubble merging process, and the results indicate that the variation of the nearby flow field during the bubble merging and leaving has a direct effect on the temperature field. In addition to the large density ratio model mentioned above, Begmohammadi et al. [161] used the distinguished lattice Boltzmann multiphase scheme based on the Cahn–Hilliard diffusion interface theory proposed by Lee to analyze the effect of density ratio on the bubble departure frequency. The results showed that the derivation between simulation and experimental results increased with increase of the density ratio.

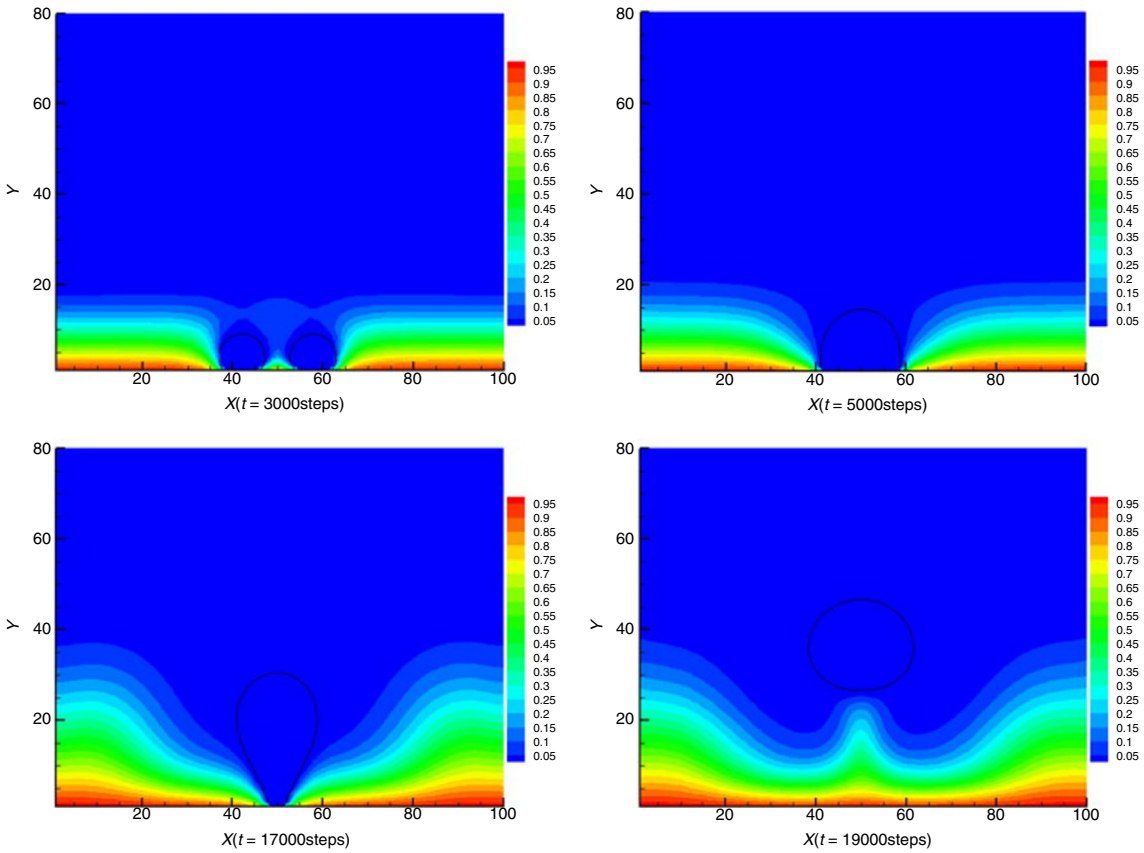

Fig. 8 Propagation of temperature fields with time during bubble horizontal merger [158]

Sun has conducted researches on isolated bubble dynamics in the early years [162, 163]. Latterly, based on the 2D model of Dong et al. [158], Sun [164] has likewise extended model to 3D and simulated the bubble growth, merger and departure, which firstly showed the merger process of four bubbles. The latent heat source term based on the phase-order parameter was introduced in phase change model that considered the Ja non-dimensional number. Shortly after, Yuan et al. [165] have investigated the variation of heat flux under bubbles from beginning of bubble coalescence to bubble departure; the results showed that there were two peaks of heat flux during the merging process. The double distribution function methods were firstly used by Gong and Cheng to successfully simulate the bubble nucleation, in which the energy source term was proposed by neglecting the viscous dissipation and based on the entropy balance equation [106]. Unlike the numerical domain of macroscopic computational methods, where micro-layer evaporation model must be considered, mesoscopic numerical methods allow the spontaneous generation of microlayer formation and evaporation processes by introducing equations of state. Furthermore, the automatic generation of surface tension by introducing intermolecular interactions and coupling the equation of state can avoid the tedious work of macroscopic simulations that require a large number of equations to satisfy the interfacial heat mass transfer. In other words, the mesoscopic lattice Boltzmann method can satisfy the spontaneous emergence of the onset of the nucleate boiling and can better describe the heat transfer and fluid flow near the initial stage of bubble growth.

Different from the aforementioned two simulation methods, the molecular dynamics method uses a large number of Leonard–Jones molecules and harmonic molecules to represent liquid and solid rather than specific phases with real thermophysical properties. Nucleation of bubbles is shown by observing density fluctuations between solid molecules in nanoscale. The solid atoms were always placed at the bottom with the arrangement of face-centered cubic structures in pool boiling simulation. Maruyama and Kimura [166] have firstly simulated the heterogeneous nucleation of a bubble on a solid surface by the molecular dynamics method. The liquid region was represented by 5488 Lennard–Jones molecules. The research results obtained the bubble size variation with the pressure during the bubble nucleation process.

Next part will introduce the numerical results of bubble behaviors under various factors, including surface modification, gravity level, superheated surface heat transfer conjugate and external fields.

Surface modification

The superheated surface plays a significant role in the bubble dynamics, such as bubble nucleation and bubble departure dynamics, and therefore affects the critical heat flux and heat transfer coefficient. It has always been a research hotspot in the field of pool boiling.

Wettability

For adjusting the contact angle, the source term always was added in the momentum equation in Continuum model, while the fluid–solid interaction force was introduced to change the contact angle in LBM [167–169]. In particularly, the wettability change in molecular dynamics simulation is obtained by changing the potential between liquid molecules and solid molecules [170].

Mukherjee and Kandlikar [171] have extended the method of Son et al. [32] to investigate the effect of dynamic contact and static contact angle on vapor volume increasing rate. The results have showed that the vapor volume growth rate increases with increase in the advancing contact angle and the bubble departure diameter decrease with the increase the surface wettability, which was the same as the numerical result of Son et al. [32]. It is worth pointing out that their model discards the micro-layer evaporation model and instead considers fluid perturbations and transient conduction caused by bubbles, which may lead to incorrect predictions of bubble dynamics. In addition to the contact angle theory, Ding et al. [172] also considered the evolution of the microlayer at different locations of the bubble base over time. Moreover, Huber and Tanguy [173] introduced the ghost fluid method based on the simulation model of Son to solve the mass transfer by introducing ghost cells near the phase interface to couple the jump energy model, and based on this, it quantified the effect of apparent contact angle on bubble dynamics and heat flux near the contact line. For improving the computational performance, the millimeter-scale sub-grid contact angle control model proposed by Li was applied to the growth of individual bubble with couples of the evaporation and condensation model [174]. This also provides the implementation conditions for controlling the forward and backward contact angles in the model by applying subgrid control forces. In their subsequent study, the model was performed to investigate the interaction between two adjacent nucleate sites at different contact angles [175].

Hsu and Lin [176] have used the VOF method to capture the interface and simulate the surface wettability effect among large region that from 5° to 180°, and the bubble dynamics simulation results are very close to LBM. The variation trend of CHF with contact angles was in good agreement with the experimental or theoretical results of other scholars [177, 178]. Furthermore, the effects of mixed superhydrophilic and superhydrophobic surfaces on pool boiling efficient have been also studied [179]. In the above study, in order to ensure the stability of the numerical simulation, the gas–liquid two-phase was not used real physical parameters, so further data correlation was performed using dimensionless parameters. However, this may also cause the simulation results to be unrealistic. Taking into account the dynamic contact angle treatment that proposed by Kistler [180] and developed by Vontas et al. [181], Pontes et al. [182] have addressed a numerical investigation of bubble dynamics on a biphilic surface, which superhydrophobic region was surrounded by a hydrophilic region, but lack of the conjugate of thermal response of surface. Moreover, their group has also considered the combination effects of the nanofluids and previous surfaces pattern on pool boiling [183]. Different from the phase change model used in Re. [182] that named Hardt and Wondra model, Li et al. [184] have simulated the effects of hydrophilic–hydrophobic ratio on boiling heat transfer introduced by the Lee model [185], and found that the bubble departure dynamics can be controlled by adjusting the different wettability region mixed ratios. In the Hardt and Wondra model, the bubble is assumed to be spherical and the detachment frequency is considered to be constant, and additional empirical constants are required to control it. In contrast, the Lee model, which does not require additional empirical constants, has been shown to be able to handle bubble dynamics better. The boiling behaviors on the 5:1 mixed surface are shown in Fig. 9. The bubble nucleation, growth and coalescence are well mimicked in the simulations. The modified VOF model involved the smoothing interface curvature using the initially volume fraction values has proposed to investigate the pool boiling by Georgoulas et al. [186, 187]. The Schrage model is used to solve the mass transfer problem at the vapor–liquid interface.

After Gong and Cheng successfully simulated bubble growth and detachment in pool boiling using improved pseudopotential LBM for the first time [106], this method has been widely used by a large number of scholars to investigate bubble dynamics. Gong and Cheng [112] have extended their model to investigate the contact angle effects on bubble departure diameter and departure frequency. The numerical results have shown the weak effect of contact angle on bubble departure diameter with the bubble departure frequency, which increase with the increasing contact angle. They calculated the latent heat of vaporization in the simulation from the P–R equation with an error of no more than 4% from the experiment. Furthermore, the increased contact angle has facilitated the nucleation temperature reduction. In their following simulation studies [188], the effects of surfaces with mixed wettability on pool boiling have been investigated. By changing the size of the hydrophobic spots on smooth

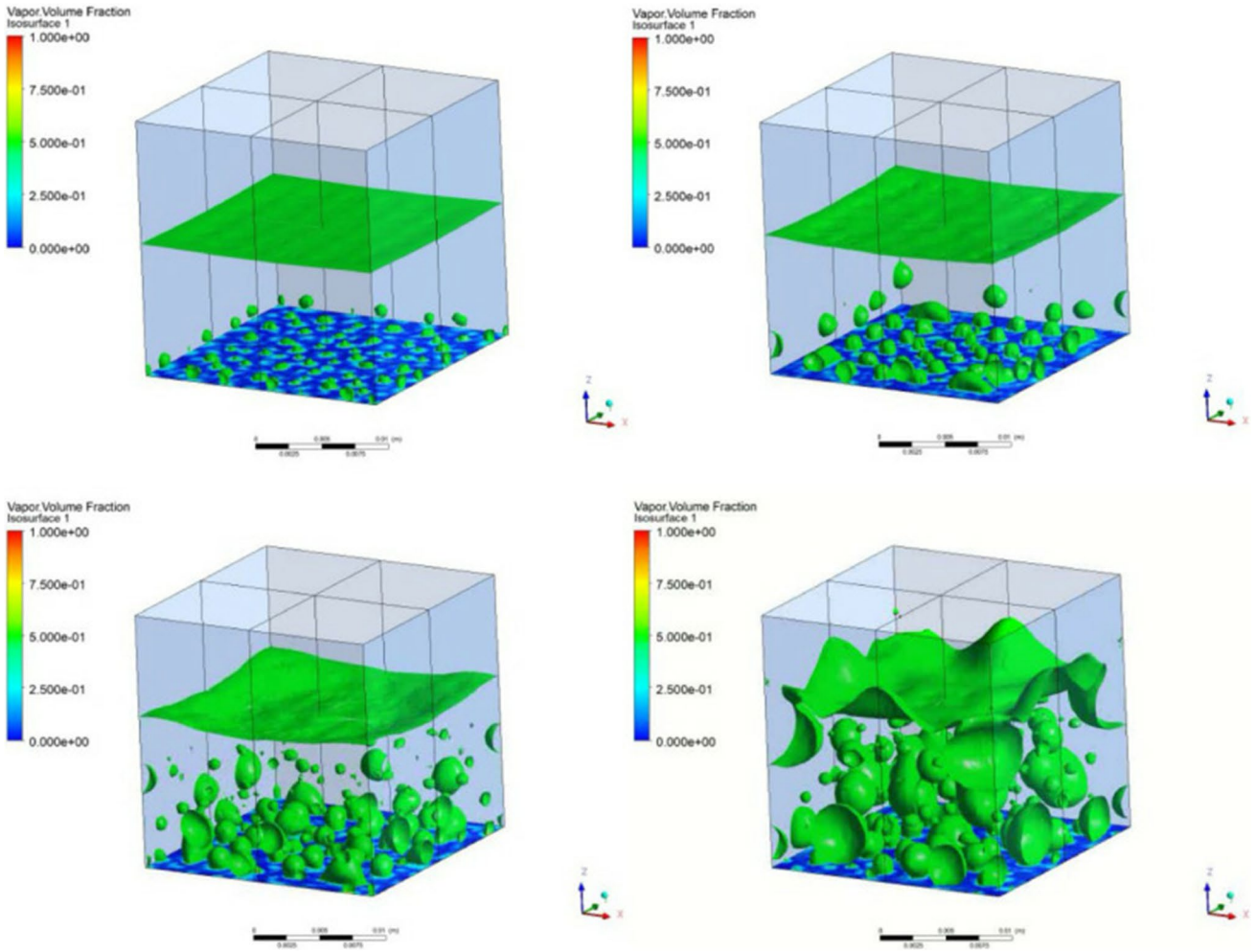

Fig. 9 Bubble dynamics of pool boiling on 5:1 mixed surface [184]

hydrophilic surfaces and the pitch distance between these spots, the various bubble phenomena have been obtained as shown in Fig. 10, also the local heat flux at the bubble base has been analyzed, which conjugated with the solid temperature thermal response. The conclusion obtained is same as the results of Li et al. [184]. The local heat flux and the temperature at the triple contact line on different smooth wettability surfaces also have been investigated [189].

Lee and Lee [190] have proposed adaptive fraction control of the pitch of hydrophobic dots, and the CHF change tendency has also been revealed by employing the model of Gong and Cheng [106]. The checkerboard pattern introduced in their research was same as the surfaces pattern in Li et al. [184]. In their following researches, multiple shape surfaces with mixed wettability have been performed to investigate the bubble coalescence, including cross, interlaced, eccentricity pattern [191–193]. Zhang et al. [194] have modified the model of Gong and Cheng [105] which determining the equilibrium distribution function by half-implicit scheme to reveal the effects of heater size on boiling curves of horizontal smooth hydrophilic and hydrophobic surfaces. The subcooling impact on bubble dynamics was also considered. To investigate the boiling hysteresis in transition boiling, different thermal methods were employed in their subsequent research [195]. It is worth mentioning that a new exact expression for the source term in thermal distribution equation was used, in which the similar formulations also performed by others [196, 197]. In the improved source term model, additional property changes are considered. The 3D pool boiling numerical simulation performed by Ma and Cheng [198] was to analyze the details of multiple bubble dynamics on different wettability surfaces, also including the change of dry spots. The results obtained have shown that compared with the hydrophilic surface, the expansion speed and average size of spots on hydrophobic surface were much faster and larger, respectively. The first, second, and third rows of Fig. 11 show bubble patterns, the corresponding

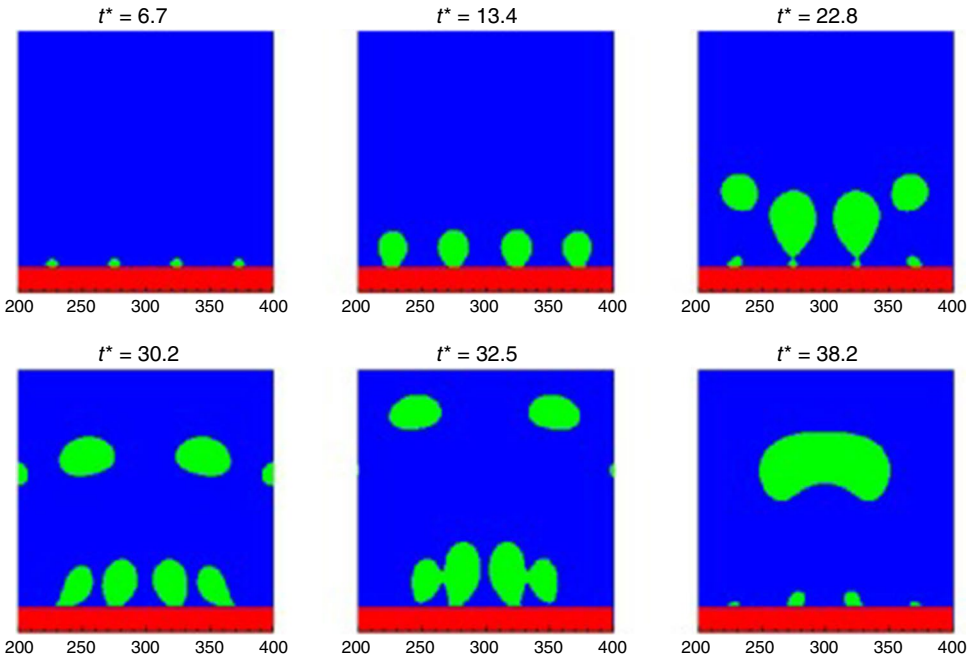

Fig. 10 Bubble dynamics on mixed wettability surface #1 with hydrophobic spots at Ja = 0.062 [188]

liquid–vapor distributions and wall temperature distributions at the solid/liquid interface of a hydrophilic heater ($\theta = 56°$) at CHF (Ja = 0.16).

The hybrid thermal lattice Boltzmann model, which was based on an improved LBM, was used to simulate the effects of the surface wettability on pool boiling heat transfer by Li et al. [199]. It is worth noting that the modified model was avoided the spurious term caused by the forcing-term effect. In this method, the temperature was calculated with iterative methods named fourth-order Runge–Kutta scheme. The LB equation with MRT collision operator is shown as follows:

$$f_i(\mathbf{x} + \mathbf{e}_i\delta_i, t + \delta_t) - f_i(\mathbf{x}, t) = -(\mathbf{M}^{-1}\Lambda\mathbf{M})_{ij}(f_j(\mathbf{x}, t) - f_j^{(eq)}(\mathbf{x}, t)) + \delta_i F_i \tag{5-1}$$

where **M** is an orthogonal transformation matrix, Λ is a diagonal Matrix. More details about this method can be obtained from reference [38]. Zhang et al. [200] have proposed a surface with temperature-dependent wettability to compare boiling heat flux with the different surfaces with fixed wettability by using MRT method. The numerical results obtained were consistent with the previous experimental, including the necking phenomenon on hydrophobic surface and the obviously waiting period on hydrophilic surface. It is worth mentioning that, compared with the BGK model, the MRT model can adjust the shear and kinematic viscosity of the fluid by modifying multi-relaxation parameters in the collision term. This ability to independently adjust the relaxation parameters enhances the simulation stability of the method. By changing the virtual density of the wall to change the density gradient of the fluid point near the wall, Wang et al. [201] studied the influence of the contact angle hysteresis on the bubble dynamics and found that the hydrophilic hysteresis would make the bubble detach and leave residual bubbles. In addition, Zhan et al. [202] used the lattice Boltzmann method to deeply study the bubble dynamics of different wettability surfaces, especially the temperature field and flow field in the adjacent area of bubbles.

In computational boiling of Nagayama et al. [203], the modified form of the L–J potential that combined with the models of Din and Michaelides [204] and Barrat and Bocquet [205] was used to adjust the surface wettability as shown below:

$$\phi_{sl}(r_{ij}) = 4\varepsilon_{sl}\left[\left(\frac{\sigma_{sl}}{r_{ij}}\right)^{12} - \beta\left(\frac{\sigma_{sl}}{r_{ij}}\right)^{6}\right] \tag{5-2}$$

where $\sigma_{sl} = (\sigma_l + \sigma_s)/2, \varepsilon_{sl} = \alpha\sqrt{\varepsilon_l\varepsilon_s}$. The values of parameters α and β were obtained by simulation the droplet formation on a solid substrate. Although the different bubble nucleation behaviors were observed in numerical results, the Young–Laplace equation that widely used to analyze the interaction between three different phases was deemed not adequate to describe the nanobubble. The possible reason was thought to be that fewer vapor molecules cannot satisfy the mechanical equilibrium state of the external liquid with it.

Soon after, Matsumoto and Yamamoto [206] have proposed the different potential equation to adjust the contact angle as follows:

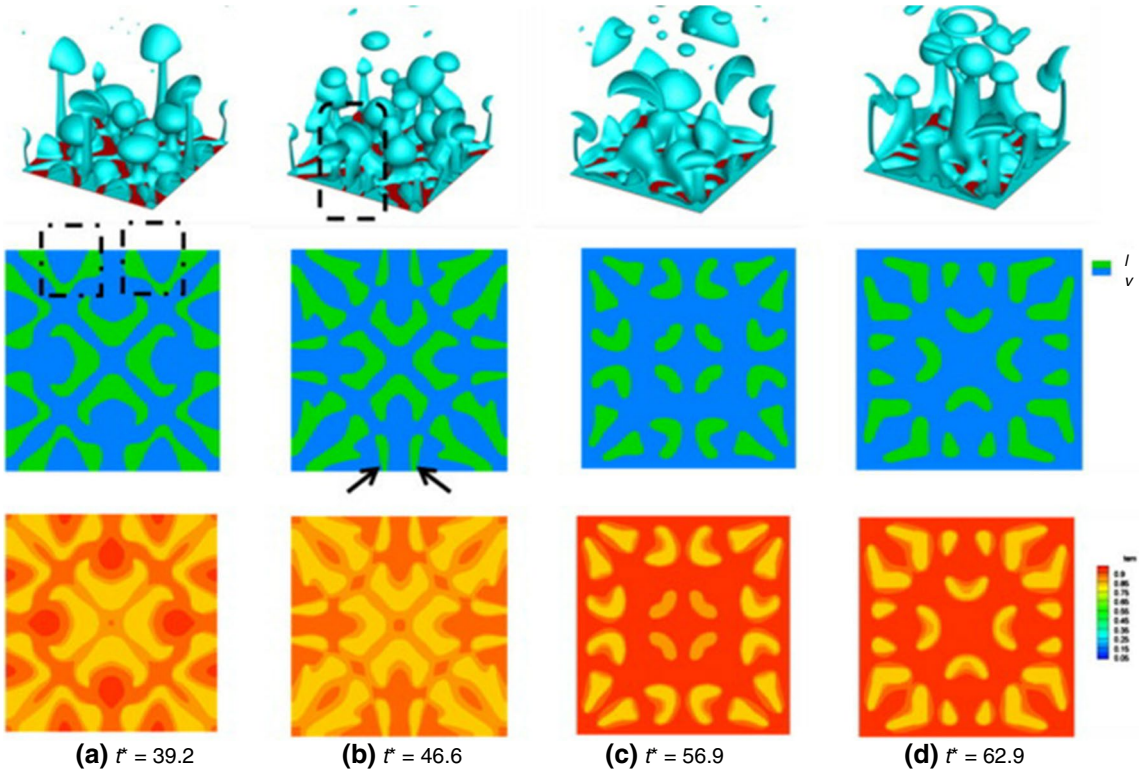

Fig. 11 Different bubble patterns, liquid–vapor distributions and surface temperature distribution at four moments [198]

$$\phi_{sl}(r_{ij}) = \alpha \cdot 8\pi\varepsilon_{sl} n \left[\frac{1}{90} \left(\frac{\sigma_{sl}}{r_{ij}} \right)^{12} - \frac{1}{12} \left(\frac{\sigma_{sl}}{r_{ij}} \right)^{6} \right] \quad (5\text{-}3)$$

where n is uniform distribution number density of particles. The non-dimensional parameter α was introduced to control the surface wettability and in their study, when α less than 1 as the hydrophobic surface; otherwise, it is a hydrophilic surface. They found the bubble size oscillation phenomenon when the surface is hydrophobic and the heating area is small. This has also observed in their next numerical study literature [207]. They has also presented that the bubble nucleation during boiling was depended on thermal expansion and pressure fluctuations adjacent to the solid–liquid interface. Hens et al. [208] have investigated the bubble nucleation at the different wettability condition, which was defined by varying solid–liquid energy parameter ε. The nanodroplet was placed to verify the contact angles on the surfaces under the NVT at 80 K, and the results have shown the quite reasonable interaction potential model. In order to reveal the complete boiling regime map, Zhang et al. [209] have changed the wettability of surfaces from superhydrophobic to superhydrophilic; meanwhile, the surface energy method was used to analyze the nucleation of nanobubble. Moreover, a three-dimensional molecular dynamics analysis of surface potential energy was used to investigate the relationship between boiling characteristics and wettability by Bai et al. [210], in which a long-Coulombic pairwise interaction was considered in L–J potential. Figure 12 shows the wetting behavior and boiling behavior of two different wettability surfaces. The results have showed that the hydrophilic surface can significantly promote the pool boiling heat transfer, including the low onset of nucleation boiling temperature and higher heating rate and the main reason was the decrease of the interfacial thermal resistance with the increasing wettability capacity.

Furthermore, Zhou et al. [211] have carried out the 2D molecular dynamics simulation to study the effects of different surface temperature on bubble nucleation of various surfaces with different wettability area fraction. Interesting, they have observed that the nucleation site moves from hydrophobic to the hydrophilic part with the increasing temperature. They explained this phenomenon using the temperature and density of argon molecules near the wall and proposed an optimal area ratio factor. The initial process of nucleate boiling was divided into two stages in their subsequent research, which named slow nucleation stage at the nucleus occurs and the rapid stage during the stable bubble growth [212]. Zhou et al. [213] used molecular dynamics to study the bubble dynamics on a superhydrophilic surface, and obtained an optimal parameter of solid–liquid

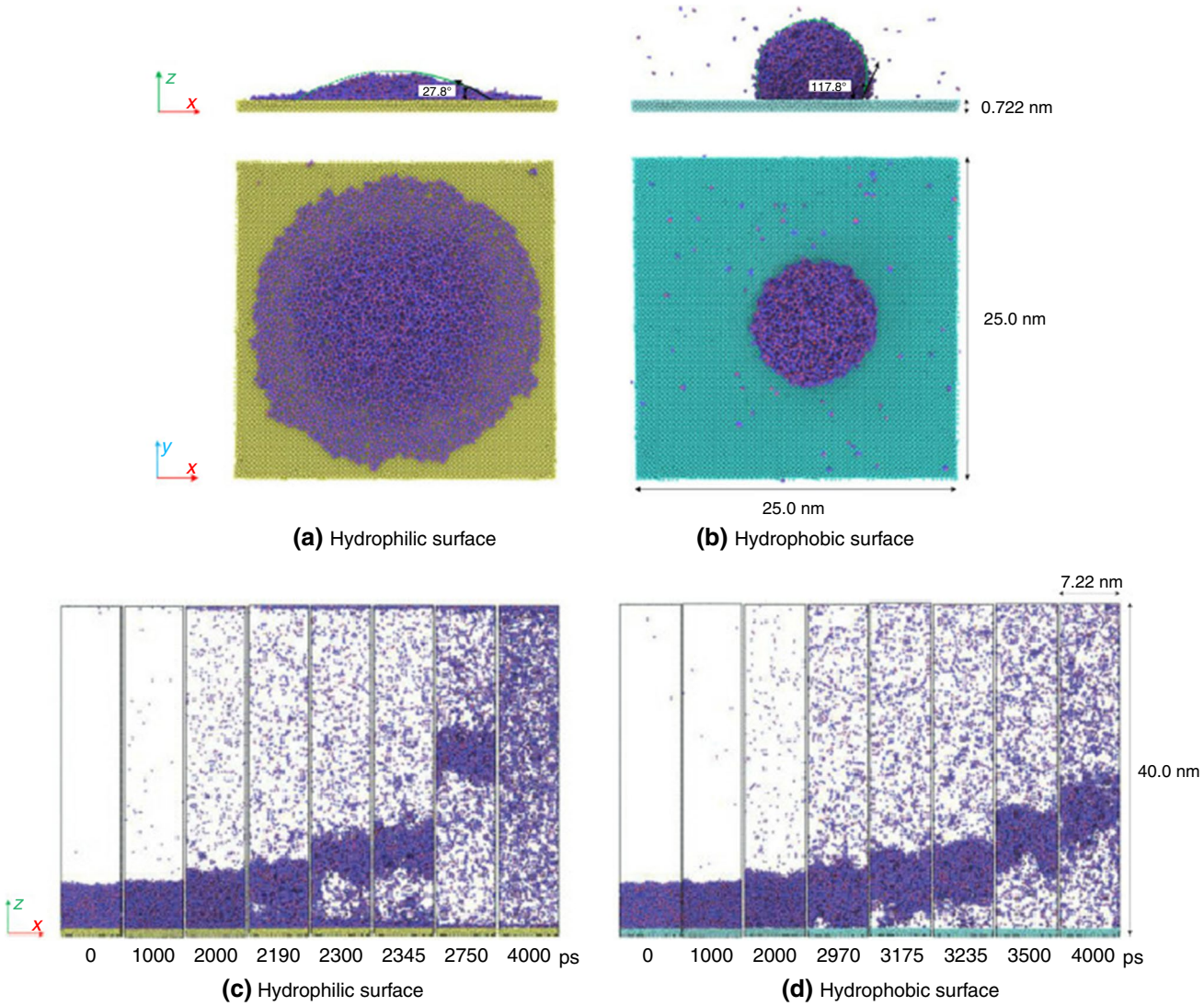

Fig. 12 Snapshots of equilibrium states for a water droplet and boiling behavior over hydrophilic and hydrophobic surfaces [210]

interaction ($\alpha = 1.5$) for achieving maximal nucleate boiling enhancement with minimum costs that are obtained in their study.

Structured Surfaces

Compared to the wettability defined surfaces, the structured surfaces could provide the additional heat transfer area that attached with the boiling fluid and the bubble dynamics also variation. The main structures of the simulation are micro-fin and micro-cavity with different sizes.

Lee et al. [214] have carried out the numerical investigation of various fin spacing and height effects on bubble dynamics and the heat transfer with LS method. The results demonstrated that due to the enhancing contact area between the bubble and fins, the heat transfer of modified surfaces has enhanced by about 40%–60%. The bubble departure diameter on the smooth surface also was introduced to represent the optimal fin spacing and height, which were 0.6D and 0.2D, respectively.

The modified VOF model, which introduced several novel schemes to make multi-scale surfaces in a tractable manner, was proposed by Yazdani et al. [215] to simulate the pool boiling heat transfer efficient on re-entrant surfaces. The heat transfer coefficient variation with the time evolution is shown in Fig. 13, which demonstrated the ability of model to respond to subtle changes in the surface.

Chen et al. [216] have studied the effects of nucleation sites on pool boiling heat transfer by 3D VOF model with energy jump phase change model. The nucleation at the pillar corner was found that the growth period was shorter

than the nucleation at the center between two pillars due to the asymmetric temperature distribution. Furthermore, they have carried out the numerical simulations to investigate the bubble dynamics and heat transfer mechanism of microlayer at the bubble base with different pillar heights [217]. The structured surface with the larger height has effectively enhanced the bubble departure parameters and evaporation of the microlayer, respectively. For eliminating the two-phase interface problem, the partition function and unstructured storage were combined to simulate the pool boiling by Cao et al. [218, 219]. In their VOSET model, the temperature at the interface could be obtained by introducing the cubic linear interpolation method. In addition to study the effect of micro-fin size on bubble dynamics, they also found that vortices generated near the three-phase contact line play an important role in bubble growth and boiling heat transfer.

LBM was widely performed to investigate the pillars surfaces as well due to the terseness advantage in deal with boundary conditions. Sun et al. [220] have combined the multiphase model and thermal model to investigate the triangular and the rectangular structure surfaces on boiling heat transfer. But the results were lack of the description on local variation heat flux under bubbles. Similarly research was studied by Chang et al. [221], which also considered the capillary number. The convective heat transfer capacity on structural surfaces was considered to affect the pool boiling heat transfer performance. Zhou et al. [222] have extended the double distribution functions method to study the pool boiling of micro-pillar surface with three-dimensional, in which the increasing height caused the decreasing heat flux which is contrary to the conclusion obtained by Chen et al. [217] using the VOF model. According to the results of Mondal and Bhattacharya [223], the large height was not conducive to the nucleation of bubbles at the pillar top. MRT method was used by Yu et al. [224] to devise a kind of new surfaces with two-level hierarchical structures. The heat transfer coefficient variation was proved that dependent on the bubble departure frequency and the dry spot area fraction, it was affected by the characteristics of secondary pillars. Wang and Liang [225] used a three-dimensional LBM method to study the bubble dynamics during boiling of upward layered columnar microstructures, and the results showed that the presence of upper layered columnar microcolumns enhanced the capillary wicking.

According to the molecular dynamics simulation, Wang et al. [226] have carried out the boiling nanobubble dynamics on nanopillar structured surfaces and a kind of nanoscale vertical convection was observed, which results in the delay of the vapor layer formation. Liu and Zhang [227] have proposed the variation between free energy and the roughness, and the numerical simulation has shown that the two sequentials exist before nanobubbles nucleation: Wenzel-to-Cassie transition and Cassie-to-nanobubble transition. The similar results were obtained by Zhang et al. [228], in which the high free energy was improved by the nucleation process

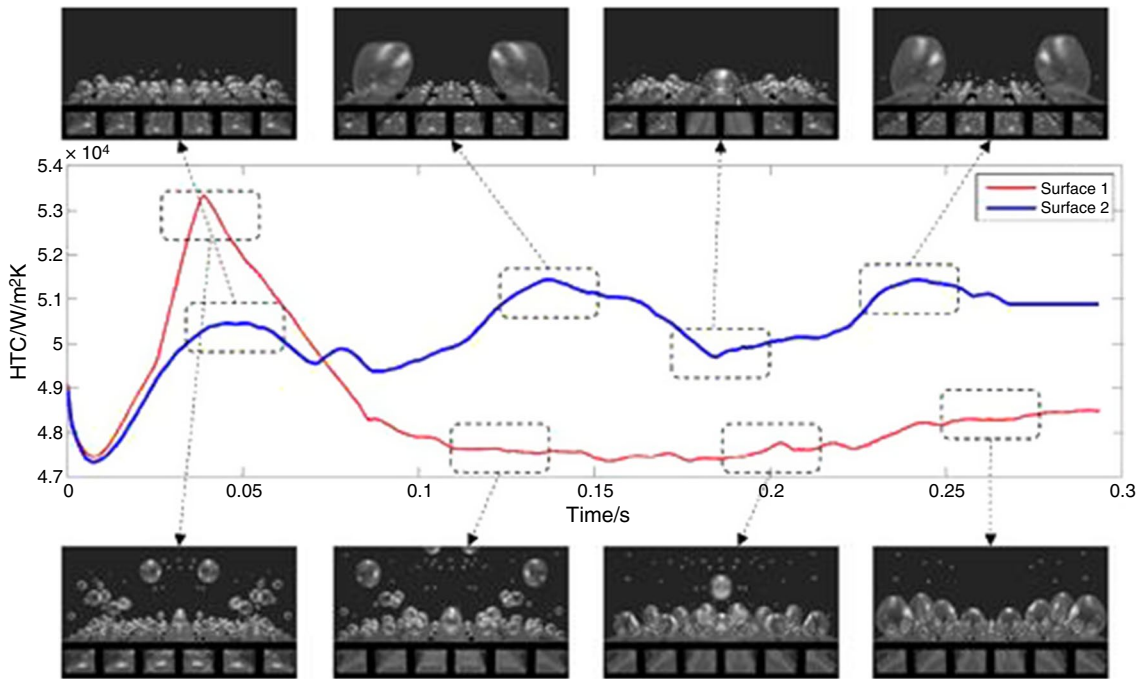

Fig. 13 Time evolution of heat transfer coefficient of pool boiling on enhanced surface 1 and enhanced surface 2 and the corresponding snapshots of pool boiling behavior [215]

whatever the cavity or pillar surfaces. Moreover, five different configurations of nanostructure surfaces were established to simulate the bubble nucleation by Chen et al. [229], and the results have shown that the higher nanostructure was beneficial for improving the bubble nucleation efficiency. Figure 14 shows the constructions of smooth and nanostructure surfaces. The heating region with red color in the middle of the surface, and the cooling regions with blue color on both sides of the surface. Ahmad et al. [230] have studied the nanoboiling of three different double-layer gradient porosity structures on copper surface by using molecular dynamics simulations, and they discussed the effect of porosity on the evaporation rate. In addition, they found that the bubble formation time was significantly reduced compared to the smooth surface.

In addition to micropillars, microcavities are performed to enhance pool boiling heat transfer performance as well. Lee et al. [231] have modified the LS method to investigate the effect of microcavity types. It was worth mentioned that the micro-layer model was simplified in their research. The truncated conical cavity was proved to be more effective for bubble formation. This model continued and used to study the boiling heat transfer enhancement on different microcavity size surfaces [232].

In 2011, Márkus and Házi [110] have investigated the bubble nucleation on the cavity and the heat conduction in the solid, which has also been taken into account. The bubble formation in the cavity was simulated well compared to the actual experiment. Furthermore, the LB model proposed by Márkus and Házi [233] was used in their subsequent literature. Different cavity configurations were established to investigate the bubble dynamics. They have found that the competition mechanism of bubble nucleation was existed between neighbor nucleation sites at low heat flux. It is obvious that the bubble in left cavity was gradually disappeared with the growth of bubble in right cavity as shown in Fig. 15.

The similar survey research was performed by Mu et al. [196] using 3D MRT LBM. Five different cavity shapes were applied to study the bubble dynamics and the heat transfer capacity. The power density on the heating surface was decreased due to bubble nucleation at the cavity, which after taking into account the solid thermal conjugate. However, in the treatment of conjugate heat transfer in the source term, they assume the heat capacities in the system to be equal, which may lead to inaccuracies in the calculation results. This issue can be solved by incorporating the temperature dependence of heat capacity in the source term of the LBM simulation, or by using more complex thermodynamic models that can account for the phase change and energy transfer between different components in the boiling pool. Soon after, the model of Gong and Cheng [106] was used by Zhou et al. [234] to investigate the bubble dynamics on four

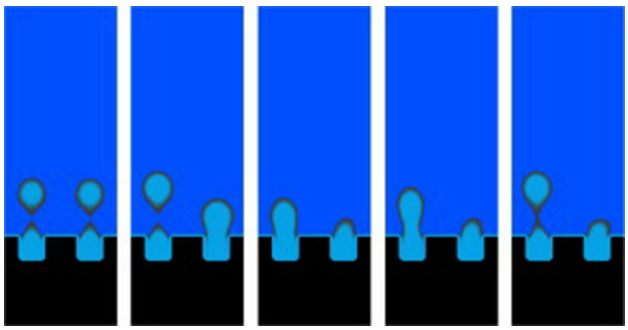

Fig. 15 Interaction of bubbles at low heat flux with 31 lattices spacing between cavities [233]

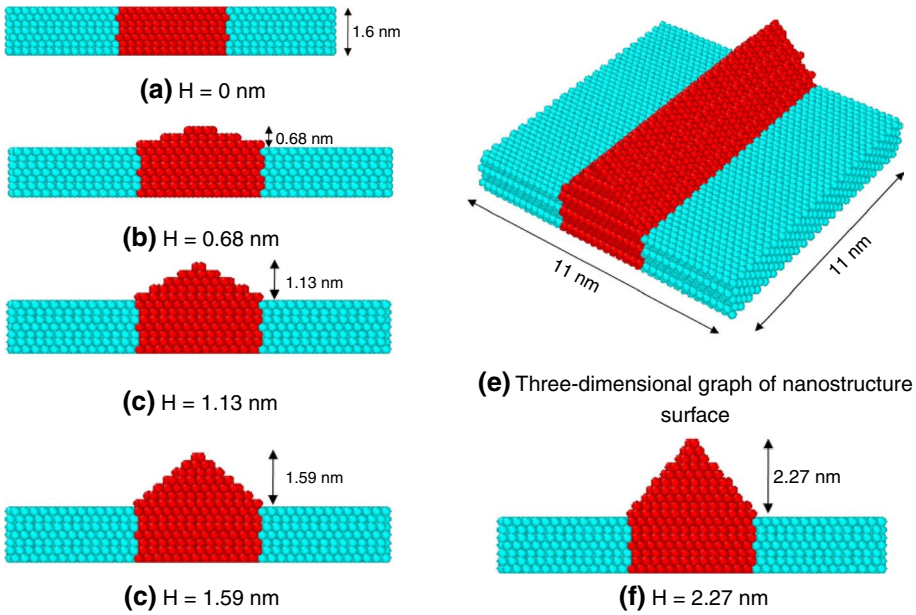

Fig. 14 Different configurations of nanostructure surfaces [229]

different cavities surfaces. The cavity opening radius was verified that mainly effected the onset of nucleation boiling temperature, which the heat transfer performance enhanced with decreasing the cavity opening radius.

According to the work of Novak et al. [235], the presence of nanoscale grooves can increase the nucleation rate, which is about two orders of magnitude higher than that of smooth surfaces at constant temperature. Then, the bubble growth rate as a function of different cavities parameters was studied by Mukherjee et al. [236] by using MD. The results that the heat transfer rate increases with the enhancing notch size, which were different from the obtained literature of Zhou et al. [234]. The different bubble dynamics mechanisms result in different boiling heat transfer mechanisms at different scales, resulting in the above phenomenon. Zhang et al. [237] constructed three different shapes of accessible cavities, and the nucleation time shortening results were the same as those of the predecessors. They also found that the higher the sealing degree of the accessible cavities, the shorter the nucleation time of bubbles and explained this phenomenon by using the energy accumulation effect. Then, this conclusion was also found by Zhou et al. [238]; their research results showed that reducing the groove size can not only promote nucleation, but also effectively reduce the degree of the onset of nucleate boiling.

Hybrid surfaces

The combination of microstructure and wettability are widely applied to enhance the heat transfer performance of pool boiling, but the influence of specific parameters on heat transfer efficiency is still worthy of in-depth study. Zhao et al. [239] have studied the pool boiling performance by using two-dimensional transient VOF model with Lee phased change model. Compared to the hydrophilic microstructures, the bubble volume growth rates of mixed hydrophilic and hydrophobic microstructures have shown the obviously enhancing. But it was worth noting that the evaporation of the microlayer was not taken into in model. With adding the microlayer evaporation model, Chen et al. [240] have proposed a conceptual microstructure surface with time-varying wettability model, which the bubble dynamics were changed. In their numerical results, a thin liquid films were generated between the bubble and micropillar due to the local curvature of bubble increasing that enhancing the heat transfer.

The numerical bubble dynamics on hybrid surfaces were carried out by Li et al. [241] with MRT LBM, and the enhancement mechanism was also explained. The bubble nucleation at the corner of pillars was verified that speed up the bubble departure due to the interaction with the top nucleation bubbles. Furthermore, the trends that increasing contact angle enhances the heat transfer performance also were revealed. Similar research was simulated by Ma et al. [242] with the introduction of the double distribution functions, where two contact angles were performed to combine with microstructures, 53° and 103°. The competition mechanism of bubble nucleation between the wettability effect and the wall temperature effect was proposed, and computation results have shown that the onset of nucleation boiling temperature will significantly decreased if contact angle was large enough. The orthogonal array tests were performed to study the hydrophilic region effect of 3D boiling heat transfer on hybrid surface by Yu et al. [243], and they found that the optimal contact angle of the hydrophilic region was conducive to bubble departure. Moreover, different from single microstructure used in research of Yu et al. [243] and the fixed microstructure numbers that involved in Ref. [241, 242], Feng et al. [244] have investigated the effects of pillars number on boiling heat transfer performance. The simulation results have shown that with the increasing number, the variation of boiling heat transfer performance increased firstly and decreased drastically due to the different bubble dynamics. In combination with experiments, Xu et al. [245] have found that when the contact angle was raised from 98.7° to 131.8°, the vapor film generated on heated surface that hindered liquid supplement. Bubble dynamics and normalized heat flux changes on microstructure and wetted mixed surfaces are discussed in Wang et al. [246], and they found that the bubble detachment frequency, detachment diameter and average heat flux are regulated by wettability, microcolumn spacing and main height.

With control of the energy parameter ε, the interaction force between solid and liquid molecular was regulated effectively. Introducing this method, the pool boiling heat transfer characteristics of the three hybrid surfaces were studied by Diaz and Guo [247]. The results shown that the surface with combination of argon-philic nano-pillar and argon-philic wall can improve the heat transfer performance best, which was in line with their subsequent research. It is worth pointing out that the literature [247, 248] does not provide a snapshot of the changing behavior of nanobubbles. The criterion was introduced to determine the number of liquid or vapor molecular number that based on the threshold coordination number. The improvement simulation was carried out by Chen et al. [249], and the bubble nucleation process was observed clearly. The different nanostructures that applied to pool boiling with same height and strong-hydrophilic region have shown the little impact on bubble nucleation, although showed the apparently improved compared with smooth surface. After then, Bai et al. [250] have proposed the temperature-dependent wettability hybrid surface that firstly the hydrophilic nanostructure surface with high interaction energy between solid and liquid molecules and then transfer to hydrophobic nanostructure surface

when absorbing enough energy which conductive to bubble nucleation.

Compared with the protruding structure, the cavity structure is considered to be beneficial to lower the onset of nucleation boiling temperature. Gong and Cheng [251] performed the previous model to investigate the effects of different contact angle surface with single cavity on bubble dynamics. In addition to the bubble departure dynamics, the variation of three-phase contact line on wettability mixed surfaces was also checked. Furthermore, the mutual inhibition between adjacent sites nucleation on rough was verified in their subsequent literature [252], which observed by Márkus and Házi [233] as well, and the effects of cavity parameters on this mechanism were also shown. The simulation results shown that the hydrophilic surface with hydrophobic cavity has the best boiling heat transfer performance. In order to estimate the thermal interaction between adjacent cavities, Zhang et al. [253] have introduced the temperature correlation coefficient that according to the nucleation sites and bubble departure diameter, which the strongest thermal action observed at $S/D_d = 0.65$. This method was then worked well in the similar research of Ahmad et al. [254].

She et al. [255] have analyzed difference of the repulsive forces, density gradients and potential energy between cavity with wettability and normal surfaces, while the repulsive force in strong-hydrophobic cavity is also investigated by Chen et al. [256]. More than that, the onset of nucleation obtained on different wettability was shown the great accordance with macro-experiments, which the mechanism was analyzed by the method that based on the relationship between atomic potential energy and atomic kinetic energy in their following simulation investigation [257]. Taken into account the pressure control, Shahmardi et al. [258] have studied the bubble dynamics and the heat transfer characteristic on surfaces with single cavity by using the open-source software GROMACS. In addition to the phenomenon that nanostructure determined the nucleation sites position as same as other researchers observed, the mechanism of which hydrophilic surfaces accelerate the nucleation was also proposed. The interaction of cavity width-to-depth ratio, wall superheat and surface wettability were considered to investigate the bubble dynamics and heat transfer performance during nucleate boiling by Lavino et al. [259], and the phase diagram was proposed as shown in Fig. 16. AR in Fig. 16 means the aspect ratio of the cavity width to height. Figure 16 reveals the effects of cavity parameters and wettability on bubble nucleation time and bubble interaction.

Table 1 shows the details of model parameters in molecular dynamics numerical of pool boiling. The atomic species of the solids and liquids used in the simulations are also given in Table 1, as well as the number of atoms in their corresponding densities. The purpose is to provide a basis for future computational studies using molecular dynamics.

In general, the lattice Boltzmann method shows outstanding advantages in studying the effect of surface modification on pool boiling using different simulation methods, especially in the bubble nucleation and bubble growth stages. Although the predecessors have proposed improved algorithms for calculating the temperature field, such as the fourth-order Runge–Kutta, how to ensure numerical stability under the condition of relatively large density is still a difficult point worth studying. Furthermore, the bubble nucleation simulation results of molecular dynamics and the bubble growth simulation results of macroscopic methods can be used to provide a mechanistic analysis of the bubble dynamics obtained by mesoscopic methods, especially after considering the surface modification, respectively. In turn, the simulation results of lattice Boltzmann can

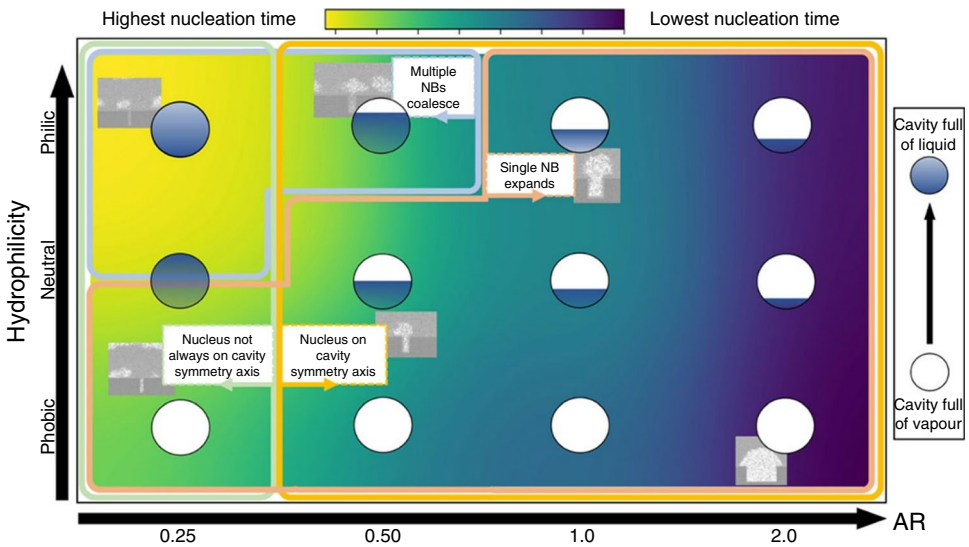

Fig. 16 Phase diagram summarizing the main results and the key mechanisms observed in the MD simulations carried out in this work [259]

Table 1 Summary of model parameters in molecular dynamics simulation

Year and Ref. No,	Solid particles and number	Liquid particles and number	Solid–liquid interaction parameters	Ensemble	Remarks
2006 [203]	Platinum, 2688	Argon, 1440,2000	$\alpha = 0.14, 0.5, 1,$ $\beta = 0.1,0.3,0.5,1,$ $\theta\ (^\circ) = 0, 95,150,180,$	NVT	The Young–Laplace equation claimed that inadequate to describe a nanobubble
2014 [208]	Platinum, 5600	Argon, 2187	$\varepsilon_{ll}/\ \varepsilon_{wl} = 2, \theta = 132^\circ$ $\varepsilon_{ll}/\ \varepsilon_{wl} = 1, \theta = 96^\circ$ $\varepsilon_{ll}/\ \varepsilon_{wl} = 0.2, \theta = 43^\circ$	NVT/NVE	Different wettability surface combination was considered
2019 [211]	Platinum, 8100	Argon, 49,692	$\alpha = 1.5$, hydrophilic, $\alpha = 0.4$, hydrophobic	NVE	The effects of patterned surfaces with different wettability were investigated
2016 [226]	Copper, 16,000	Oxygen, hydrogen, 16,000	–	NVT/NVE	Taken into account the subcooled and nanostructured
2020 [228]	Platinum, 14,400	Argon, 73,724	–	NVT	The onset of nucleation boiling on cavity surface, pillar surface and smooth surfaces were investigated
2016 [247]	Copper, 5296	Argon, 5324	$\varepsilon_{wl} = 0.0653$ eV, philic $\varepsilon_{wl} = 0.0327$ eV, phobic	NVE	Introducing different wettability nano-pillars
2021 [250]	Copper	Oxygen, 6570	$\alpha = 0.639$, $\varepsilon_{wl} = 0.0342$ eV, $\theta = 30.8^\circ$ $\alpha = 0.172$, $\varepsilon_{wl} = 0.0092$ eV, $\theta = 112.5^\circ$	NVT/NVE	A surface with smart wettability transition combined nanostructure has proposed to enhance heat transfer
2016 [255]	Platinum, 8970	Argon, 8886,9257,10,253	$\alpha = 0.14,0.5,1$, $\beta = 1$, hydrophilic, $\alpha = 0.14$, $\beta = 0.1,0.3,0.5$, hydrophobic	NVT	Effects of cavity on bubble nucleation was analyzed
2018 [256]	Platinum	Argon, 28,000	$\alpha = 1, \beta = 1$, hydrophilicity, $\alpha = 0.14, \beta = 0.5, 0.3, 0.1,$ Hydrophobicity	NVT/NVE	Considered the surface combined with Hydrophobicity cavity and hydrophilicity smooth region
2019 [312]	Cu, Pt, Si, Ni, 720 ~ 2185	Oxygen, hydrogen, 3192	–	NVT/NVE	880 Graphene atoms were arranged above the substrate and the CHF variation with thermal conductivity capacity was also investigated

be used to verify the heat transfer processes of the macroscopic approach, such as the typical three heat transfer sub-processes.

Effect of gravity

In space applications, the boiling heat transfer is the preferred choice for thermal management technique due to the space constraints. However, reducing gravity will significantly affect the bubble dynamics, thereby reducing boiling heat transfer performance and critical heat flux. Hence, the key drawback in pool boiling experiment under microgravity is difficult to set up accurate environment under the normal gravity of the earth, so simulation has provided an effective alternative tool.

Abarajith et al. [260] have carried out the numerical simulation and experimental validation of the bubble growth and departure of multiple merging bubbles under variable gravity conditions. The level-set method was performed to capture the phase change interface. The merger bubbles departure occurred earlier compared with the single bubble, which was explained by the additional lift off-force generated during merger process. The LS scheme conjunction with ghost fluid methods was introduced by Lee et al. [231]

to investigate the bubble performance under microgravity on different cavity surfaces. The immersed solid surface method was introduced to solve the solid–liquid contact surface problem, which avoids the complex processability of meshes when using solid walls. The truncated conical cavity is found to be more effective for bubble formation in nucleate boiling, which same as the results that obtained by nanoscale simulation in Ref. [237]. Moreover, a numerical method that coupling the LS function with the moving mesh method was employed to simulate the nucleate boiling, which subcooling was also considered by Wu and Dhir [261]. Two saddle points in the isotherms at high subcooling condition were observed, and the thermal layer turns thins down was explained by the condensed liquid along the interfaces flew downward. In their following reports, the effects of presence of a noncondensable gas was taken into account on nucleation embryo initial mass fraction, and the mass fraction was observed that decrease over time [262]. After a while, this model was performed to predict the bubble departure diameter and heat transfer performance, which the results show a remarkably good agreement with the experimental data [263]. The improvement of the above literature was studied by Aktinol et al. [264], which the fluid was Perfluoro-n-Hexane and the mass fraction of dissolved gas in the liquid was 25 times higher. The bubble shape and the heat flux comparison between numerical and experiment are shown in Fig. 17, and the peaks shown from the simulations coincide with the location of pinning of the liquid–vapor interface on the wall although there are obvious differences between the bubble shape in the two images on the right.

Urbano et al. [265] employed a combined LS and ghost-fluid approach to simulate the subcooled pool boiling of water under microgravity conditions. The ratio of the condensation Jacob number and the evaporation Jacob number was defined to evaluate the bubble dynamics. The equilibrium radius they proposed was found that was inversely proportional to the temperature gradient between the superheated wall and the subcooled bulk fluid. Except for the LS method, the phase field method also used to capture the vapor–liquid interface. The gravity level effects on bubble dynamics observed by Yi et al. [266] have a same tendency with the results simulated by other methods. But in their model, the microlayer evaporation underneath the growing bubble was neglected.

Ryu and Ko [267] presented a numerical study on the boiling heat transfer involving single nucleate site and

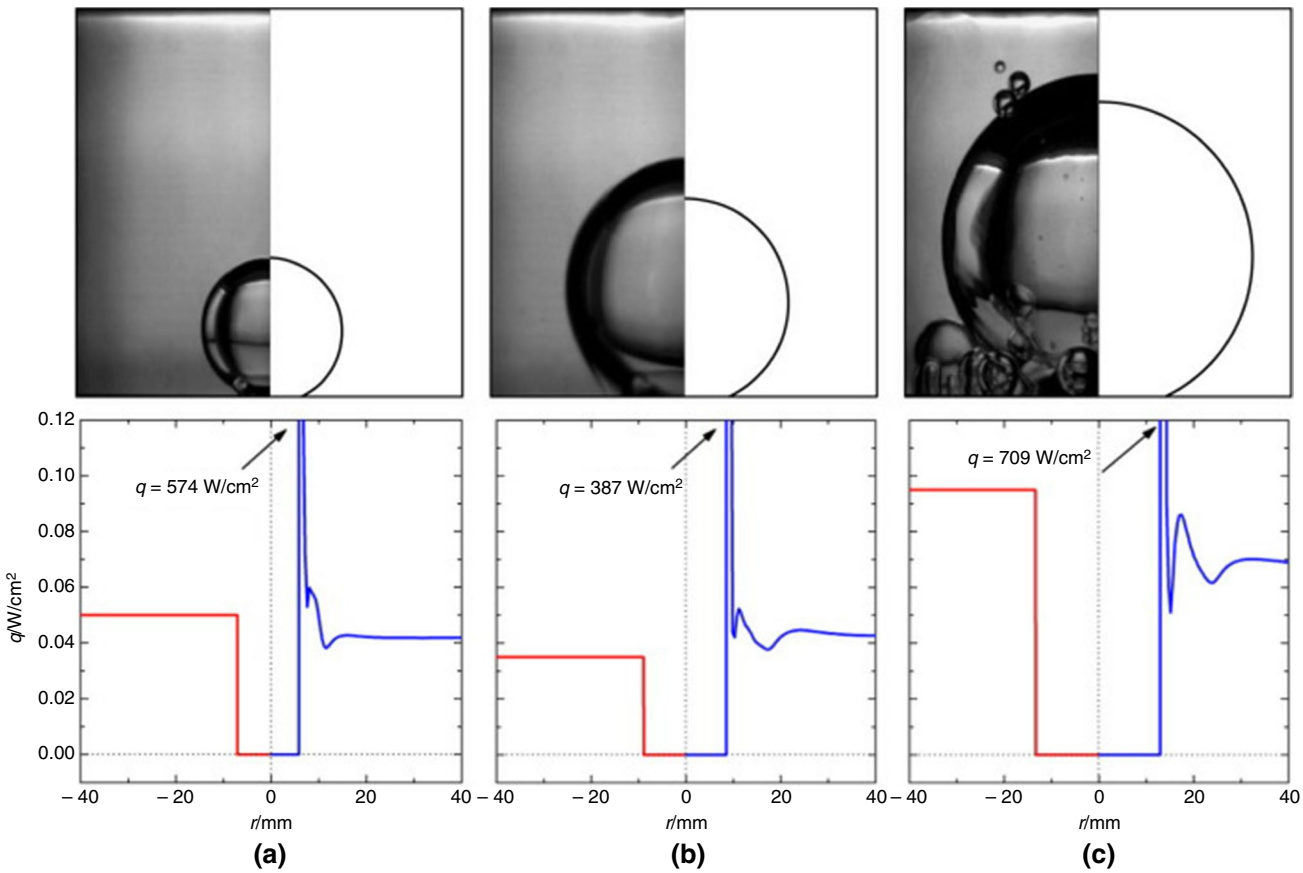

Fig. 17 Bubble shape and heat flux comparison between simulations and experiments [264]

multiple nucleate sites based on the free energy LB model, which a free parameter was introduced to control the thermal diffusivity coefficient. The bubble departure diameter is proportional to $g^{-0.5}$ that was obtained, and a power-law relationship between the Nusselt number and the number of nucleate sites was proposed as well. Sadeghi et al. [268] have extended the phase-field LBM model of Safari and Rahimian [160] from two to three dimensions to investigate pool boiling, which the Lee model was coupled to solve the density ratio issue [269]. They observed that bubble departure diameter increases with decreasing the gravity acceleration and the decrement is proportional to $g^{-0.354}$. BGK model and MRT model were performed by Guzella et al. [270] to investigate the bubble dynamics, which the traditional forcing scheme proposed by Guo et al. [271] was applied. The bubble dynamics at different gravitational accelerations were observed and the results shown that bubble departure diameters and period increase with the decreasing gravity. It is worth mentioning that the numerical results of bubble departure period predicted by the BGK model were smaller than the one obtained by the MRT model at $T_r = 0.76$ and the $g = 3.125 \times 10^{-5}$, which may due to the modified velocity that influence the kinematic viscosity, hence affecting the densities. Feng et al. [272] have modified the pseudopotential model to study the effects of gravity on bubble dynamics and heat transfer performance, which a new gravity scaling model was introduced to predict heat flux at different gravity acceleration. It is worth noting that when using LBM method to simulate pool boiling, the variation trend of bubble detachment frequency and diameter with gravity is often used to verify the accuracy of the model and shows good predictive ability. Therefore, this method is a very potential method to study boiling in space.

It makes sense that molecular dynamics simulations that take into account the effects of gravity do not appear in the existing literature. The effect of gravity is minimal where intermolecular forces dominate at the nanoscale, but this seems to be part of the future.

Nanofluids

Nanofluids can change the boiling heat transfer performance by changing the physical properties of the working fluid, while the results shown the different effects. Mohammadpourfard et al. [273] have coupled the mixture model with the multi mass transfer equations to simulate the heat transfer during nucleate boiling of a magnetic water nanofluid, which pointed out that due to the presence of Ferro-particle, additional forces are exerted on the bubble, which results in the elongate of the bubble in the direction of the magnetic lines of force and a shorter departure time at negative magnetic field gradients. Moreover, in their latest paper, in order to consider the effect of nanoparticle deposition, the variation of the liquid contact angle is considered in the specified correlation between the bubble departure diameter and the active nucleation site density, and the RPI model is improved based on the above relationship [274]. The mixture model was used to simulate the effects of TiO_2 nanofluid concentration on bubble dynamics and boiling heat transfer by Qi et al. [275]. They found that the diameter of bubbles in nanofluids is one-third of that in pure water, which is attributed to the weakening of surface tension in nanofluids, thus weakening boiling heat transfer. Niknam et al. [276] carried out the numerical investigation of nanofluid pool boiling at low concentration. The effect of nanoparticle size and surface roughness was checked and revealed that fixed or increasing of nucleation site is feasible. The pool boiling simulation study of Salehi and Hormozi [277] used the Euler model coupled with the k-ε turbulence model, and after the introduction of the heat flux partitioning (HFP) model, the prediction precision of boiling bubble parameters in the silicon water nanofluid were very high. This model was employed to investigate the pool boiling of Al_2O_3 nanofluids as well [278]. According to the response surface methodology, the least effective parameter that contributes to the boiling heat transfer was the bubble departure diameter. The HFP model was introduced by Kamel et al. [279] to simulate the pool boiling with Silica-Water either, while the results showed that the boiling heat coefficient of 0.01% nanofluid was worse than pure water. The new correlation for the correction of a bubble waiting time coefficient was proposed in their article. The numerical results of Emlin et al. [280] on the pool boiling of alumina nanofluids based on the Euler–Eulerian model showed that the HFP model can obtain good accuracy in predicting the heat flux curve and critical heat flux. On the basis of simulation research, Zaboli et al. [281] proposed numerical relational expressions for calculating heat transfer coefficient, bubble detachment diameter, and nucleation point density. The Ranz and Marshall relation is widely used for the interaction of different phase surfaces in nanofluid pool boiling, but additional assumptions and uncertainties are introduced in the modified version of this relation in order to solve the heat conduction problem of nanofluids, so it should be used with caution and its limitations in predicting the behavior of nanofluids should be carefully considered. The VOF method was performed by Gajghate et al. [282] to investigate the ZrO_2 nanofluids during nucleate boiling, which the concentration was 0.001% and 0.01%. The bubble departure velocity with 0.001% nanofluid concentration was observed faster than that with 0.01%. Majdi et al. [283] coupled the VOF method and the Euler method to study the pool boiling of microstructured surfaces in nanofluids, but the model needs to be further compared with experimental results to verify its correctness and rationality.

The pseudopotential multiphase lattice Boltzmann method was used to investigate the boiling heat performance of pure water and Al_2O_3 with 1% concentration by Rostamzadeh et al. [284]. The evaporation power of bubble growth was obtained by following equation:

$$p(t) = \rho_v h_{lv} \frac{dV}{dt} = m h_{lv} \tag{5-4}$$

The vaporization power calculated for nanofluids and water was compared and results shown that the bubble growth power in nanofluids is stronger than pure water.

Combined the solid–liquid LBM and the single component multiphase model, Wang and Cheng [285] have simulated the bubble coalescence in nanofluid with hydrophilic nanoparticles that contact angle range at 33°~51°. Not only the four interaction forces of nanoparticle were introduced, including the impinging force, momentum exchanging force, repulsion force, adhesion force, but also the rotational motion was considered. The results shown that the bubble coalescence period was prolonged and the bubble departure diameter in nanofluids is smaller than that in pure water. Figure 18 shows the velocity field of liquid film drainage before two bubbles coalescence. When moderately hydrophilic nanoparticles are adsorbed on the bubble interface, the drainage resistance of the liquid film is much greater than when no nanoparticles are adsorbed on the bubble interface which delayed the bubble merger.

Zhang et al. [286] have taken into consideration the non-condensable gas effects on single bubble dynamics in seawater boiling, which the modified P–R equation was applied in the multiphase multicomponent (MCMP) pseudopotential model to solve the phase-change process. Dou et al. [98] have reported the pool boiling heat transfer performance with the working medium was NaCl solutions by using MRT-LBM. The semi-empirical formula was used to adjust the NaCl solution surface tension parameter in the model. The results shown that the bubble departure diameter increasing with the NaCl concentration reinforce, while the departure frequency decreased.

Combined the NVT and NVE, Yin et al. [287] have investigated the nanofluids on boiling performance by using molecular dynamics method, although only one nanoparticle was arranged in liquid region. Nanoparticle enhancement effect was manifested that obviously at high superheat temperature surface and big nanoparticle.

The deposition of nanoparticles is gradually enhanced as boiling continues in a nanofluidic cell. In contrast to the assumption that nanofluids are single-phase solutions with specific physical properties, the molecular dynamics approach is a very promising method to provide mechanistic support for heat transfer by nanoparticles adjacent to the heated surface through analysis of local potential energy changes in the nanoscale range.

Thermal conjugate with solid

As we all know, pool boiling can effectively reduce the wall temperature. It is necessary to consider the coupling mechanism of a series of bubble behaviors and wall temperature changes for understanding the cooling mechanism. Kunkelmann and Stephan [288] have introduced the transient heat flux at the triple-phase line under the bubble by using VOF model. The results verified that the temperature at the triple point was the lowest due to the evaporation of the microlayer. In their model, the phase interface temperature is no longer assumed as the saturation temperature, but calculated by establishing a relationship between the evaporation mass flux and the saturation temperature. Two level-set functions were used by Zhang et al. [289] to capture the liquid–vapor–solid interfaces. The results shown that the thermal diffusivity of the solid walls significantly influences the bubble departure dynamics, which the bubble departure diameter increased with the thermal diffusivity decreasing while the bubble released period decreased. A

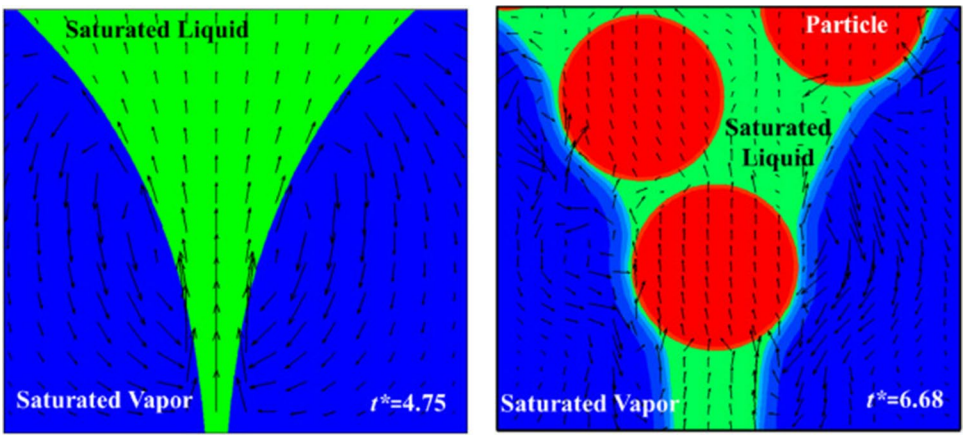

(a) Pool boiling of water **(b)** Pool boiling of a nanofluid

Fig. 18 Velocity fields of the liquid drainage flow between two bubbles in different working medium ($\theta = 47$ /°) [285]

simple isothermal boundary condition was deduced to solve the pool boiling with the high thermal conductivity thick substrate only by Huber et al. [173] using LS method. The simplified correlation on the dimensionless bubble departure variation with Jakob number was proposed.

Different from the single bubble investigated in Ref. [10, 288, 289], several bubble dynamics on a major plate was simulated by Pezo and Stevanovic [290], which the two-phase mixture model was performed. The relationship between nucleation sites density with the critical heat flux was proposed to predict the boiling crisis, which the vapor void fraction at different height was also compared as shown in Fig. 19. It is worth pointing out that due to the chaotic feature of the two-phase flow, the simulated results of the void fraction are smaller than the experimental results near the wall. This model was performed by Petrovic and Stevanovic [291] to simulate the transient boiling heat transfer as well. In the subsequent study, they considered a partitioned heat transfer model and they replaced the conventional model based on the average wall temperature with the temperature difference between the nucleated and non-nucleated regions. The rewetting heat flux also considered in simulation of Giustini et al. [292]. But the model that established has an obviously heat flux predicted deviation at the three-phase contact line compared with experimental, which caused by different evaporation rates.

Gong and Cheng [188] have shown the dimensionless temperature field of pool boiling on mixed wettability surface, and the dimensionless local heat flux on the surface was shown as well. The lowest temperature and the highest local heat flux indicated that the phase change process was taking place as shown in Fig. 20. The thermal response was performed in their subsequent literatures [189, 251, 252, 293], and the publication based on their model [194, 234, 242, 294]. Compared with the BGK model used in Gong and Cheng model, the MRT collision operator has been proved to be shown the better performance in pool boiling simulation. The MRT method can provide better accuracy than the BGK method by allowing independent control of

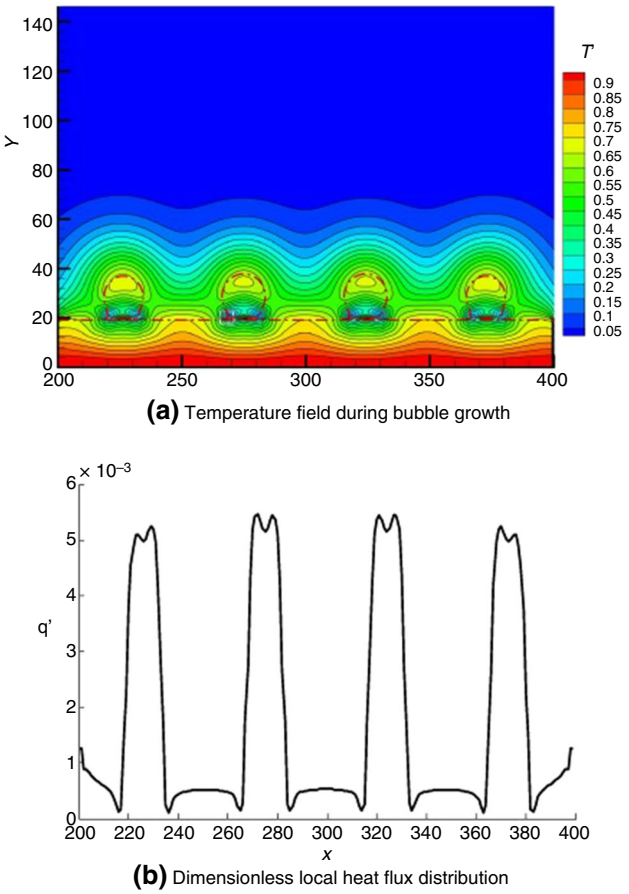

Fig. 20 Temperature field and dimensionless local heat flux on surface #1 [188]

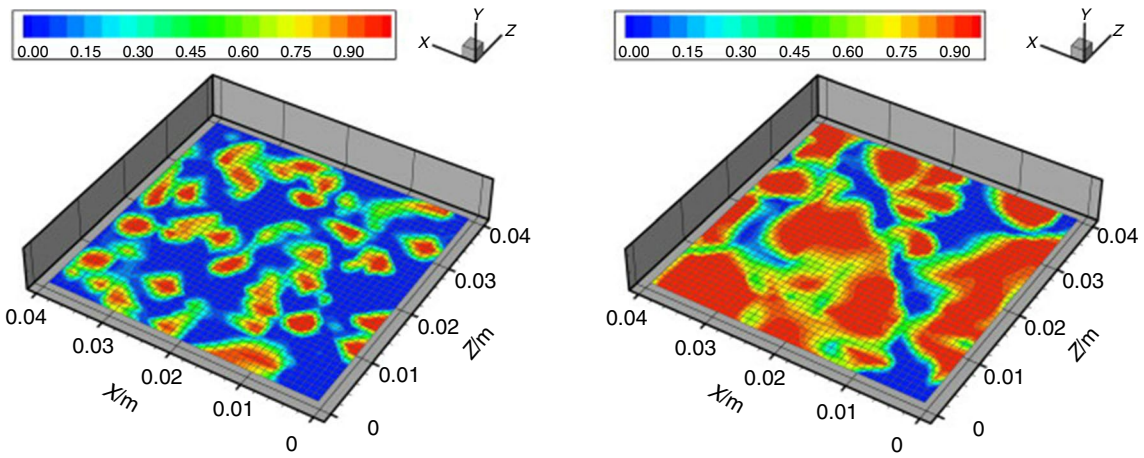

Fig. 19 Void fraction at the superheat surface at 200 /kW·m^{-2} (left) and 1000 /kW·m^{-2}(right) [290]

relaxation times for different moments of the distribution function, which can lead to improved resolution of complex flow features. The improved hybrid LBM, which introduced the infinite volume discrete to deal with the diffusion term in the energy equation, was performed by Hu and Liu [295] to investigate the different cavity characteristic surface effects on the surface thermal responses. Moreover, multi-bubbles growth, departure and coalescence were analyzed by Zhao et al. [296], which the solid–fluid interface conjugate heat transfer was dealt with the finite volume method scheme proposed by Hu and Liu [295].

The introduction of the coupled solid-flow-vapor thermal response method in the pool boiling simulation process can help to further understand the heat transfer mechanism at the three-phase point. In particular, the heat transfer mechanism of the modified surface, including wettability and microstructure, is difficult to obtain in experiments. The method provides a new idea to study pool boiling, especially from the perspective of lattice spacing and critical temperature.

Other factors

This section introduces the establishment of the pool boiling model and the research results under the conditions of external pressure field and electric field. The effect of surface orientation and substrate material on bubble behavior is also discussed.

The modified color function was performed to capture the interface by Murallidharan et al. [297], and the modified CSF model was used to investigate the bubble growth during nucleate boiling at high-pressure conditions. And the correlation proposed showed the good agree with the experiment at 44.7-bar by Sakashita [298]. Sielaff et al. [299] simulated the bubble coalescence using the VOF scheme in the CFD software OpenFOAM in 3D domain, which the Hardt and Wondra [300] phase change model was used. The results showed that the optimal bubble merger rate appeared at the given pressure once the spacing between nucleation sites determined. Same as the phase change model used in the literature [239], the Lee model was also introduced into the model by Ren and Zhou [301] to analyze the pool boiling heat transfer characteristics, and the results showed that the heat transfer on horizontal surfaces is more sensitive in the subatmosphere compared to vertical pipes.

In addition to system pressure, an external electric field is also often used to study boiling heat transfer. Hristov et al. [302] simulated the growth and departure of a single bubble during nucleate boiling under the uniform electric field by using LS method with software MATLAB and COMSOL. The bubble departure shape was observed elongated under the 5 MV/m electric field intensity. Moreover, a two-dimensional hybrid LB model was developed by Feng et al. [303] to simulate bubble dynamics under the uniform electric field. The same bubble dynamic that bubble elongated was observed as well as shown in Fig. 21. The un-uniform electric field was introduced to simulate gravity effects on the bubble dynamics in their subsequent numerical study with previous LB model [304]. The numerical results shown that decreasing gravitational acceleration could enhance the effects of electric field on bubble dynamics, which the bubble departure diameter and frequency decrease with the stronger electric field. Yao et al. [305] coupled the pseudopotential MRT and the leaky dielectric assumption to analyze the bubble dynamics under different electric field distributions, but lacked the analysis of the impact on heat transfer. Then, Li et al. [306] have investigated the pool boiling with microcolumn structure under the action of electric field, and the results showed that the existence of electric field force will hinder the fluid replenishment in the channel, but it can also prevent the merging of column top bubbles and channel bubbles. In addition, the local normalized heat flux distribution on the micropillar surface is also discussed and analyzed in detail.

The effect of surface orientation is often considered in the study of nuclear pool boiling, especially when it changes the contact angle between bubbles and the surface. The lubrication theory applied to the nucleate boiling at inclined heated surface was introduced by Tondro et al. [307], and heat transfer under the bubble was investigated. In their following research, the bubble departure diameter was analyzed under different inclined surfaces by using modified Lay and Dhir model [308]. The bubble exhibited the largest bubble detachment diameter on the surface with an inclination angle of 30°; hence, the heat transfer rate was also the largest. However, the bubble dynamics in their article may need further experimental verification, as the bubbles should not remain perpendicular to the platform under the effect of buoyancy at larger inclination conditions. Sun et al. [309] performed the phase-field LBM to simulate the bubble dynamics on vertical surface. The interface capture was modeled by the convective Cahn–Hilliard equation, while the phase change was accomplished by the C–H equation obtained by adding an extension of the source term in a non-isothermal system as proposed by Dong et al. [158]. A series of multi bubbles growth, departure and coalescence were observed, and the heat transfer mechanisms were analyzed. The LB model with large density ratio proposed by Zheng et al. [159] was applied by Dong et al. [310] to simulate the effects of surface orientation on nucleate pool boiling, besides the microcavities. The results obtained in their numerical shown the larger angle was conducive to bubble departure, the bubble would split into multiple bubbles once the departure bubble is unable to maintain the circle shape that also observed.

Some scholars have also studied the properties and arrangement of pool boiling substrates. Chen et al. [311] used the modified VOF model to study the influence of thermal conductivity

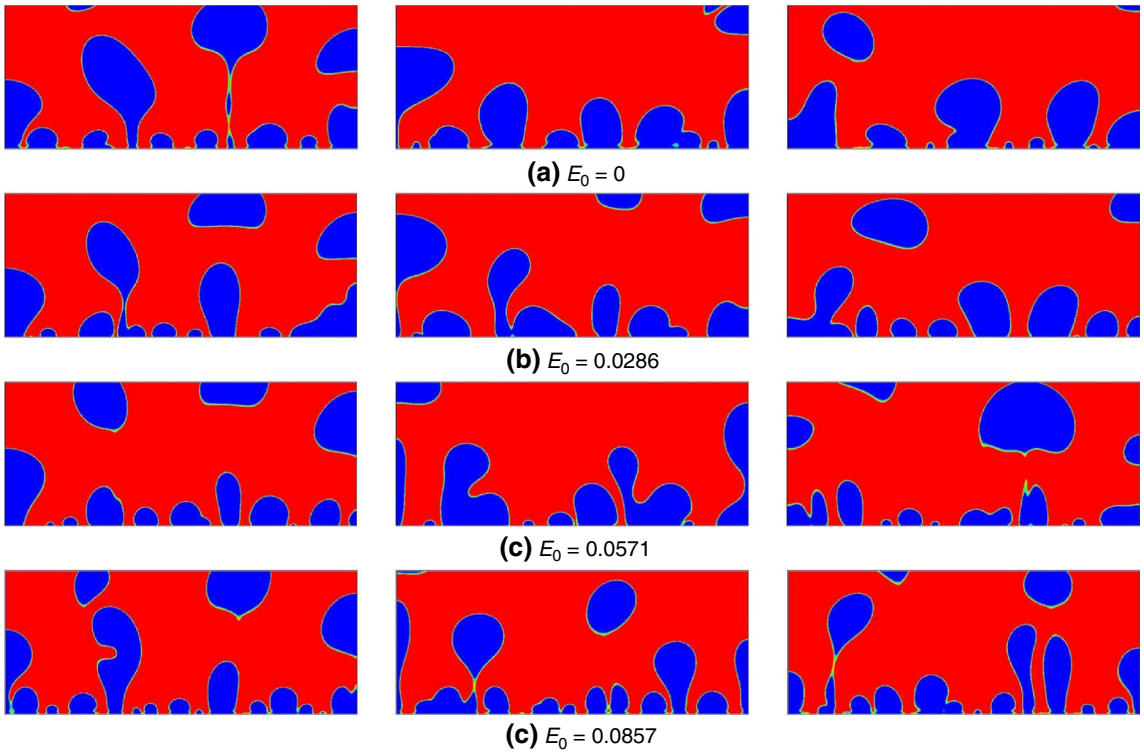

Fig. 21 The snapshots of bubble dynamics under electric field at $T_w = 0.13$ [303]

of heat transfer plates on the microlayer evaporation, including copper, brass, stainless steel, glass. The results shown that the evaporation rate increases with the larger thermal conductivity. Moreover, the molecular dynamics was employed by Diaz and Guo [312] to investigate the boiling heat transfer on the planes of Cu, Ni, Pt and Si with single-layer graphene. Based on the numerical results on LBM, Sattari et al. [313] concluded the heater extended has more effect than increasing heat flux on bubble departure diameter. Shan et al. [314] have focused on the bubble behavior on two separate heated plates. The bubbles on the surfaces at different spacing plates shown a total of four detachment behaviors, which the pattern of bubble merging shown the large heat flux and departure frequency.

Up to now, there are still few simulation studies on the above-mentioned influencing factors, and the establishment of the model still involves more assumptions. Furthermore, more experiments are needed to verify the simulation results.

Boiling curve and CHF

In the past decade, the numerous simulations focusing on prediction of nucleate boiling heat flux were carried out along with the state-of-the-art computational methods and technique appeared. Abarajith [33] have carried out the simulation of pool boiling performance on surface with different cylindrical cavities. The heat flux, which obtained by interpolating method, as a function of wall superheat was compared with the data from experiments, in which the active cavities number and the locations were used as an input in simulations. Besides that, the boiling curve at reduced gravity was compared as well and shown the agreement with data in experiment.

Wei et al. [315] have focused on the mushroom vapor region nucleate boiling, and the Marangoni convection in the microlayer region was considered. The heat flux prediction value was compared with the existing data and shown the good consistent. The macrolayer model was considered in numerical of He et al. [74] as well, and the

boiling curves shown the great consistent with the data of Gaetner et al. [316], while the large deviation existed in the low heat flux region. Besides, the CHF was favorably consistent with the value calculated by equation of Katto and Yokoyo [317]. The coupled map lattice methods were proposed to simulate pool boiling with nanofluids and water [318, 319]. The variation trend of the boiling curves caused by the nanofluid concentration change was similar to the experiment, but there is an obviously different with the experimental data at high heat flux that the deviation approximately to 50%.

Using level-set interface capture method, Son and Dhir [320] successfully simulated the bubble dynamics at high surface temperature. The heat flux obtained from the present 2D analyzed was within 25% error with that predicted from correlation of Stephan and Abdelsalam [321]. Besides that, the average heat flux obtained from 2D computation with higher quality grid and 3D computations with coarser grid was compared as shown in Fig. 22 while the large error verified the importance of grid quality in simulation. Furthermore, Grag and Dhir [322] obtained the complete pool boiling curve with the LS method, while the film boiling curve shown the larger error compared with the results of Berenson [323].

Wang et al. [324] presented a numerical study that introduced evaporation–condensation model on the pool boiling associated with modified heated surfaces with hemispheres in different orientations. Although the boiling curve shown a great consistent with the data of Nukiyama et al. [4] when heat flux $q < 60 W/cm^2$, the prediction of CHF was not satisfactory. The surface with the downward facing hemispheres has the lowest CHF, which has the best heat transfer coefficient. The numerical simulation was performed to investigate the pool boiling of liquid nitrogen and the boiling curve simulated results showed a large error compared with the experiment in nucleate boiling region, although the curve shape was similar [325], which may be due to the deviation

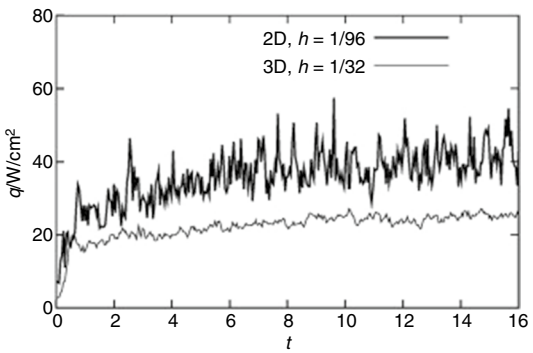

Fig. 22 Wall heat fluxes obtained from two- and three-dimensional computations [320]

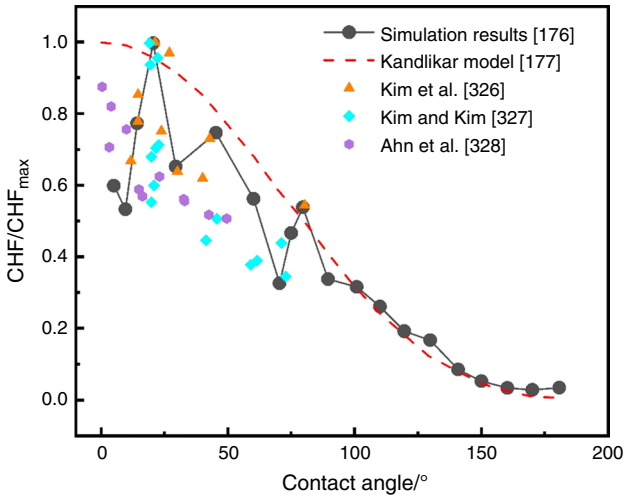

Fig. 23 Critical heat flux normalized by the corresponding maximum value of CHF in simulation, model, and experimental data [176]

in wall heat transfer caused by the multicomponent liquid rewetting mechanism not considered in the model.

Modified VOF model was applied to simulate the pool boiling with different contact angles, and the various boiling curves are obtained in Ref. [176]. The normalized CHF data were also plotted to enable compared with another models and experiments [177, 326–328] as shown in Fig. 23. Except for a few points, the overall trend is good consistent with the experimental or model results. The hybrid wettability surfaces were investigated in their subsequent literature as well [179].

The effect of pressure on boiling curve was investigated by introduced Lee model, and the numerical results showed the well consistent with the experiment data at 1 kPa and 2 kPa [301, 329].

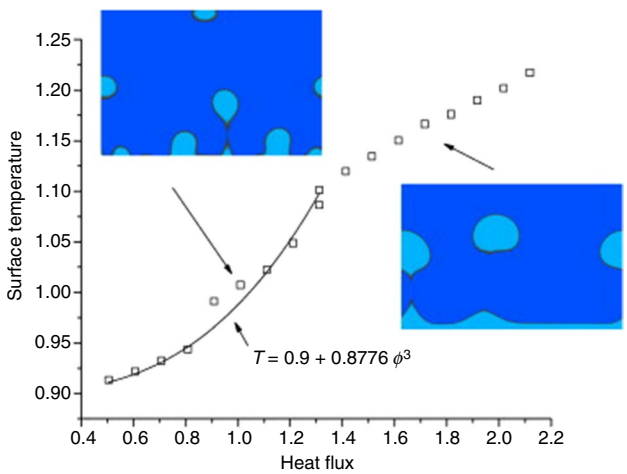

Fig. 24 Variation of the surface temperature with the heat flux [330]

Márkus and Házi [330] firstly carried out the LBM simulation to form the pool boiling curve that controlled the surface heat flux as shown in Fig. 24. It was obvious that the typical transition region does not appear in their curve, which suffers from the spurious term caused by the forcing-term effect and error term proportional. A few years later, the complete pool boiling curve, including the transition process, was successfully simulated using pseudopotential LBM by Gong and Cheng [189] as shown in Fig. 25. The variation trend of critical heat flux on different wettability surfaces is also in line with the results of macroscopic experiments, that is, the hydrophobic surface is smaller than the hydrophilic surface. The only regret is the lack of trend curves for conventional wettability surfaces for comparison ($\theta = 75$–$85°$).

Table 2 lists the primary contents related to the LBM models, equation of state, parameters and the details of boiling curves simulated by LBM.

In addition to the research content in Table 1, some scholars have also used the LBM method to obtain the boiling curves of microstructure surfaces [104, 221, 223], wettability surfaces [190, 193, 195, 199, 200], and the hybrid surfaces [241–244]. It was worth mentioning that different heating models in LB computation were performed to control the surface temperature verifying the diversity of curve trend in transition region [195]. The similar result was confirmed by Ma and Cheng [331], while the different trends appeared except in nucleate boiling. The boiling heat transfer curves for the two heating modes are shown in Fig. 26. In addition, the critical heat flux, the minimum heat flux, and the theoretical predictions for the film boiling stage are also given in the figure [15, 323]. A detailed explanation of the theoretical model can be found in reference [331]. When the heating method of controlling the wall temperature is adopted, the variation trend of the boiling curve is very similar to the experimental results, especially in the convective heat transfer area and the film boiling area. The transition from the convective region to nucleate boiling has never occurred in the previous literature. In addition, the heat flux in the film boiling stage is also in excellent agreement with the theoretical value [323]. The only shortcoming is that the critical heat flux is significantly lower than theoretical value. There is no significant difference between the boiling heat transfer curve obtained by controlling the heat flow and that obtained by controlling the wall temperature in the nucleate boiling stage. But when the heat flux exceeds the CHF point, the wall temperature rises sharply, and then, the heat flux increases. This conclusion has also been found by other scholars [293, 332]. This conclusion provides an important basis for future scholars to use mesoscopic methods to study pool boiling.

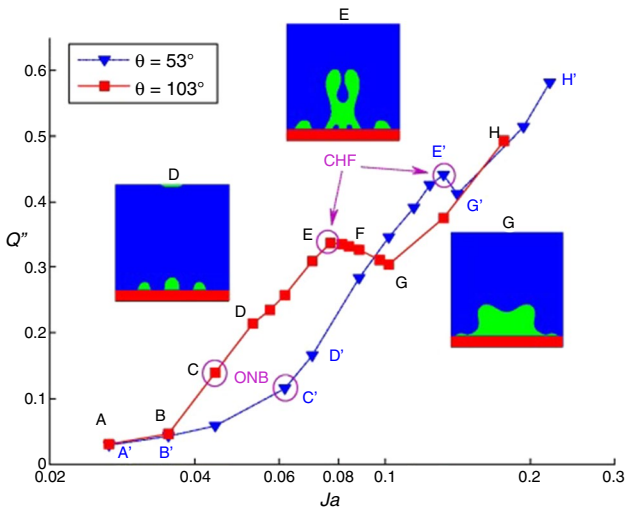

Fig. 25 Boiling curves on hydrophilic heating surface (53°) and hydrophobic heating surface (103°) under constant wall temperature [189]

According to the numerical results of Feng et al. [303], the increasing electric field intensity has enhancing the boiling heat flux as shown in Fig. 27, in which E_0 means the characteristic electric field intensity. As shown in Fig. 27, the effect of the electric field has weak effect on the heat transfer performance at the initial stage of nucleate boiling. But with the increase of the electric field intensity, the heat flux in the stage after nucleate boiling, CHF and film boiling also increased.

In conclusion, the macro-scale simulation methods that introduce the micro-liquid layer model and phase distribution theory, including LS and VOF, still have great potential in predicting the heat flux, although the current research content is still relatively sparse. However, the establishment of the model requires a lot of assumptions and simplicity, and the nucleation sites need to be set in the early stage of the simulation. In addition, the stability of mass transfer and the continuity of the interface increase the modeling difficulty of this method. Therefore, this method still needs continuous development to improve the reliability of use. The lattice Boltzmann method, as a new simulation method, can obtain certain boiling curve trend at the present stage, which is mainly reflected in the accurate prediction of film boiling, but the prediction of nucleation boiling and onset of nucleation boiling temperature still need to be further verified by comparison of experimental results. Scale-limited molecular dynamics simulations have not yet achieved effective research progress in this field.

Challenges and future directions

The published studies about three-dimensional pool boiling simulation in the past two decades are shown in Fig. 28. It is clear that the literatures using the LBM method in the past

Table 2 Summary on the application of LBM to the study of boiling curves

Ref. No.	Density model	Thermal model	Parameters	Equation of state	Heat flux Remarks
[199]	Multi-relaxation-time (MRT)	Finite-difference method	2D, Wettability (44.5°,50°,55.5°)	Peng–Robinson (P–R), $T=0.86\ T_c$	Obviously heat flux decreasing at the transition boiling region was existed but no film boiling region
[189]	BGK	Thermal LBM	2D, wettability (53°,103°)	Peng–Robinson (P–R), $T=0.9\ T_c$	Complete boiling curves and CHF at the wettability surfaces were compared
[194]	BGK	Thermal LBM	2D, wettability	Peng–Robinson (P–R), $T=0.85\ T_c$	Half-implicit scheme was introduced. No obviously heat flux decreasing at the transition boiling region
[195]	MRT	Thermal LBM	2D, Wettability (52.9°,62.8°,73.5°)	Peng–Robinson (P–R), $T=0.53\ T_c$	With the density ratio of 4560.28 and considered the cavity shapes
[196]	BGK	Thermal LBM	3D, Wettability (56°,85°,107°)	Peng–Robinson (P–R), $T=0.9\ T_c$	The CHF of surface with contact angle 85° was consistent well with the prediction of model of Kandlikar et al.[176]
[199]	Multi-relaxation-time (MRT)	Finite-difference method	2D, Wettability (44.5°,50°,55.5°)	Peng–Robinson (P–R), $T=0.86\ T_c$	Obviously heat flux decreasing at the transition boiling region was existed but no film boiling region
[244]	MRT	Thermal LBM	2D, Wettability combined with micro structure	Peng–Robinson (P–R), $T=0.9\ T_c$	The influence of pillar number was taken into considered
[302]	MRT	Finite-difference method	2D, Electric field	Peng–Robinson (P–R), $T=0.86\ T_c$	The boiling curves variation trends with the change electric filed were simulated
[329]	Bhatnagar–Gross–Krook (BGK)	Thermal LBM	2D, Cavity	Van der Waals, $T=0.9T_c$	No Transition region in boiling curve

five years are almost the same as the classical macro-method, which is obviously less than macroscopic scale method before 2011 years. The mesoscopic LBM clearly account for a large increasing rate, of which the published literatures after 2011 has the same as the classical methods, while there are relatively few researches using molecular dynamics methods, especially for the period that before 2017 years, which can be attributed to the dimensional limitation and the power of computer. Figure 29 shows the number of literatures on different influencing factors of pool boiling by different computational methods. It is obvious from the figure that the macroscopic and the mesoscopic numerical methods have adequate capacity to simulate the pool boiling with various effect factors, while the macroscopic scale focuses more on the working medium and the mesoscopic scale focuses on different surface modification. The molecular dynamics approach shows obvious limitations, which has the huge potential in boiling mechanism explore, which need further consideration and improvement. Figure 30 shows the main content in this paper. Overall, different simulation methods have shown great abilities to explore and investigate the pool boiling, but the author believes that further theoretical analysis and experimental verification are needed to propose a more accurate prediction model to explain pool boiling phenomenon and heat transfer enhanced mechanism in the future. After a careful analysis, we could identify the following problematic points for numerical methods.

(1) Most of the papers on the macroscopic pool boiling simulation model have studied the nucleation of bubbles, but it is difficult to determine the physical cause of nucleation through simulation due to the existence of a prior conditions, such as the advance placement of small bubble species and the presetting of wall

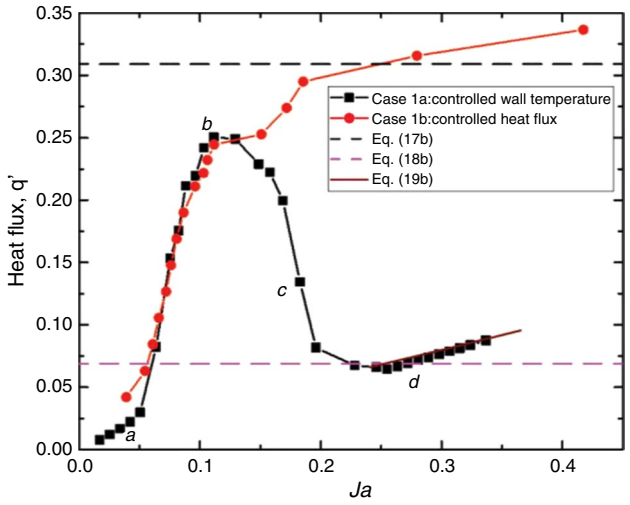

Fig. 26 Effects of heating modes on pool boiling curves for infinite smooth heaters [331]

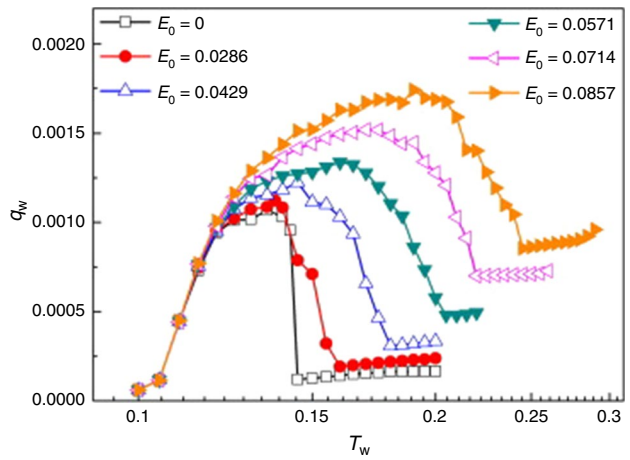

Fig. 27 Boiling curves under different electric field [303]

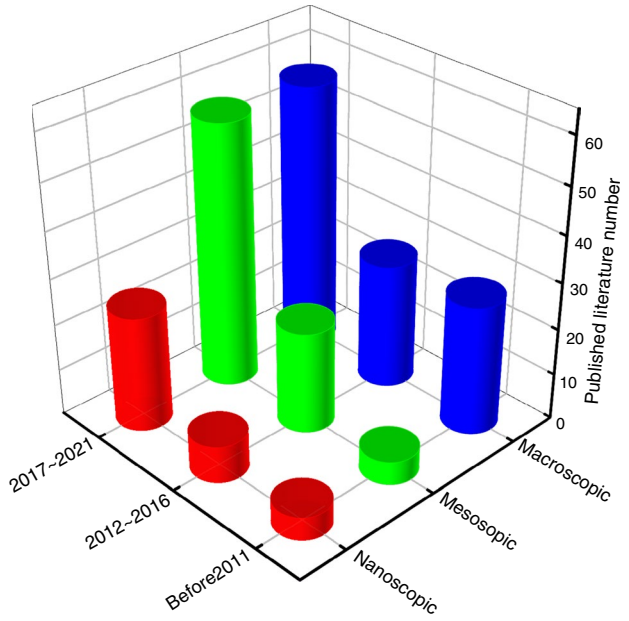

Fig. 28 Comparison of the published literature numbers on the simulation of pool boiling by different methods in the last two decades

temperature. Besides, the micro-layer model also has obvious defects. The existing simplified models that rely on external parameters are all empirically based axisymmetric models. This also hampers the development of macroscopic methods for investigating surface modification and boiling curves.

(2) The turbulent flow effect is rarely considered in the published literature. In the nucleate boiling stage, the detachment of the bubbles will cause the violent fluctuations of the boiling working medium, that is, induce turbulence. The large eddy turbulence model has been introduced in some literatures, and although certain conclusions have been obtained, since this mechanism has not been resolved in experiments, it is worth further discussion whether it is reasonable to apply this model.

(3) When coupling a multiphase LBM model and a thermal LBM model, the error terms in the recovery of the macroscopic equations deserve attention. In addition, the invariance of mechanical stability conditions needs to be ensured when using the pseudopotential LB model to simulate boiling, which affects the applicable range of the coexistence density of the pseudopotential LB model. In the case of the phase field LBM using the evolution of the C–H equation to describe the gas–liquid interface, interface nonphysical oscillations or deformations may arise due to the nonzero thickness of the interface. In addition, the absence of Galilean invariance may affect the heat and mass transfer near the interface. The effective solution of these problems is also a challenging issue for future research.

(4) An important problem in the simulation of molecular dynamics method is that the determination of the potential function is difficult to construct the atomic potential between single molecules between different fluids, which increases the difficulty of establishing the boiling model. Furthermore, how to effectively capture and analyze the energy and heat transfer changes near the gas–liquid phase interface under finite time and length-scale conditions is also a major modeling challenge in this approach.

(5) In order to properly model the variation of properties with temperature during pool boiling, it is necessary to couple a database containing fluid or solid properties (e.g. density, viscosity, thermal conductivity, specific heat, etc.) to the process, which can also be addressed

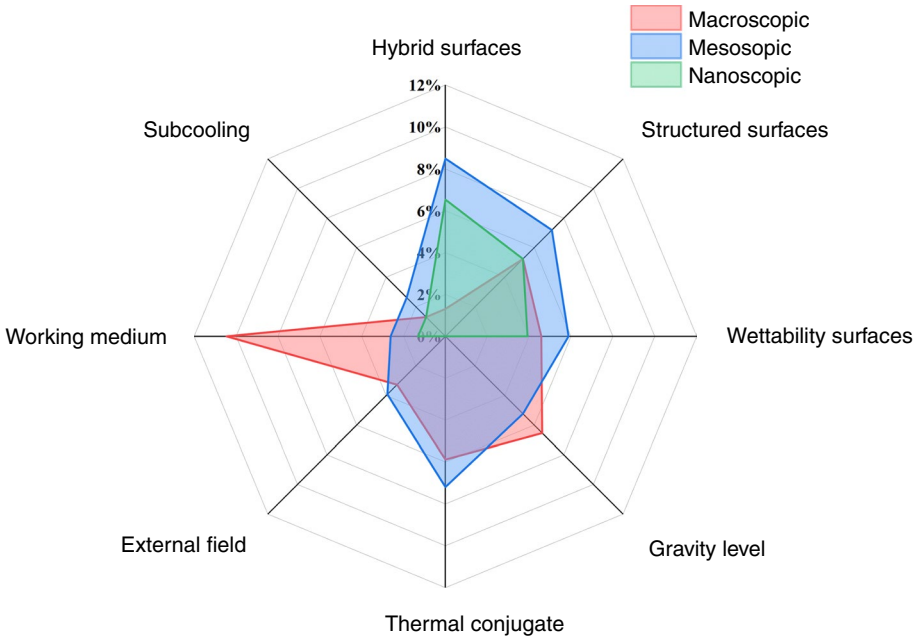

Fig. 29 The proportion of literatures on different influencing factors of pool boiling by different computational methods

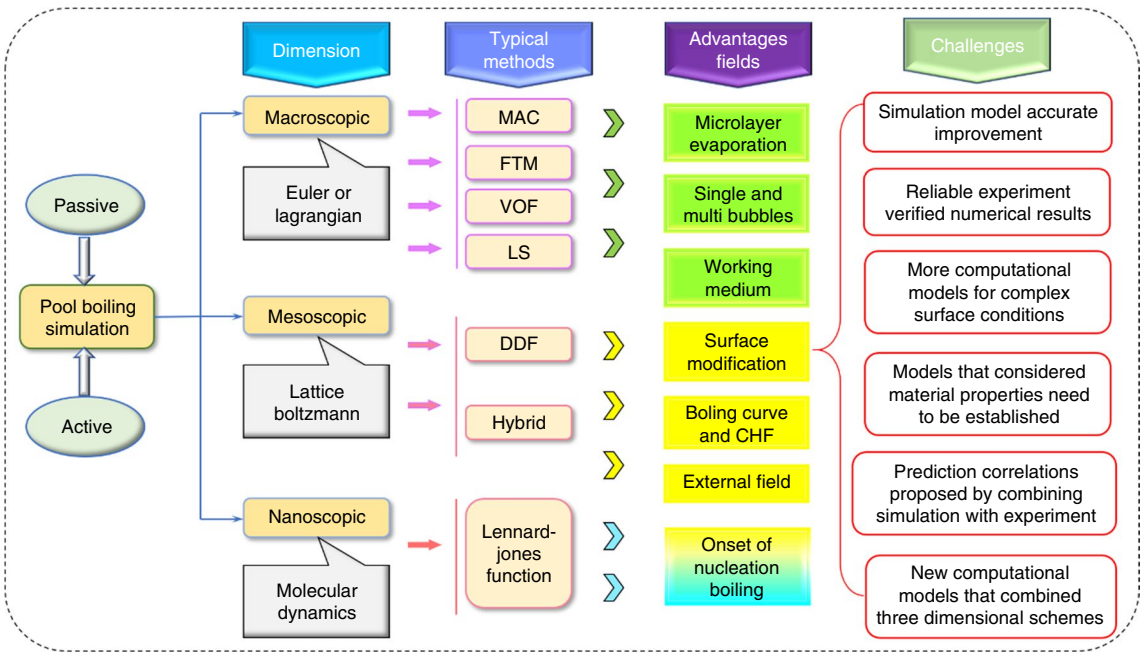

Fig. 30 Overall remarks regarding this research

by the introduction of user-defined property functions and thermodynamic equations of state, as these properties exhibit a strong correlation with temperature. How to guarantee the correctness of the physical parameters during the boiling process at each time step variation requires the consideration of a theoretical model instead of a semi-empirical correlation equation and a more detailed database in combination with a simulation code for parameter sensitivity analysis. This poses a challenge to propose a pool boiling model with a wider range of applications.

(6) Although literature results show that single-phase treatment of nanofluids with different concentrations can predict the pool boiling heat flux, during the actual boiling process, the concentration of nanofluids may change due to the violent perturbations caused by bubble departure, Brownian motion, nanoparticle aggregation, and continuous particle deposition. Missing

nanofluidic database and use of empirical formulas may lead to incorrect predictions of bubble dynamics and heat flux. This requires detailed consideration and modeling of the combined effect between changes in nanofluid suspension properties in macroscopic regions and nanoparticle deposition altering the heated surface properties, which poses a challenge for the study of bubble dynamics using simulation.

The rapid development of industrial technology worldwide has led to the proliferation of devices with high heat flux, especially in the field of compact heat exchangers, nuclear industry, deep space exploration, etc. Accurate modeling of pool boiling heat transfer is necessary, because in the future one needs to get rid of experimental tasks requiring high consumption and to depend on two-phase studies of pool boiling. However, in order to obtain a calculation method with higher accuracy, wider applicability, clear physical meaning and high computational efficiency, it is important to solve the following problems before achieving the above goal:

- Further consideration of complex microlayer evolutionary mechanism is required when simulating the violent interactions between the large number of bubbles near the superheat surface, and in the case of bubble nucleation on modified surfaces. Obtaining microlayer transient change data purely from experiments may be very difficult, and analytical solutions may need to be derived theoretically to solve this problem.
- When using boiling models based on interface trapping and interface tracking, new or improved mass and energy transfer models need to be proposed. In pool boiling, the shape of bubbles undergoes continuous changes under various forces, ultimately changing the pressure near the bubbles, further causing the surface temperature of the bubbles to no longer be a fixed saturation temperature. Different energy transfer models based on saturation temperature may produce erroneous flux estimates when calculating evaporation mass flux. The problem of assuming the saturation temperature of the liquid–vapor phase interface must be efficiently resolved.
- The most commonly used surface capture simulation methods include phase field method, level-set method, VOF method, and front tracking method. However, front tracking, VOF, and LS methods may lose the smoothness of the underlying velocity field and the uniqueness of particle trajectories when the topology changes. The phase field rule does not have this problem, but this method may have physical interpretation difficulties and require a large number of grid points near the interface to accurately capture physical changes. Therefore, it may be necessary to further develop new coupling methods on the basis of the above methods to balance the respective shortcomings of existing interface capture methods. In addition, the development of adaptive grids will facilitate the transition of pool boiling simulation from two-dimensional to three-dimensional.
- A large number of empirical or semi-empirical formulas, such as bubble departure diameter, nucleation site density, and bubble departure frequency, need to be added to the commonly used RPI model to ensure the integrity of the two-phase model based on Eulerian theory. Most of these correlations are obtained based on experimental fitting, so the scope of application is very limited. It will be an important direction in the future to use theoretical analysis, including methods such as energy conservation or mechanical conservation, to derive theoretical correlation suitable for a wider range to replace empirical formulas.
- Nanofluidic pool boiling based on a two-phase model is the focus of future research. Experimental studies have shown that during pool boiling, hydrophilic nanoparticles are adsorbed on the bubble surface and deposited on the heated surface as the wall temperature increases [333]. In addition, the agglomeration phenomena of nanoparticles are also issues that must be addressed. Obviously, these phenomena cannot be extracted from the single-phase model-based bubble dynamics for analysis. Moreover, in the current pool boiling experiments, two conclusions have been made regarding the effect of nanofluid on pool boiling performance: enhancement and weakening. The introduction of the two-phase model can provide more detailed insight into the above issues, but at the same time, gas, liquid and solid phases will exist simultaneously in the boiling zone, which increases the difficulty of establishing the control equations, but this is a problem that must be solved in the future.
- The S–C pseudopotential model has shown good performance when dealing with large density ratio problems, so a large number of studies on pool boiling are based on pseudopotential LBM, but the mechanical stability issues related to the forcing scheme deserve further improvement and control. In addition, the treatment of the error term in the recovery of the macroscopic formulation needs to be further considered when coupling the thermal LB model.
- The detachment of bubbles in pool boiling and the oscillations during ascent will cause fluctuations in the fluid near the bubbles. At high heat flux, these oscillations will be made more intense by the occurrence of violent bubble coalescence and detachment, which may produce induced turbulence phenomena. A key issue is to determine the strength of the bubble disturbance in the isolated bubble region and the fully developed region

in nucleate boiling, especially the vorticity fluctuation phenomenon near the bubble may be more special. In addition to considering the turbulence model in boiling, whether the turbulence model developed based on unidirectional flow is suitable for multiphase flow is an important point to be considered in the future.

- The nucleation mechanism of bubbles on microscopic walls can be studied by molecular dynamics, which is difficult to obtain by using macroscopic or mesoscopic simulation methods. But at the present stage, molecular dynamics still has certain limitations in capturing the gas–liquid interface. In addition, the potential characteristics of molecular dynamics should be exploited in the future, considering the influence mechanism of insoluble gas and external field on nanoboiling, and further revealing the mechanism of the non-evaporating liquid layer at the base of the microliquid layer in pool boiling will be the main research direction in the future.
- The macroscopic simulation method based on the continuum theory cannot simulate the nucleation of bubbles, and only the multi-scale coupling method can effectively solve this problem. In other words, molecular dynamics or lattice Boltzmann methods can be used to complete the nucleation of bubbles, and then, macroscopic simulation methods such as VOSET or CLSVOT can be used to further complete the growth and detachment of bubbles. The key to multiscale simulation theory is the selection of coupling algorithms and the conservation problem in the coupling region of different methods. Future research on pool boiling simulation should strive in this direction.

Conclusions

A large number of literatures on numerical pool boiling heat transfer have been overviewed, including different computational fluid dynamics dimension. Some significant progress has been proposed to numerically simulate pool boiling over the last decade. The results of different numerical simulations and their validation with experimental data have been discussed. The bubble growth, bubble merger, bubble coalescence and bubble nucleation have been investigated for various surfaces modified conditions, level of gravity, nanofluids, thermal conjugate, external field and surface orientation. The simulation capabilities of different methods for pool boiling curve and critical heat flux are also discussed. The primary findings of this review are summarized as follows:

(1) When using Lagrangian and Eulerian methods based on continuous medium models, dealing with mass conservation, phase interface capture problems, and microfluidic layer change processes is the key to successful simulation of pool boiling. The added assumptions in dealing with mass and energy changes reduce the accuracy of the model, especially at the phase interface where the assumption of uniform and saturated temperature affects the heat and mass transfer process. With the introduction of the RPI model, the prediction of heat flux and the bubble shape are well predicted, but the study of boiling heat transfer characteristics on modified surfaces is still a short direction for the method because of the need to introduce additional empirical formulas. In addition, the Eulerian–Eulerian mixing model based on the RPI theory shows excellent ability in simulating the boiling heat exchange of nanofluidic pools, which can effectively reveal the mechanism of the enhanced boiling heat exchange properties of nanofluids. Overall, the method makes an excellent approach in the bubble growth phase, but the empirical formulation in the model still needs further optimization.

(2) The advantage of the mesoscale LBM approach is that fewer assumptions are made, the SC model has been shown to be applicable for large density ratios, and the free energy model requires careful treatment of the density ratio versus the error term to reduce model error. Therefore, it is understandable that the SC model coupled with the thermal LB method is widely used to simulate pool boiling. Unlike SRT, MRT methods can provide multiple relaxation factor control and can be coupled with fourth-order Longo Kutta, finite difference method and other methods dealing with energy fields to make hybridization currents less. The introduction of density-based flow-solid interaction forces is that the LBM can deal with surface wettability well, and further coupling with the solid domain can provide detailed insight into the transient corresponding to the nucleation process. The effective treatment of the P–R equation of state with interaction forces can increase the stability of the simulation at high density ratios, so the method shows good capability in the prediction of boiling curves, but the prediction of critical heat flux prediction is lacking.

(3) The molecular dynamics approach with Newton's second law focuses on the simulation analysis of pool boiling at the nanoscale (Micron system consisting of a large scale of 1 ~ 100 nm, the simulation time is nanoseconds and the step size is generally set to different femtosecond in nano dimensional). The establishment of intermolecular potentials and the determination of small-time steps control the accuracy of the model. The method explains the classical nucleation theory for different wettability and structured surfaces on the basis of potential energy changes and reveals the mechanism of enhanced boiling on hydrophilic surfaces in terms

of changes in phenomenological aspects such as pressure and molecular density. The transient change of energy near the wall is explained at the molecular level by the change of intermolecular distance induced by the change of molecular force strength. However, the gas–liquid interface capture still lacks some accuracy due to the violent molecular motion characteristics during the phase transition. In addition, large-scale simulations require higher computer performance and increase the computational time. Therefore, it is currently limited to pool boiling studies in a very limited area.

(4) For two-phase boiling simulations, a number of commercially available CFD software have been developed. The most widely used in engineering field are FLUENT, CFX, and STAR-CCM + . The solvers of these packages are based on structured \ unstructured meshes and use the finite volume method to discretize each physical field. In addition, COMSOL Multiphysics is also used to perform calculations for two-phase interface flows. In addition to the above software, the open-source software Openfoam has been widely used, which allows the user to modify the code from the bottom and can change the solver according to the user's simulation goals. Powerflow provides a code for single-phase LBM simulations, but has not yet addressed two-phase flows. Therefore, the LBM study of multiphase flow aspect still relies on the underlying code to implement, which makes the LBM method take several times more CPU time than the macroscopic method. In contrast, molecular dynamics, which is supported by the LAMMPS software package, requires more computer requirements than the first two methods. Therefore, there is still a long way to go to apply LBM and molecular dynamics methods to industry. Further, excellent commercial software needs to be developed for macroscopic methods and to embed theories such as front tracking, CLSVOF, VOSET, phase field, etc.

(5) The literature on multi-scale pool boiling simulations shows that the simulations can effectively address the problems and difficulties in experiments. Details of pool boiling phenomena and property changes that are difficult to observe and analyze in experiments, such as local temperature changes on mixed surfaces, bubble dynamics during nanofluid boiling, and temperature response of superheated surfaces, can be well handled. In addition, the introduction of prediction methods for boiling heat transfer properties could provide some basis for future industrial applications [334]. However, current research still faces many challenges, such as how to deal with complex micro- and nanostructures in various physical and chemical ways in the real world, how to build materials on nanostructures, and how to obtain more detailed experimental data to verify simulation results. A reasonable solution to these problems can lay the foundation for future industrial computing applications.

Acknowledgements This work was supported by National Natural Science Foundation of China (Nos. 52276019, 51976146) and the authors declare no conflicts of interest.

Author contributions HJ did writing, original draft, conceptualization, methodology, investigation, software, data curation, and formal analysis. YL was involved in supervision, project administration, funding acquisition, writing—review and editing. HC performed resources, supervision, and project administration.

References

1. Mudawar I. Assessment of high-heat-flux thermal management schemes. IEEE Trans Comp Pack Man. 2001;24:122–41. https://doi.org/10.1109/6144.926375.
2. Mudawar I. Two-phase microchannel heat sinks: theory, applications, and limitations. J Electron Packag. 2011;133:041002. https://doi.org/10.1115/1.4005300.
3. Chu HQ, Yu XY, Jiang HT, Wang DD, Xu N. Progress in enhanced pool boiling heat transfer on macro-and micro-structured surfaces. Int J Heat Mass Transf. 2023;200:123530. https://doi.org/10.1016/j.ijheatmasstransfer.2022.123530.
4. Nukiyama S. The maximum and minimum values of the heat Q transmitted from metal to boiling water under atmospheric pressure. Int J Heat Mass Transf. 1966;9:1419–33. https://doi.org/10.1016/0017-9310(84)90112-1.
5. Chu HQ, Yu BM. A new comprehensive model for nucleate pool boiling heat transfer of pure liquid at low to high heat fluxes including CHF. Int J Heat Mass Transf. 2009;52:4203–10. https://doi.org/10.1016/j.ijheatmasstransfer.2009.04.010.
6. Sajjad U, Sadeghianjahromi A, Ali HM, Wang CC. Enhanced pool boiling of dielectric and highly wetting liquids-A review on surface engineering. Appl Therm Eng. 2021;195:117074. https://doi.org/10.1016/j.applthermaleng.2021.117074.
7. Bergles AE. Some perspectives on enhanced heat transfer-second-generation heat transfer technology. J Heat Trans-T ASME. 1988;110:1082–96. https://doi.org/10.1115/1.3250612.
8. Kim JM, Kim T, Yu DI, Kim MH, Moriyama K, Park HS. Time effect on wetting transition of smart surface and prediction of the wetting transition for critical heat flux in pool boiling. Int J Heat Mass Transf. 2017;114:735–42. https://doi.org/10.1016/j.ijheatmasstransfer.2017.06.114.
9. Shen B, Hamazaki T, Ma W, Iwata N, Hidaka S, Takahara A, Takahashi K, Takata Y. Enhanced pool boiling of ethanol on wettability-patterned surfaces. Appl Therm Eng. 2019;149:325–31. https://doi.org/10.1016/j.applthermaleng.2018.12.049.
10. Dong L, Quan X, Cheng P. An experimental investigation of enhanced pool boiling heat transfer from surfaces with micro/nano-structures. Int J Heat Mass Transf. 2014;71:189–96. https://doi.org/10.1016/j.ijheatmasstransfer.2013.11.068.
11. Yu XY, Xu N, Yu S, Han Y, Chu HQ. Effect of orthogonal channel structure on the heat transfer in pool boiling and its heat flux prediction model. Int J Therm Sci. 2023;187:108193. https://doi.org/10.1016/j.ijthermalsci.2023.108193.
12. Deng D, Feng J, Huang Q, Tang Y, Lian Y. Pool boiling heat transfer of porous structures with reentrant cavities. Int J Heat Mass Transf. 2016;99:556–68. https://doi.org/10.1016/j.ijheatmasstransfer.2016.04.015.

13. Ujereh S, Fisher T, Mudawar I. Effects of carbon nanotube arrays on nucleate pool boiling. Int J Heat Mass Transf. 2007;50:4023–38. https://doi.org/10.1016/j.ijheatmasstransfer.2007.01.030.
14. Raj R, Kim J, Mcquillen J. Subcooled pool boiling in variable gravity environments. J Heat Trans-T ASME. 2009;131:091502. https://doi.org/10.1115/1.3122782.
15. Raj R, Kim J. Heater size and gravity based pool boiling regime map: transition criteria between buoyancy and surface tension dominated boiling. J Heat Trans-T ASME. 2010;132:091503. https://doi.org/10.1115/1.4001635.
16. Deng DX, Wan W, Feng JY, Huang QS, Qin Y, Xie YL. Comparative experimental study on pool boiling performance of porous coating and solid structures with reentrant channels. Appl Therm Eng. 2016;107:420–30. https://doi.org/10.1016/j.applthermaleng.2016.06.172.
17. Liu Y, Tang JQ, Li LX, Shek YN, Xu DY. Design of Cassie-wetting nucleation sites in pool boiling. Int J Heat Mass Transf. 2019;32:25–33. https://doi.org/10.1016/j.ijheatmasstransfer.2018.11.146.
18. Jo HS, Kim TG, Lee JG, Kim MW, Park HG, James SC, Choi J, Yoon SS. Supersonically sprayed nanotextured surfaces with silver nanowires for enhanced pool boiling. Int J Heat Mass Transf. 2018;123:397–406. https://doi.org/10.1016/j.ijheatmasstransfer.2018.02.092.
19. Hayes A, Raghupathi PA, Emery TS, Kandlikar SG. Regulating Flow of Vapor to Enhance Pool Boiling. Appl Therm Eng. 2019;149:1044–51. https://doi.org/10.1016/j.applthermaleng.2018.12.091.
20. Rohsenow WM, Griffith P. Correlation of maximum heat transfer data for boiling of saturated liquids. Chem Eng Prog. 1955;52:47–9.
21. Zuber N. Hydrodynamic aspects of boiling heat transfer. United States Atomic Energy Commission, Technical Information Service. 1959.
22. Haramura Y, Katto Y. A new hydrodynamic model of critical heat flux, applicable widely to both pool and forced convection boiling on submerged. Int J Heat Mass Transf. 1983;26:389–99. https://doi.org/10.1016/0017-9310(83)90043-1.
23. Yagov VV. A physical model and calculation formula for critical heat fluxes with nucleate pool boiling of liquids. Therm Eng. 1988;35:333–9.
24. Mudawar I, Howard AH, Gersey CO. An analytical model for near-saturated pool boiling critical heat flux on vertical surfaces. Int J Heat Mass Transf. 1997;40:2327–39. https://doi.org/10.1016/S0017-9310(96)00298-0.
25. Utaka Y, Nakamura K, Sakurai A, Itagaki K, Sonoda A. Configuration of microlayer in nucleate boiling. Trans Jpn Soc Mech Eng. 2008;74:2358–64.
26. Utaka Y, Kashiwabara Y, Ozaki M. Microlayer structure in nucleate boiling of water and ethanol at atmospheric pressure. Int J Heat Mass Transf. 2013;57:222–30. https://doi.org/10.1016/j.ijheatmasstransfer.2012.10.031.
27. Utaka Y, Kashiwabara Y, Ozaki M, Chen Z. Heat transfer characteristics based on microlayer structure in nucleate pool boiling for water and ethanol. Int J Heat Mass Transf. 2014;68:479–88. https://doi.org/10.1016/j.ijheatmasstransfer.2013.09.063.
28. Kossolapov A, Phillips B, Bucci M. Can LED lights replace lasers for detailed investigations of boiling phenomena? Int J Multiphase Flow. 2021;135:103522. https://doi.org/10.1016/j.ijmultiphaseflow.2020.103522.
29. Lee RC, Nyadhl JE. Numerical Calculation of Bubble Growth in Nucleate Boiling from inception to departure. J Heat Trans-T ASME. 1989;111:474–9. https://doi.org/10.1115/1.3250701.
30. Mei R, Chen W, Klausner JF. Vapor Bubble Growth in Heterogeneous Boiling- II. Growth Rate and Thermal Fileds. Int J Heat Mass Transf. 1995;38;921–934. https://doi.org/10.1016/0017-9310(94)00196-3.
31. Welch SWJ. Direct Simulation of Vapor Bubble Growth. Int J Heat and Mass Transf. 1998;41:1655–66. https://doi.org/10.1016/S0017-9310(97)00285-8.
32. Son G, Dhir VK, Ramanujapu N. Dynamics and Heat Transfer Associated With a Single Bubble During Nucleate Boiling on a horizontal surface. J Heat Trans-T ASME. 1999;121:623–31. https://doi.org/10.1115/1.2826025.
33. Abarajith HS. Numerical Prediction and Experimental Validation of Pool Nucleate Boiling Heat Flux Under Variable Gravity Conditions. United States: Thesis;2006.
34. Dhir VK. Mechanistic prediction of nucleate boiling heat transfer-achievable or a hopeless task? J Heat Trans-T ASME. 2006;128:1–12. https://doi.org/10.1115/1.2136366.
35. Kunugi T. Brief review of latest direct numerical simulation on pool and film boiling. Nucl Eng Technol. 2012;44(8):847–54. https://doi.org/10.5516/NET.02.2012.717.
36. Dhir VK, Warrier GR, Aktinol E. Numerical simulation of pool boiling: a review. J Heat Trans-T ASME. 2013;135:061502. https://doi.org/10.1115/1.4023576.
37. Dhir V K. Advances in Understanding of Pool Boiling Heat Transfer-From Earth on to Deep Space. J Heat Trans-T ASME. 2019;141:050802. https://doi.org/10.1115/1.4043282.
38. Li Q, Luo KH, Kang QJ, He YL, Chen Q, Liu Q. Lattice Boltzmann methods for multiphase flow and phase-change heat transfer. Prog Energ Combust. 2016;52:62–105. https://doi.org/10.1016/j.pecs.2015.10.001.
39. Kharangate CR, Mudawar I. Review of computational studies on boiling and condensation. Int J Heat Mass Transf. 2017;108:1164–96. https://doi.org/10.1016/j.ijheatmasstransfer.2016.12.065.
40. Dadhich M, Prajapati OS. A brief review on factors affecting flow and pool boiling. Renew Sust Energ Rev. 2019;112:607–25. https://doi.org/10.1016/j.rser.2019.06.016.
41. Harlow FH, Welch JE. Numerical calculation of time-dependent viscous incompressible flow of fluid with free surface. Phys Fluid. 1996;8:2182–9. https://doi.org/10.1063/1.1761178.
42. Madhavan S, Mesler B. A Study of Vapor bubble growth on surfaces. Int Heat Transf Conf. 1970;4.
43. Takagi S. Three-dimensional deformation of a rising bubble. In Proc. German-Japanese Symp. on Multi-Phase Flow. 1994;499.
44. Hirt CW, Amsden AA, Cook JL. An arbitrary lagrangian-eulerian computing method for all speeds. J Comput Phys. 1974;14:227–53. https://doi.org/10.1016/0021-9991(74)90051-5.
45. Hughes TJR, Liu WK, Zimmermann TK. Lagrangian-Eulerian finite element formulation for incompressible viscous flows. Comput Method Appl M. 1981;29:329–49. https://doi.org/10.1016/0045-7825(81)90049-9.
46. Donea J, Giuliani S, Halleux JP. An arbitrary Lagrangian-Eulerian finite element method for transient dynamic fluid-structure interaction. Comput Method Appl M. 1982;33:689–723. https://doi.org/10.1016/0045-7825(82)90128-1.
47. Belytschko TB, Kennedy JM. Computer models for subassembly simulation. Nucl Eng Des. 1978;49:7–38. https://doi.org/10.1016/0029-5493(78)90049-3.
48. Belytschko T, Kennedy JM, Schoeberle DF. Quasi-Eulerian finite element formulation for fluid-structure interaction. J Press Vess-T ASME. 1980;102:62–9. https://doi.org/10.1115/1.3263303.
49. Chern IL, Glimm J, McBryan O, Plohr B, Yaniv S. Front tracking for gas dynamics. J Comput Phys. 1986;62:83–110. https://doi.org/10.1016/0021-9991(86)90101-4.
50. Glimm J, Grove JW, Li XL, Oh W, Sharp DH. A critical analysis of Rayleigh-Taylor growth rates. J Comput Phys. 2001;169:652–77. https://doi.org/10.1006/jcph.2000.6590.

51. Marshall G. A front tracking method for one-dimensional moving boundary problems. SIAM J Sci Stat Comput. 1986;7:252–63. https://doi.org/10.1137/0907017.
52. Charrier P, Tessieras B. On front-tracking methods applied to hyperbolic systems of nonlinear conservation laws. SIAM J Numer Anal. 1986;23:461–72. https://doi.org/10.1137/072303 1.
53. Unverdi SO, Tryggvason G. A front-tracking method for viscous, incompressible, multi-fluid flows. J Comput Phys. 1992;100:25–37. https://doi.org/10.1016/0021-9991(92)90307-K.
54. Unverdi SO, Tryggvason G. Computations of multi-fluid flows. Physica D. 1992;60:70–83. https://doi.org/10.1016/0167-2789(92)90227-E.
55. Esmaeeli A, Tryggvason G. Direct numerical simulations of bubbly flows. Part 1. Low Reynolds number arrays. J Fluid Mech. 1998;377:313–345. https://doi.org/10.1017/S00221120980031 76.
56. Esmaeeli A, Tryggvason G. Direct numerical simulations of bubbly flows Part 2. Moderate Reynolds number arrays. J Fluid Mech. 1999;385:325–358. https://doi.org/10.1017/S002211209 9004310.
57. Hirt CW, Nichols BD. Volume of fluid (VOF) method for the dynamics of free boundaries. J Comput Phys. 1981;39:201–25. https://doi.org/10.1016/0021-9991(81)90145-5.
58. Rudman M. Volume-tracking methods for interfacial flow calculations. Int J Numer Meth Fluids. 1997;24:671–91. https://doi.org/10.1002/(SICI)1097-0363.
59. Ubbink O, Issa RI. A method for capturing sharp fluid interfaces on arbitrary meshes. J Comput Phys. 1999;153:26–50. https://doi.org/10.1006/jcph.1999.6276.
60. Noh WF, Woodward P. SLIC (simple line interface calculation). In: Lecture notes in physics, Springer, New York. 1976;59:330–340.
61. Youngs DL. Time-dependent multi-material flow with large fluid distortion. Numer Meth Fluid. 1982;24:273–85.
62. Ashgriz N, Poo JY. FLAIR: Flux line-segment model for advection and interface reconstruction. J Comput Phys. 1991;93:449–68. https://doi.org/10.1016/0021-9991(91)90194-P.
63. Price GR, Reader GT, Rowe RD, Bugg JD. A piecewise parabolic interface calculation for volume tracking. in: Proceedings of the Sixth Annual Conference of CFD Society of Canada 1998:71–77.
64. Ginzburg I, Wittum G. Two-phase flows on interface refined grids modeled with VOF, staggered finite volumes, and spline interpolants. J Comput Phys. 2001;166:302–35. https://doi.org/10.1006/jcph.2000.6655.
65. Mukherjee A, Dhir VK. Study of lateral merger of vapor during nucleate pool boiling. J Heat Trans-T ASME. 2004;126:1023–39. https://doi.org/10.1115/1.1834614.
66. Sussman M, Smereka P, Osher S. A level set approach for computing solutions to incompressible two-phase flows. J Comput Phys. 1994;114:146–59. https://doi.org/10.1006/jcph.1994.1155.
67. Son G, Dhir VK. Numerical simulation of film boiling near critical pressures with a level-set method. J Heat Trans-T ASME. 1998;120:183–92. https://doi.org/10.1115/1.2830042.
68. Sun DL, Tao WQ. A coupled volume-of-fluid and level set (VOSET) method for computing incompressible two-phase flows. Int J Heat Mass Transf. 2010;53:645–55. https://doi.org/10.1016/j.ijheatmasstransfer.2009.10.030.
69. Ling K, Li ZY, Tao WQ. A direct numerical simulation for nucleate boiling by the VOSET method. Numer Heat Tr A-Appl. 2014;65:949–71. https://doi.org/10.1080/10407782.2013.850971.
70. Sussman M, Puckett EG. A coupled level set and volume-of-fluid method for computing 3D and axisymmetric incompressible two-phase flows. J Comput Phys. 2000;162:301–37. https://doi.org/10.1006/jcph.2000.6537.
71. Antanovskii LK. A phase field model of capillarity. Phys Fluid. 1995;7:747–53. https://doi.org/10.1063/1.868598.
72. Jacqmin D. Calculation of two-phase Navier-Stokes flows using phase-field modeling. J Comput Phys. 1999;155:96–127. https://doi.org/10.1006/jcph.1999.6332.
73. Jing Y, Guo L, Zhang X. A numerical simulation of pool boiling using CAS model. Int J Heat Mass Transf. 2003;46:4789–97. https://doi.org/10.1016/S0017-9310(03)00353-3.
74. He Y, Shoji M, Maruyama S. Numerical Study of high heat flux pool boiling heat transfer. Int J Heat Mass Transf. 2001;44:2357–73. https://doi.org/10.1016/S0017-9310(00)00269-6.
75. Kaneko K. Theory and Applications of Coupled Map Lattices. Chichester: Chichester John Wiley and Sons; 1993.
76. Yanagita T. Phenomenology for Boiling: A Coupled Map Lattice Model. Chaos. 1992;2:343–50. https://doi.org/10.1063/1.165877.
77. Laurila T, Carlson A, Do-Quang M, Ala-Nissila Y, Amberg G. Thermohydrodynamics of boiling in a van der Waals fluid. Phys Rev E. 2012;85:026320. https://doi.org/10.1103/PhysRevE.85.026320.
78. Xu X, Liu C, Qian T. Hydrodynamic boundary conditions for one-component liquid-gas flows on non-isothermal solid substrates. Commun Math Sci. 2012;10:1027–53. https://doi.org/10.4310/CMS.2012.v10.n4.a1.
79. Succi S. The lattice Boltzmann equation for fluid dynamics and beyond. Oxford: Oxford University Press; 2001.
80. Chen S, Chen H, Martnez D, Matthaeus W. Lattice Boltzmann model for simulation of magnetohydrodynamics. Phys Rev Lett. 1991;67:3776–9. https://doi.org/10.1103/PhysRevLett.67.3776.
81. Qian YH, d'Humières D, Lallemand P. Lattice BGK models for Navier-Stokes equation. Europhys Lett. 1992;17:479–84. https://doi.org/10.1209/0295-5075/17/6/001.
82. Swift MR, Osborn WR, Yeomans JM. Lattice Boltzmann simulation of nonideal fluids. Phys Rev Lett. 1995;75:830–3. https://doi.org/10.1103/PhysRevLett.75.830.
83. Swift MR, Orlandini E, Osborn WR, Yeomans JM. Lattice Boltzmann simulations of liquid-gas and binary fluid systems. Phys Rev E. 1996;54:5041–52. https://doi.org/10.1103/PhysRevE.54.5041.
84. Inamuro T, Konishi N, Ogino F. A Galilean invariant model of the lattice Boltzmann method for multiphase fluid flows using free-energy approach. Comput Phys Commun. 2000;129:32–45. https://doi.org/10.1016/S0010-4655(00)00090-4.
85. He X, Chen S, Zhang R. A lattice Boltzmann scheme for incompressible multiphase flow and its application in simulation of Rayleigh-Taylor instability. J Comput Phys. 1999;152:642–63. https://doi.org/10.1006/jcph.1999.6257.
86. Li Q, Luo KH, Gao YJ, He YL. Additional interfacial force in lattice Boltzmann models for incompressible multiphase flows. Phys Rev E. 2012;85:026704. https://doi.org/10.1103/PhysRevE.85.026704.
87. Liu H, Valocchi AJ, Zhang Y, Kang Q. Phase-field-based lattice Boltzmann finite-difference model for simulating thermocapillary flows. Phys Rev E. 2013;87:013010. https://doi.org/10.1103/PhysRevE.87.013010.
88. Shi Y, Tang GH. Simulation of Newtonian and non-Newtonian rheology behavior of viscous fingering in channels by the lattice Boltzmann method. Comput Math Appl. 2014;68:1279–91. https://doi.org/10.1016/j.camwa.2014.08.024.
89. Gunstensen AK, Rothman DH, Zaleski S, Zanetti G. Lattice Boltzmann model of immiscible fluids. Phys Rev A. 1991;43:4320–7. https://doi.org/10.1103/PhysRevA.43.4320.
90. Grunau D, Chen S, Eggert K. A lattice Boltzmann model for multiphase fluid flows. Phys Fluids A. 1993;5:2557–62. https://doi.org/10.1063/1.858769.

91. Reis T, Phillips TN. Lattice Boltzmann model for simulating immiscible two-phase flows. J Phys A-Math Theor. 2007;40:4033. https://doi.org/10.1088/1751-8113/40/14/018.
92. Liu H, Valocchi AJ, Kang Q. Three-dimensional lattice Boltzmann model for immiscible two-phase flow simulations. Phys Rev E. 2012;85:046309. https://doi.org/10.1103/PhysRevE.85.046309.
93. Shan X, Chen H. Lattice Boltzmann model for simulating flows with multiple phases and components. Phys Rev E. 1993;47:1815–20. https://doi.org/10.1103/PhysRevE.47.1815.
94. Shan X, Chen H. Simulation of nonideal gases and liquid-gas phase transitions by the lattice Boltzmann equation. Phys Rev E. 1994;49:2941. https://doi.org/10.1103/PhysRevE.49.2941.
95. Falcucci G, Bella G, Shiatti G, Chibbaro S, Sbragaglia M, Succi S. Lattice Boltzmann models with mid-range interactions. Commun Comput Phys. 2007;2:1071–84.
96. Yu Z, Fan L-S. Multirelaxation-time interaction-potential-based lattice Boltzmann model for two-phase flow. Phys Rev E. 2010;82:046708. https://doi.org/10.1103/PhysRevE.82.046708.
97. Li Q, Luo KH, Li XJ. Lattice Boltzmann modeling of multiphase flows at large density ratio with an improved pseudopotential model. Phys Rev E. 2013;87:053301. https://doi.org/10.1103/PhysRevE.87.053301.
98. Dou S, Hao L, Liu H. Numerical study of bubble behaviors and heat transfer in pool boiling of water/NaCl solutions using the lattice Boltzmann method. Int J Therm Sci. 2021;170:107158. https://doi.org/10.1016/j.ijthermalsci.2021.107158.
99. Yuan P, Schaefer L. Equations of state in a lattice Boltzmann model. Phys Fluids. 2006;18:042101. https://doi.org/10.1063/1.2187070.
100. Zhang R, Chen H. Lattice Boltzmann method for simulations of liquid-vapor thermal flows. Phys Rev E. 2003;67:066711. https://doi.org/10.1103/PhysRevE.67.066711.
101. Gong S, Cheng P. Numerical investigation of droplet motion and coalescence by an improved lattice Boltzmann model for phase transitions and multiphase flows. Comput Fluids. 2012;53:93–104. https://doi.org/10.1016/j.compfluid.2011.09.013.
102. Zeng J, Li L, Liao Q, Cui W, Chen Q, Pan L. Simulation of phase transition process using lattice Boltzmann method. Chinese Sci Bull. 2009;54:4596–603. https://doi.org/10.1007/s11434-009-0734-x.
103. Li Q, Luo KH, Li XJ. Forcing scheme in pseudopotential lattice Boltzmann model for multiphase flows. Phys Rev E. 2012;86:016709. https://doi.org/10.1103/PhysRevE.86.016709.
104. Mukherjee A, Basu DN, Mondal PK. Algorithmic augmentation in the pseudopotential-based lattice Boltzmann method for simulating the pool boiling phenomenon with high-density ratio. Phys Rev E. 2021;103:053302. https://doi.org/10.1103/PhysRevE.103.053302.
105. Martys NS, Chen H. Simulation of multicomponent fluids in complex three dimensional geometries by the lattice Boltzmann method. Phys Rev E. 1996;53:743–50. https://doi.org/10.1103/PhysRevE.53.743.
106. Gong S, Cheng P. A lattice Boltzmann method for simulation of liquid-vapor phase-change heat transfer. Int J Heat Mass Transf. 2012;55:4923–7. https://doi.org/10.1016/j.ijheatmasstransfer.2012.04.037.
107. Chen L, Kang QJ, Mu YT, He YL, Tao WQ. A critical review of the pseudopotential multiphase lattice Boltzmann model: Methods and applications. Int J Heat and Mass Transf. 2014;76:210–36. https://doi.org/10.1016/j.ijheatmasstransfer.2014.04.032.
108. Gong S, Cheng P, Quan X. Lattice Boltzmann simulation of droplet formation in microchannels under an electric field. Int J Heat Mass Transf. 2010;53:5863–70. https://doi.org/10.1016/j.ijheatmasstransfer.2010.07.057.
109. Hazi G, Markus A. On the bubble departure diameter and release frequency based on numerical simulation results. Int J Heat Mass Transf. 2009;52:1472–80. https://doi.org/10.1016/j.ijheatmasstransfer.2008.09.003.
110. Márkus A, Házi G. Simulation of evaporation by an extension of the pseudopotential lattice Boltzmann method: a quantitative analysis. Phys Rev E. 2011;83:046705. https://doi.org/10.1103/PhysRevE.83.046705.
111. Biferale L, Perlekar P, Sbragaglia M, Toschi F. Convection in multiphase fluid flows using lattice Boltzmann methods. Phys Rev Lett. 2012;108:104502. https://doi.org/10.1103/PhysRevLett.108.104502.
112. Gong S, Cheng P. Lattice Boltzmann simulation of periodic bubble nucleation, growth and departure from a heated surface in pool boiling. Int J Heat Mass Transf. 2013;64:122–32. https://doi.org/10.1016/j.ijheatmasstransfer.2013.03.058.
113. Liu X, Cheng P. Lattice Boltzmann simulation of steady laminar film condensation on a vertical hydrophilic subcooled flat plate. Int J Heat Mass Transf. 2013;62:507–14. https://doi.org/10.1016/j.ijheatmasstransfer.2013.03.002.
114. Kamali MR, Gillissen JJJ, Van den Akker HEA, Sundaresan S. Lattice Boltzmann based two-phase thermal model for simulating phase change. Phys Rev E. 2013;88:033302. https://doi.org/10.1103/PhysRevE.88.033302.
115. Miyagawa H, Kitamura K. An Introduction of Molecular Dynamics Simulation. J Synth Org Chem Jpn. 1997;55:402–9.
116. Hollingsworth SA, Dror RO. Molecular Dynamics Simulation for All. Neuron. 2018;99:1129–43. https://doi.org/10.1016/j.neuron.2018.08.011.
117. Haile JM, Johnston I, Mallinckrodt AJ, McKay S. Molecular Dynamics Simulation: Elementary Methods. Comput Phys. 1993;7:625. https://doi.org/10.1063/1.4823234.
118. Giovanni C, Ryckaert JP. Molecular dynamics simulation of rigid molecules. Comput Phys Re. 1986;4:346–92. https://doi.org/10.1016/0167-7977(86)90022-5.
119. Van der Ploeg P, Berendsen HJC. Molecular dynamics simulation of a bilayer membrane. J Chem Phys. 1982;76:3271–3271. https://doi.org/10.1063/1.443321.
120. Grest G, Kremer K. Molecular dynamics simulation for polymers in the presence of a heat bath. Phys Rev. 1986;33:3628–31. https://doi.org/10.1103/PhysRevA.33.3628.
121. Raghupathi PA, Kandlikar SG, Pool boiling enhancement through contact line augmentation. Appl Phys Lett. 2017;110:204101. https://doi.org/10.1063/1.4983720.
122. Kim JS, Girard A, Jun S, Lee J, You SM. Effect of surface roughness on pool boiling heat transfer of water on hydrophobic surfaces. Int J Heat Mass Transf. 2018;118:802–11. https://doi.org/10.1016/j.ijheatmasstransfer.2017.10.124.
123. O'Hanley H, Coyle C, Buongiorno J, McKrell T, Hu LW, Rubner M, Cohen R. Separate effects of surface roughness, wettability, and porosity on the boiling critical heat flux. Appl Phys Lett. 2013;103:024102. https://doi.org/10.1063/1.4813450.
124. Fan SM, Jiao LS, Wang K, Duan F. Pool boiling heat transfer of saturated water on rough surfaces with the effect of roughening techniques. Int J Heat Mass Transf. 2020;159:120054. https://doi.org/10.1016/j.ijheatmasstransfer.2020.120054.
125. Xu ZG, Zhao CY. Thickness effect on pool boiling heat transfer of trapezoid shaped copper foam fins. Appl Therm Eng. 2013;60:359–70. https://doi.org/10.1016/j.applthermaleng.2013.07.013.
126. Xu ZG, Zhao CY. Pool boiling heat transfer of open-celled metal foams with V-shaped grooves for high pore densities. Exp Therm Fluid Sci. 2014;52:128–38. https://doi.org/10.1016/j.expthermflusci.2013.09.003.
127. Xu ZG, Zhao CY. Enhanced boiling heat transfer by gradient porous metals in saturated pure water and surfactant solutions.

Appl Therm Eng. 2016;100:68–77. https://doi.org/10.1016/j.applthermaleng.2016.02.016.
128. Xu ZG, Zhao CY. Experimental study on pool boiling heat transfer in gradient metal foams. Int J Heat Mass Transf. 2015;85:824–9. https://doi.org/10.1016/j.ijheatmasstransfer.2015.02.017.
129. Yu ck, Lu DC. Pool boiling heat transfer on horizontal rectangular fin array in saturated FC-72. Int J Heat Mass Transf. 2007;50:3624–3637. https://doi.org/10.1016/j.ijheatmasstransfer.2007.02.003.
130. Zhong D, Meng J, Li Z, Guo Z. Critical heat flux for downward-facing saturated pool boiling on pin fin surfaces. Int J Heat Mass Transf. 2015;87:201–11. https://doi.org/10.1016/j.ijheatmasstransfer.2015.04.001.
131. Jiang HT, Yu XY, Xu N, Wang DD, Yang J, Chu HQ. Effect of T-shaped micro-fins on pool boiling heat transfer performance of surfaces. Exp Therm Fluid Sci. 2022;136:110663. https://doi.org/10.1016/j.expthermflusci.2022.110663.
132. Hao W, Wang T, Jiang YY, Guo C, Guo CH. Pool boiling heat transfer on deformable structures made of shape-memory-alloys. Int J Heat Mass Transf. 2017;112:236–47. https://doi.org/10.1016/j.ijheatmasstransfer.2017.04.113.
133. Wang T, Jiang YY, Jiang HC, Guo C, Guo CH, Tang DW, Rong LJ. Surface with recoverable mini structures made of shape-memory alloys for adaptive-control of boiling heat transfer. Appl Phys Lett. 2015;107:023904. https://doi.org/10.1063/1.4926987.
134. Chibowski E. Surface free energy of a solid from contact angle hysteresis. Adv Colloid Interface. 2003;103(2):149–72. https://doi.org/10.1016/S0001-8686(02)00093-3.
135. Verlet L. Computer, "Experiments" on Classical Fluids I Thermodynamical Properties of Lennard-Jones Molecules. Phys Rev. 1967;159:98–103. https://doi.org/10.1103/PhysRev.159.98.
136. Swope WC, Andersen HC. A computer simulation method for the calculation of equilibrium constants for the formation of physical clusters of molecules: Application to small water clusters. J Chem Phys. 1982;76:637–49. https://doi.org/10.1063/1.442716.
137. Hoover WG. Canonical dynamics: Equilibrium phase-space distributions. Phys Rev A Gen Phys. 1985;31:1695–7. https://doi.org/10.1103/PhysRevA.31.1695.
138. Berendsen HJC, Postma JPM, Van Gunsteren WF, Dinola A, Haak JR. Molecular dynamics with coupling to an external bath. J Chem Phys. 1984;81:3684–90. https://doi.org/10.1063/1.448118.
139. Schneider T, Stoll E. Molecular-dynamics study of a three-dimensional one-component model for distortive phase transitions. Phys Rev B. 1978;17:1302. https://doi.org/10.1103/PhysRevB.17.1302.
140. Surblys D, Matsubara H, Kikugawa G, Ohara T. Application of atomic stress to compute heat flux via molecular dynamics for systems with many-body interactions. Phys Rev E. 2019;99:051301. https://doi.org/10.1103/PhysRevE.99.051301.
141. Plimpton S. Fast parallel algorithms for short-range molecular dynamics. J Comput Phys. 1995;117:1–19. https://doi.org/10.1006/jcph.1995.1039.
142. Wang J, Wolf RM, Caldwell JW, Kollman PA, Case DA. Development and testing of a general amber force field. J Comput Chem. 2004;25:1157–74. https://doi.org/10.1002/jcc.20035.
143. Lindahl E, Hess B, David VDS. GROMACS 3.0: a package for molecular simulation and trajectory analysis. Mol Model Ann. 2001;7:306–317. https://doi.org/10.1007/s008940100045.
144. Zhu X, Lopes PE Jr, MK. Recent developments and applications of the CHARMM force fields. Wiley Interdis Rev: Comput Mol Sci. 2012;2:167–85. https://doi.org/10.1002/wcms.74.
145. Chandrasekhar I, Bakowies D, Glättli A, Hünenberger P, Pereira C, Gunsteren WFN. Molecular dynamics simulation of lipid bilayers with GROMOS96:application of surface tension. Mol Simul. 2005;31:543–548. https://doi.org/10.1080/08927020500134243.
146. Cooper MG, Lloyd AJP. The microlayer in nucleate pool boiling. Int J Heat Mass Transf. 1969;12:895–913. https://doi.org/10.1016/0017-9310(69)90154-9.
147. Judd RL, Hwang KS. A comprehensive model for nucleate pool boiling heat transfer including microlayer evaporation. J Heat Trans-T ASME. 1976;98:623–9. https://doi.org/10.1115/1.3450610.
148. Son G, Ramanujapu N, Dhir VK. Numerical Simulation of Bubble Merger Process on a Single Nucleation Site During Pool Nucleate Boiling. J Heat Trans-T ASME. 2002;124:51–61. https://doi.org/10.1115/1.1420713.
149. Sato Y, Niceno B. A depletable micro-layer model for nucleate pool boiling. J Comput Phys. 2015;300:20–52. https://doi.org/10.1016/j.jcp.2015.07.046.
150. Sato Y, Ničeno B. A sharp-interface phase change model for a mass-conservative interface tracking method. J Comput Phys. 2013;249:127–61. https://doi.org/10.1016/j.jcp.2013.04.035.
151. Jia HW, Zhang P, Fu X, Jiang SC. A numerical investigation of nucleate boiling at a constant surface temperature. Appl Therm Eng. 2015;88:248–57. https://doi.org/10.1016/j.applthermaleng.2014.09.022.
152. Mobli M, Bayat M, Li C. Estimating bubble interfacial heat transfer coefficient in pool boiling. J Mol Liq. 2022;350:118541. https://doi.org/10.1016/j.molliq.2022.118541.
153. Salehi A, Mortazavi S, Amini M. A numerical study of heat transfer in saturated nucleate pool boiling process: a new analysis based on the inherent physics. Acta Mech. 2022;233:3601–22. https://doi.org/10.1007/s00707-022-03290-8.
154. Inamuro T, Ogata T, Ogino F. Numerical simulation of bubble flows by the Lattice Boltzmann method. Future Gener Comp Sy. 2004;20:959–64. https://doi.org/10.1016/j.future.2003.12.008.
155. Inamuro T, Ogata T, Tajima S, Konishi N. A Lattice Boltzmann method for incompressible two-phase flows with large density differences. J Comput Phys. 2004;198:628–44. https://doi.org/10.1016/j.jcp.2004.01.019.
156. Inamuro T, Ogata T, Ogino F. Lattice Boltzmann simulation of droplet collision dynamics. Int J Heat Mass Transf. 2004;47:4649–57. https://doi.org/10.1016/j.ijheatmasstransfer.2003.08.030.
157. Sakakibara B, Inamuro T. Lattice Boltzmann simulation of collision dynamics of two unequal-size droplets. Int J Heat Mass Transf. 2008;51:3207–3216.https://doi.org/10.1016/j.ijheatmasstransfer.2008.02.004.
158. Dong Z, Li W, Song Y. A numerical investigation of bubble growth on and departure from a superheated wall by lattice Boltzmann method. Int J Heat Mass Transf. 2010;53:4908–16. https://doi.org/10.1016/j.ijheatmasstransfer.2010.06.001.
159. Zheng HW, Shu C, Chew YT. A lattice Boltzmann for multiphase flows with large density ratio. J Comput Phys. 2006;218:353–71. https://doi.org/10.1016/j.jcp.2006.02.015.
160. Safari H, Rahimian MH, Krafczyk M. Extended lattice Boltzmann method for numericalsimulation of thermal phase change in two-phase fluid flow. Phys Rev E. 2013;88:013304. https://doi.org/10.1103/PhysRevE.88.013304.
161. Begmohammadi A, Farhadzadeh M, Rahimian MH. Simulation of pool boiling and periodic bubble release at high density ratio using lattice Boltzmann method. Int Commun Heat Mass Transf. 2015;61:78–87. https://doi.org/10.1016/j.icheatmasstransfer.2014.12.018.
162. Sun T, Li W, Yang S. Numerical simulation of bubble growth and departure during flow boiling period by lattice Boltzmann method. Int J Heat Fluid Flow. 2013;44:120–9. https://doi.org/10.1016/j.ijheatfluidflow.2013.05.003.

163. Sun T, Li W. Three-dimensional numerical simulation of nucleate boiling bubble by lattice Boltzmann method. Comput Fluids. 2013;88:400–9. https://doi.org/10.1016/j.compfluid.2013.10.009.
164. Sun T. A numerical study on dynamics behaviors of multi bubbles merger during nucleate boiling by lattice Boltzmann method. Int J Multiphase Flow. 2019;118:128–40. https://doi.org/10.1016/j.ijmultiphaseflow.2019.04.011.
165. Yuan J, Ye X, Shan Y. Modeling of the bubble dynamics and heat flux variations during lateral coalescence of bubbles in nucleate pool boiling. Int J Multiphase Flow. 2021;142:103701. https://doi.org/10.1016/j.ijmultiphaseflow.2021.103701.
166. Maruyama S, Kimura T. A molecular dynamics simulation of a bubble nucleation on solid surface. Trans Japan Soci Mech Engi Series B. 1999;65:3461–7. https://doi.org/10.1299/kikaib.65.3461.
167. Brackbill JU, Kothe DB, Zemach C. A continuum method for modeling surface tension. J Comput Phys. 1992;100:335–54. https://doi.org/10.1016/0021-9991(92)90240-Y.
168. Lafaurie B, Nardone C, Scardovelli R, Zaleski S, Zanetti G. Modelling merging and fragmentation in multiphase flows with SURFER. J Comput Phys. 1994;11:134–47. https://doi.org/10.1006/jcph.1994.1123.
169. Li Q, Luo KH, Kang QJ, Chen Q. Contact angles in the pseudopotential lattice Boltzmann modeling of wetting. Phys Rev E. 2014;90:053301. https://doi.org/10.1103/PhysRevE.90.053301.
170. Chen Y, Zou Y, Yu B, Sun D, Chen X. Effects of surface wettability on rapid boiling and bubble nucleation: a molecular dynamics study. Nanosc Microsc Therm. 2018;22:198–212. https://doi.org/10.1080/15567265.2018.1475526.
171. Mukherjee A, Kandlikar SG. Numerical study of single bubbles with dynamic contact angle during nucleate pool boiling. Int J Heat Mass Transf. 2007;50:127–38. https://doi.org/10.1016/j.ijheatmasstransfer.2006.06.037.
172. Ding W, Krepper E, Hampel U. Evaluation of the microlayer contribution to bubble growth in horizontal pool boiling with a mechanistic model that considers dynamic contact angle and base expansion. Int J Heat Fluid Flow. 2018;72:274–87. https://doi.org/10.1016/j.ijheatfluidflow.2018.06.009.
173. Huber G, Tanguy S, Sagan M, Colin C. Direct numerical simulation of nucleate pool boiling at large microscopic contact angle and moderate Jakob number. Int J Heat Mass Transf. 2017;113:662–82. https://doi.org/10.1016/j.ijheatmasstransfer.2017.05.083.
174. Li M, Bolotnov IA. The evaporation and condensation model with interface tracking. Int J Heat and Mass Transf. 2020;150:119256. https://doi.org/10.1016/j.ijheatmasstransfer.2019.119256.
175. Li MN, Moortgat J, Bolotno I. Nucleate boiling simulation using interface tracking method. Nucl Eng Des. 2020;369:110813. https://doi.org/10.1016/j.nucengdes.2020.110813.
176. Hsu HY, Lin MC, Popovic B, Lin CR, Patankar NA. A numerical investigation of the effect of surface wettability on the boiling curve. PLoS ONE. 2017;12:0187175. https://doi.org/10.1371/journal.pone.0187175.
177. Kandlikar SG. A theoretical model to predict pool boiling CHF incorporating effects of contact angle and orientation. J Heat Trans-T ASME. 2001;123:1071–9. https://doi.org/10.1115/1.1409265.
178. Kutateladze SS. On the transition to film boiling under natural convection. Kotloturbostroenie. 1948;3:10–2.
179. Lin CW, Lin YC, Hung T, Lin MC, Hsu HY. A numerical investigation of the superbiphilic surface on the boiling curve using the volume of fluid method. Int J Heat Mass Transf. 2021;171:121058. https://doi.org/10.1016/j.ijheatmasstransfer.2021.121058.
180. Kistler SF. Hydrodynamics of wetting. New York: Marcel-Dekker; 1993.
181. Vontas K, Andredaki M, Georgoulas A, Nikas KS, Marengo M. Numerical investigation of droplet impact on smooth surfaces with different wettability characteristics: Implementation of a dynamic contact angle treatment in OpenFOAM. Proceedings of ILASS-Europe. 2017:58–65. https://doi.org/10.4995/ilass2017.2017.5020.
182. Pontes P, Cautela R, Teodori E, Moita AS, Georgoulas A, Moreira ALNM. Bubble Dynamics and Heat Transfer on Biphilic Surfaces: Experiments and Numerical Simulation. J Bionic Eng. 2020;17:1–13. https://doi.org/10.1007/s42235-020-0064-x.
183. Freitas E, Pontes P, Cautela R, Bahadur V, Miranda J, Ribeiro A, Souza RR, Oliveira JD, Copetti JB, Lima R, Pereira JE, Moreira ALN, Moita AS. Pool Boiling of Nanofluids on Biphilic Surfaces: An Experimental and Numerical Study. Nanomaterials. 2021;11:125. https://doi.org/10.3390/nano11010125.
184. Li Y, Li Y, Jiao W, Chen XQ, Lu G. Manipulating the heat transfer of pool boiling by tuning the bubble dynamics with mixed wettability surfaces. Int J Heat Mass Transf. 2021;170:120996. https://doi.org/10.1016/j.ijheatmasstransfer.2021.120996.
185. Lee WH. A pressure iteration scheme for two-phase flow modeling. Multiphase Transport Fundamentals, Reactor Safety, Applications. Washington DC: Hemisphere Publishing;1980.
186. Georgoulas A, Koukouvinis P, Gavaises M, Marengo M. Numerical investigation of quasi-static bubble growth and detachment from submerged orifices in isothermal liquid pools: The effect of varying fluid properties and gravity levels. Int J Multiphase Flow. 2015;74:59–78. https://doi.org/10.1016/j.ijmultiphaseflow.2015.04.008.
187. Georgoulas A, Andredaki M, Marengo M. An Enhanced VOF Method Coupled with Heat Transfer and Phase Change to Characterise Bubble Detachment in Saturated Pool Boiling. Energies. 2017;10:272. https://doi.org/10.3390/en10030272.
188. Gong S, Cheng P. Numerical simulation of pool boiling heat transfer on smooth surfaces with mixed wettability by lattice Boltzmann method. Int J Heat Mass Transf. 2015;80:206–16. https://doi.org/10.1016/j.ijheatmasstransfer.2014.08.092.
189. Gong S, Cheng P. Lattice Boltzmann simulations for surface wettability effects in saturated pool boiling heat transfer. Int J Heat Mass Transf. 2015;85:635–46. https://doi.org/10.1016/j.ijheatmasstransfer.2015.02.008.
190. Lee JS, Lee JS. Critical heat flux enhancement of pool boiling with adaptive fraction control of patterned wettability. Int J Heat Mass Transf. 2016;96:504–12. https://doi.org/10.1016/j.ijheatmasstransfer.2016.01.044.
191. Lee JS, Lee JS. Numerical study of hydrophobic-island shapes with patterned wettability for pool boiling. Appl Therm Eng. 2017;127:1632–41. https://doi.org/10.1016/j.ijheatmasstransfer.2016.01.044.
192. Lee JS, Lee JS. Numerical approach to the suppression of film boiling on hot-spots by radial control of patterned wettability. Int J Multiphase Flow. 2016;84:165–75. https://doi.org/10.1016/j.ijmultiphaseflow.2016.04.021.
193. Lee JS, Lee JS. Conjugate heat transfer analysis for the effect of the eccentricity of hydrophobic dot arrays on pool boiling. Appl Therm Eng. 2017;110:844–54. https://doi.org/10.1016/j.applthermaleng.2016.08.209.
194. Zhang CY, Cheng P, Hong FJ. Mesoscale simulation of heater size and subcooling effects on pool boiling under controlled wall heat flux conditions. Int J Heat Mass Transf. 2016;101:1331–42. https://doi.org/10.1016/j.ijheatmasstransfer.2016.05.036.
195. Zhang CY, Cheng P. Mesoscale simulations of boiling curves and boiling hysteresis under constant wall temperature and constant heat flux conditions. Int J Heat Mass Transf. 2017;11:319–29. https://doi.org/10.1016/j.ijheatmasstransfer.2017.03.039.

196. Mu YT, Chen L, He YL, Kang QJ, Tao WQ. Nucleate boiling performance evaluation of cavities at mesoscale level. Int J Heat Mass Transf. 2016;106:708–19. https://doi.org/10.1016/j.ijheatmasstransfer.2016.09.058.
197. Fang WZ, Chen L, Kang QJ, Tao WQ. Lattice Boltzmann modeling of pool boiling with large liquid-gas density ratio. Int J Therm Sci. 201;114:172–183. https://doi.org/10.1016/j.ijthermalsci.2016.12.017.
198. Ma XJ, Cheng P. 3D simulations of pool boiling above smooth horizontal heated surfaces by a phase-change lattice Boltzmann method. Int J Heat Mass Transf. 2019;131:1095–108. https://doi.org/10.1016/j.ijheatmasstransfer.2018.11.103.
199. Li Q, Kang QJ, Francois MM, He YL, Luo KH. Lattice Boltzmann modeling of boiling heat transfer: The boiling curve and the effects of wettability. Int J Heat and Mass Transf. 2015;85:787–96. https://doi.org/10.1016/j.ijheatmasstransfer.2015.01.136.
200. Zhang L, Wang T, Jiang YY, Kim S, Guo CH. A study of boiling on surfaces with temperature-dependent wettability by lattice Boltzmann method. Int J Heat Mass Transf. 2018;122:775–84. https://doi.org/10.1016/j.ijheatmasstransfer.2018.02.026.
201. Wang H, Lou Q, Liu G, Li L. Effects of contact angle hysteresis on bubble dynamics and heat transfer characteristics in saturated pool boiling. Int J Therm Sci, 2022;178:107554. https://doi.org/10.1016/j.ijthermalsci.2022.107554.
202. Zhan H, Li S, Jin Z, Zhang G, Wang L, Li Q, Zhang Z. Study on boiling heat transfer of surface modification based on Lattice Boltzmann and experiments. J Mech Sci Technol. 2022;36:1025–39. https://doi.org/10.1007/s12206-022-0148-0.
203. Nagayama G, Tsuruta T, Cheng P. Molecular dynamics simulation on bubble formation in a nanochannel. Int J Heat Mass Transf. 2006;49:4437–43. https://doi.org/10.1016/j.ijheatmasstransfer.2006.04.030.
204. Din XD, Michaelides EE. Kinetic theory and molecular dynamics simulations of microscopic flows. Phys Fluids. 1997;9:3915–25. https://doi.org/10.1063/1.869490.
205. Barrat JR, Bocquet L. Large slip effect at a nonwetting fluid–solid interface. Phys Rev Lett. 1999;82:4671–4. https://doi.org/10.1103/PhysRevLett.82.4671.
206. Matsumoto M, Yamamoto T. Initial stage of nucleate boiling at atomic scale. ASME/JSME Thermal Engineering Joint Conference. 2011;38921. https://doi.org/10.1115/AJTEC2011-44435.
207. Yamamoto T, Matsumoto M. Initial Stage of Nucleate Boiling: Molecular Dynamics Investigation. J Therm Sci Tech. 2012;7:334349. https://doi.org/10.1299/jtst.7.334.
208. Hens A, Agarwal R, Biswas G. Nanoscale study of boiling and evaporation in a liquid Ar film on a Pt heater using molecular dynamics simulation. Int J Heat Mass Transf. 2014;71:303–12. https://doi.org/10.1016/j.ijheatmasstransfer.2013.12.032.
209. Zhang LY, Xu JL, Lei JP, Liu GL. The connection between wall wettability, boiling regime and symmetry breaking for nanoscale boiling. Int J Therm Sci. 2019;145:106033. https://doi.org/10.1016/j.ijthermalsci.2019.106033.
210. Bai P, Zhou LP, Huang X, Du XZ. How wettability affects boiling heat transfer: A three-dimensional analysis with surface potential energy. Int J Heat Mass Transf. 2021;175:121391. https://doi.org/10.1016/j.ijheatmasstransfer.2021.121391.
211. Zhou WJ, Li Y, Li MJ, Wei JJ, Tao WQ. Bubble nucleation over patterned surfaces with different wettabilities: Molecular dynamics investigation. Int J Heat Mass Transf. 2019;136:1–9. https://doi.org/10.1016/j.ijheatmasstransfer.2019.02.093.
212. Li Y, Zhou WJ, Zhang YH, Qi BJ, Wei JJ. A molecular dynamics study of surface wettability effects on heterogeneous bubble nucleation. Int Commun Heat Mass Transf. 2020;119:104991. https://doi.org/10.1016/j.icheatmasstransfer.2020.104991.
213. Zhou W, Han D, Xia G. Maximal enhancement of nanoscale boiling heat transfer on superhydrophilic surfaces by improving solid-liquid interactions: Insights from molecular dynamics. Appl Surf Sci. 2022;591:153155. https://doi.org/10.1016/j.apsusc.2022.153155.
214. Lee W, Son G, Yoon HY. Numerical study of bubble growth and boiling heat transfer on a microfinned surface. Int Commun Heat Mass Transf. 2012;39(1):52–7. https://doi.org/10.1016/j.icheatmasstransfer.2011.09.008.
215. Yazdani M, Radcliff T, Soteriou M, Alahyari AA. A high-fidelity approach towards simulation of pool boiling. Phys Fluids. 2016;28:365–401. https://doi.org/10.1063/1.4940042.
216. Chen HX, Sun Y, Xiao HY, Wang XD. Bubble dynamics and heat transfer characteristics on a micropillar structured surface with different nucleation site positions. J Therm Anal Calorim. 2020;141:547–58. https://doi.org/10.1007/s10973-020-09301-x.
217. Chen HX, Sun Y, Li LH, Wang XD. Bubble dynamics and heat transfer performance on micro-pillars structured surfaces with various pillars heights. Int J Heat Mass Transf. 2020;163:120502. https://doi.org/10.1016/j.ijheatmasstransfer.2020.120502.
218. Cao ZZ, Zhou J, Wei JJ, Sun DL, Yu B. Direct numerical simulation of bubble dynamics and heat transfer during nucleate boiling on the micro-pin-finned surfaces. Int J Heat Mass Transf. 2020;163:120504. https://doi.org/10.1016/j.ijheatmasstransfer.2020.120504.
219. Cao ZZ, Zhou J, Liu A, Sun DL, Yu B, Wei JJ. A three dimensional coupled VOF and Level set (VOSET) method with and without phase change on general curvilinear grids. Chem Eng Sci. 2020;223:115705. https://doi.org/10.1016/j.ces.2020.115705.
220. Sun T, Qin H, Liu Z. A Numerical Investigation of Nucleate Boiling on Enhanced Surfaces by Lattice Boltzmann Method. Int J Comput Meth. 2018;1850053. https://doi.org/10.1142/S0219876218500536.
221. Chang XT, Huang HB, Cheng YP, Lu XY. Lattice Boltzmann study of pool boiling heat transfer enhancement on structured surfaces. Int J Heat Mass Transf. 2019;139588–599. https://doi.org/10.1016/j.ijheatmasstransfer.2019.05.041.
222. Zhou P, Liu W, Liu ZJ. Lattice Boltzmann simulation of nucleate boiling in micro-pillar structured surface. Int J Heat Mass Transfer. 2019;131:1–10. https://doi.org/10.1016/j.ijheatmasstransfer.2018.11.038.
223. Mondal K, Bhattacharya A. Numerical Study of Pool Boiling Heat Transfer From Surface With Protrusions Using Lattice Boltzmann Method. J Heat Trans-T ASME. 2021;143:021603. https://doi.org/10.1115/1.4049031.
224. Yu Y, Li Q, Qiu Y, Huang RZ. Bubble dynamics and dry spot formation during boiling on a hierarchical structured surface: A lattice Boltzmann study. Phys of Fluids. 2020;33:083306. https://doi.org/10.1063/5.0056894.
225. Wang J, Liang G. Boiling heat transfer on two-tier hierarchical structured surface. Chem Eng Sci. 2023;270:118547. https://doi.org/10.1016/j.ces.2023.118547.
226. Wang W, Huang S, Luo X. MD simulation on nano-scale heat transfer mechanism of sub-cooled boiling on nano-structured surface. Int J Heat Mass Transf. 2016;100:276–86. https://doi.org/10.1016/j.ijheatmasstransfer.2016.04.018.
227. Liu YW, Zhang XR. Molecular dynamics simulation of nanobubble nucleation on rough surfaces. J Chem Phys. 2017;146:1–5. https://doi.org/10.1063/1.4981788.
228. Zhang LY, Xu JL, Liu GL, Lei JP. Nucleate boiling on nanostructured surfaces using molecular dynamics simulations. Int J Therm Sci. 2020;152:106325. https://doi.org/10.1016/j.ijthermalsci.2020.106325.
229. Chen YJ, Yu Z, Sun DL, Wang Y, Yu B. Molecular dynamics simulation of bubble nucleation on nanostructure surface. Int J

Heat Mass Transf. 2018;118:1143–51. https://doi.org/10.1016/j.ijheatmasstransfer.2017.11.079.
230. Ahmad S, Khan SA, Ali HM, Huang X, Zhao J. Molecular dynamics study of nanoscale boiling on double layered porous meshed surfaces with gradient porosity. Appl Nanosci. 2022;12:2997–3006. https://doi.org/10.1007/s13204-022-02568-6.
231. Lee W, Son G, Jeong J. Numerical Analysis of Bubble Growth and Departure from a Microcavity. Numer Heat Tr B-Fund. 2010;58:323–42. https://doi.org/10.1080/10407790.2010.522871.
232. Lee W, Son G. Numerical simulation of boiling enhancement on a micro structured surface. Int Commun Heat Mass Transf. 2011;38:168–73. https://doi.org/10.1016/j.icheatmasstransfer.2010.11.017.
233. Márkus A, Házi G. Numerical simulation of the detachment of bubbles from a rough surface at microscale level. Nucl Eng Des. 2012;248:263–9. https://doi.org/10.1016/j.nucengdes.2012.03.040.
234. Zhou P, Liu ZC, Liu W, Duan XL. LBM simulates the effect of sole nucleate site geometry on pool boiling. Appl Therm Eng. 2019;160:114027. https://doi.org/10.1016/j.applthermaleng.2019.114027.
235. Novak BR, Maginn EJ, Mccready MJ. An Atomistic Simulation Study of the Role of Asperities and Indentations on Heterogeneous Bubble Nucleation. J Heat Trans-T ASME. 2008;130:88–96. https://doi.org/10.1115/1.2818771.
236. Mukherjee S, Datta S, Das AK. Molecular Dynamic Study of Boiling Heat Transfer Over Structured Surfaces. J Heat Trans-T ASME. 2018;140:054503. https://doi.org/10.1115/1.4038480.
237. Zhang L, Yang Y, Han J. Microscopic mechanism of effects of nanostructure morphology on bubble nucleation: A molecular dynamics simulation. Numer Heat Tr A-appl. 2023;1–16. https://doi.org/10.1080/10407782.2023.2180461.
238. Zhou W, Han D, Ma H, Hu Y, Xia G. Molecular dynamics study on enhanced nucleate boiling heat transfer on nanostructured surfaces with rectangular cavities. Int J Heat Mass Transf. 2022;191:122814. https://doi.org/10.1016/j.ijheatmasstransfer.2022.122814.
239. Zhao ZC, Zhang J, Jia DD, Zhao K, Zhang X, Jiang PP. Thermal performance analysis of pool boiling on an enhanced surface modified by the combination of microstructures and wetting properties. Appl Therm Eng. 2017;117:417–426. https://doi.org/10.1016/j.applthermaleng.2017.02.014.
240. Chen HX, Li LH, Wang YR, Guo YX. Heat transfer enhancement in nucleate boiling on micropillar-arrayed surfaces with time-varying wettability. Appl Therm Eng. 2022;200:117649. https://doi.org/10.1016/j.applthermaleng.2021.117649.
241. Li Q, Yu Y, Zhou P, Yan HJ. Enhancement of boiling heat transfer using hydrophilic-hydrophobic mixed surfaces: A lattice Boltzmann study. Appl Therm Eng. 2017;132:490–9. https://doi.org/10.1016/j.applthermaleng.2017.12.105.
242. Ma XJ, Cheng P, Quan XJ. Simulations of saturated boiling heat transfer on bio-inspired two-phase heat sinks by a phase-change lattice Boltzmann method. Int J Heat Mass Transf. 2018;127:1013–24. https://doi.org/10.1016/j.ijheatmasstransfer.2018.07.082.
243. Yu Y, Wen ZX, Li Q, Zhou P, Yan HJ. Boiling heat transfer on hydrophilic hydrophobic mixed surfaces: a 3D lattice Boltzmann study. Appl Therm Eng. 2018;142:846–54. https://doi.org/10.1016/j.applthermaleng.2018.07.059.
244. Feng Y, Chang FC, Hu ZT, Liu HX, Zhao JF. Investigation of pool boiling heat transfer on hydrophilic-hydrophobic mixed surface with micro-pillars using LBM. Int J Therm Sci. 2021;163:106814. https://doi.org/10.1016/j.ijthermalsci.2020.106814.
245. Xu ZG, Qin J, Ma XF. Experimental and numerical investigation on bubble behaviors and pool boiling heat transfer of semi-modified copper square pillar arrays. Int J Therm Sci. 2021;160:106680. https://doi.org/10.1016/j.ijthermalsci.2020.106680.
246. Wang J, Liang G, Yin X, Shen S. Pool boiling on micro-structured surface with lattice Boltzmann method. Int J Therm Sci. 2023;187:108170. https://doi.org/10.1016/j.ijthermalsci.2023.108170.
247. Diaz R, Guo Z. A molecular dynamics study of phobic/philic nano-patterning on pool boiling heat transfer. Heat Mass Transf. 2017;53:1061–71. https://doi.org/10.1007/s00231-016-1878-2.
248. Diaz R, Guo Z. Molecular dynamics study of wettability and pitch effects on maximum critical heat flux in evaporation and pool boiling heat transfer. Numer Heat Tr A-Appl. 2017;72:891–903. https://doi.org/10.1080/10407782.2017.1412710.
249. Chen YJ, Zou Y, Wang Y, Han DX, Yu B. Bubble nucleation on various surfaces with inhomogeneous interface wettability based on molecular dynamics simulation. Int Commun Heat Mass Transf. 2018;98:135–42. https://doi.org/10.1016/j.icheatmasstransfer.2018.08.017.
250. Bai P, Zhou LP, Huang XH, Du XZ. Molecular Insight into Bubble Nucleation on the Surface with Wettability Transition at Controlled Temperatures. Langmuir. 2021;37:8765–75. https://doi.org/10.1021/acs.langmuir.1c01121.
251. Gong S, Cheng P, Quan XJ. Two-dimensional mesoscale simulations of s-aturated pool boiling from rough surfaces. Part I: Bubble nucleation in a single cavity at low superheats. Int J Heat Mass Transf. 2016;100:927–937. https://doi.org/10.1016/j.ijheatmasstransfer.2016.04.085.
252. Gong S, Cheng P, Quan XJ. Two-dimensional mesoscale simulations of saturated pool boiling from rough surfaces. Part II: Bubble interactions above multi-cavities. Int J Heat Mass Transf. 2016;100:938–948. https://doi.org/10.1016/j.ijheatmasstransfer.2016.04.082.
253. Zhang L, Wang T, Kim S, Jiang YY. The effects of wall superheat and surface wettability on nucleation site interactions during boiling. Int J Heat Mass Transf. 2020;146(7):118820. https://doi.org/10.1016/j.ijheatmasstransfer.2019.118820.
254. Ahmad S, Liu HQ, Shi Y, Chen JT, Zhao JY. The study of nucleation site interactions on the mixed wettability rough surface. Int Commun Heat Mass Transf. 2021;126(2):105372. https://doi.org/10.1016/j.icheatmasstransfer.2021.105372.
255. She XH, Shedd TA, Lindeman B, Yin YG, Zhang XS. Bubble formation on solid surface with a cavity based on molecular dynamics simulation. Int J Heat Mass Transf. 2016;95:278–87. https://doi.org/10.1016/j.ijheatmasstransfer.2015.11.082.
256. Chen YJ, Li JF, Yu B, Sun DL, Zou Y, Han DX. Nanoscale Study of Bubble Nucleation on a Cavity Substrate Using Molecular Dynamics Simulation. Langmuir. 2018;34:14234–48. https://doi.org/10.1021/acs.langmuir.8b03044.
257. Chen Y J, Yu B, Zou Y, Chen BN, Tao WQ. Molecular dynamics studies of bubble nucleation on a grooved substrate. Int J Heat Mass Transf. 2020;158:119850. https://doi.org/10.1016/j.ijheatmasstransfer.2020.119850.
258. Shahmardi A, Tammisola O, Chinappi M, Brandt L. Effects of surface nanostructure and wettability on pool boiling: A molecular dynamics study. Int J Therm Sci. 2021;167:106980. https://doi.org/10.1016/j.ijthermalsci.2021.106980.
259. Lavino AD, Smith E, Magnini M, Mater OK. Surface Topography Effects on Pool Boiling via Non-equilibrium Molecular Dynamics Simulations. Langmuir. 2021;37:5731–44. https://doi.org/10.1021/acs.langmuir.1c00779.
260. Abarajith HS, Dhir VK, Warrier G, Son G. Numerical Simulation and Experimental Validation of the Dynamics of Multiple Bubble Merger During Pool Boiling Under Microgravity Conditions.

Ann Ny Acad Sci. 2010;1027:235–58. https://doi.org/10.1196/annals.1324.020.
261. Wu JF, Dhir VK. Numerical Simulations of the Dynamics and Heat Transfer Associated with a Single Bubble in Subcooled Pool Boiling. J Heat Trans-T ASME. 2010;132:111501. https://doi.org/10.1115/1.4002093.
262. Wu JF, Dhir VK. Numerical simulation of dynamics and heat transfer associated with a single bubble in subcooled boiling and in the presence of noncondensables, J Heat Trans-T ASME. 2011;133:041502. https://doi.org/10.1115/1.4000979.
263. Dhir VK, Warrier GR, Aktinol E, Chao D, Eggers J, Sheredy W, Booth W. Nucleate Pool Boiling Experiments (NPBX) on the International Space Station. Microgravity Sci Technol. 2011;24:307–25. https://doi.org/10.1007/s12217-012-9315-8.
264. Aktinol E, Warrier GR, Dhir VK. Single bubble dynamics under microgravity conditions in the presence of dissolved gas in the liquid. Int J Heat Mass Transf. 2014;79:251–68. https://doi.org/10.1016/j.ijheatmasstransfer.2014.08.014.
265. Urbano A, Tanguy S, Colin C. Direct numerical simulation of nucleate boiling in zero gravity conditions. Int J Heat Mass Transf. 2019;143:118521.1–118521.13. https://doi.org/10.1016/j.ijheatmasstransfer.2019.118521.
266. Yi TH, Lei ZS, Zhao JF. Numerical investigation of bubble dynamics and heat transfer in subcooling pool boiling under low gravity. Int J Heat Mass Transfer. 2019;132:1176–86. https://doi.org/10.1016/j.ijheatmasstransfer.2018.12.096.
267. Ryu S, Ko S. Direct numerical simulation of nucleate pool boiling using a two-dimensional lattice Boltzmann method. Nucl Eng Des. 2012;248:248–62. https://doi.org/10.1016/j.nucengdes.2012.03.031.
268. Sadeghi R, Shadloo MS, Jamalabadi MYA, Karimipour A. A three-dimensional lattice Boltzmann model for numerical investigation of bubble growth in pool boiling. Int Commun Heat Mass Transf. 2016;79:8–66. https://doi.org/10.1016/j.icheatmasstransfer.2016.10.009.
269. Lee T. Effects of incompressibility on the elimination of parasitic currents in the lattice Boltzmann equation method for binary fluids. Comput Math Appl. 2009;58:987–94. https://doi.org/10.1016/j.camwa.2009.02.017.
270. Guzella MD, Czelusniak LE, Mapelli VP, Alvarino PF, RibatskiG, Cabezas-Gomez L. Simulation of Boiling Heat Transfer at Different Reduced Temperatures with an Improved Pseudopotential Lattice Boltzmann Method. Symmetry. 2020;12:1358. https://doi.org/10.3390/sym12081358.
271. Guo Z, Zheng C, Shi B. Discrete lattice effects on the forcing term in the lattice Boltzmann method. Phys Rev E. 2002;65:046308. https://doi.org/10.1103/PhysRevE.65.046308.
272. Feng Y, Li HX, Zhao JF, Guo KK, Lei XL. Lattice Boltzmann Study on Influence of Gravitational Acceleration on Pool Nucleate Boiling Heat Transfer. Microgravity Sci Tec. 2021;33:1–16. https://doi.org/10.1007/s12217-020-09864-2.
273. Mohammadpourfard M, Aminfar H, Sahraro M. Numerical simulation of nucleate pool boiling on the horizontal surface for ferrofluid under the effect of non-uniform magnetic field. Heat Mass Transf. 2014;50:1167–76. https://doi.org/10.1007/s00231-014-1316-2.
274. Mortezazadeh R, Aminfar H, Mohammadpourfard M. Eulerian-Eulerian simulation of non-uniform magnetic field effects on the ferrofluid nucleate pool boiling. J Eng Thermophys. 2017;26:580–97. https://doi.org/10.1134/S1810232817040129.
275. Qi C, Wan YL, Liang L, Rao ZH, Li YM. Numerical and Experimental Investigation into the Effects of Nanoparticle Mass Fraction and Bubble Size on Boiling Heat Transfer of TiO_2-Water Nanofluid. J Heat Trans-T ASME. 2016;138:081503. https://doi.org/10.1115/1.4033353.
276. Niknam PH, Haghighi M, Kasiri N, Khanof MH. Numerical study of low concentration nanofluids pool boiling, investigating of boiling parameters introducing nucleation site density ratio. Heat Mass Transf. 2015;51:601–9. https://doi.org/10.1007/s00231-014-1433-y.
277. Salehi H, Hormozi F. Numerical study of silica-water based nanofluid nucleate pool boiling by two-phase Eulerian scheme. Heat Mass Transf. 2017;54:773–84. https://doi.org/10.1007/s00231-017-2146-9.
278. Salehi H, Hormozi F. Prediction of Al_2O_3-water nanofluids pool boiling heat transfer coefficient at low heat fluxes by using response surface methodology. J Therm Anal Calorim. 2019;137:1069–82. https://doi.org/10.1007/s10973-018-07993-w.
279. Kamel MS, Al-Agha MS, Lezsovits F, Mahian O. Simulation of pool boiling of nanofluids by using Eulerian multiphase model. J Therm Anal Calorim. 2019;142:493–505. https://doi.org/10.1007/s10973-019-09180-x.
280. Emlin V, Joshy PJ, Tide PS. Numerical Analysis of Pool Boiling of Nanofluids for High Heat Dissipation Applications. IEEE T Comp Pack Man. 2022;12:1293–301. https://doi.org/10.1109/TCPMT.2022.3193675.
281. Zaboli S, Alimoradi H, Sham M. Numerical investigation on improvement in pool boiling heat transfer characteristics using different nanofluid concentrations. J Therm Anal Calorim. 2022;147:10659–76. https://doi.org/10.1007/s10973-022-11272-0.
282. Gajghate SS, Barathula S, Cardoso EM, Saha BB, Bhaumik S. Effect of staggered V-shaped and rectangular grooves copper surfaces on pool boiling heat transfer enhancement using ZrO_2 nanofluids. J Braz Soc Mech Sci Eng. 2021;43:75. https://doi.org/10.1007/s40430-020-02759-8.
283. Majdi HS, Hussein HMA, Habeeb LJ, Zivkovic D. Pool boiling simulation of two nanofluids at multi concentrations in enclosure with different shapes of fins. Materials Today: Proceedings. 2022;60:2043–63. https://doi.org/10.1016/j.matpr.2022.01.290.
284. Rostamzadeh A, Jafarpur K, Goshtasbi Rad E. Numerical investigation of pool nucleate boiling in nanofluid with lattice Boltzmann method. J Theor App Mech 2016;54:811–825. https://doi.org/10.15632/jtam-pl.54.3.811.
285. Wang D, Cheng P. Effects of nanoparticles' wettability on vapor bubble coalescence in saturated pool boiling of nanofluids: A lattice Boltzmann simulation. Int J Heat Mass Transf. 2020;154:119669. https://doi.org/10.1016/j.ijheatmasstransfer.2020.119669.
286. Zhang D, Li SF, Li Y, Mei N, Yuan H. Lattice Boltzmann simulation of seawater boiling in the presence of non-condensable gas. Int J Heat Mass Transf. 2019;142:118415. https://doi.org/10.1016/j.ijheatmasstransfer.2019.07.065.
287. Yin X, Hu C, Bai M, Lv JZ. Molecular dynamics simulation on the effect of nanoparticles on the heat transfer characteristics of pool boiling. Numer Heat Tr B-Fund. 2018;73:94–105. https://doi.org/10.1080/10407790.2017.1420323.
288. Kunkelmann C, Stephan P. CFD Simulation of Boiling Flows Using the Volume-of-Fluid Method Within OPENFOAM. Numer Heat Tr A-App. 2009;56:631–46. https://doi.org/10.1080/10407780903423908.
289. Zhang L, Li ZD, Li K, Li HX, Zhao JF. Influence of heater thermal capacity on bubble dynamics and heat transfer in nucleate pool boiling. Appl Therm Eng. 2015;88:118–26. https://doi.org/10.1016/j.applthermaleng.2014.11.080.
290. Pezo M, Stevanovic V. Numerical prediction of critical heat flux in pool boiling with the two-fluid model. Int J Heat Mass Transf. 2011;54:3296–303. https://doi.org/10.1016/j.ijheatmasstransfer.2011.03.057.

291. Petrovic MM, Stevanovic VD. Coupled two-fluid flow and wall heat conduction modeling of nucleate pool boiling. Numer Heat Tr A-Appl. 2021;80(3):63–91. https://doi.org/10.1080/10407782.2021.1935047.
292. Giustini G, Kim I, Kim H. Comparison between modelled and measured heat transfer rates during the departure of a steam bubble from a solid surface. Int J Heat Mass Transf. 2020;148:119092. https://doi.org/10.1016/j.ijheatmasstransfer.2019.119092.
293. Gong S, Cheng P. Direct numerical simulations of pool boiling curves including heater's thermal responses and the effect of vapor phase's thermal conductivity. Int Commun Heat Mass Transf. 2017;87:61–71. https://doi.org/10.1016/j.icheatmasstransfer.2017.06.023.
294. Qin J, Xu Z, Ma X. Pore-Scale Simulation on Pool Boiling Heat Transfer and Bubble Dynamics in Open-Cell Metal Foam by Lattice Boltzmann Method. J Heat Trans-T ASME. 2021;143:011602. https://doi.org/10.1115/1.4048734.
295. Hu AJ, Liu D. 2D Simulation of boiling heat transfer on the wall with an improved hybrid lattice Boltzmann model. Appl Therm Eng. 2019;159:113788. https://doi.org/10.1016/j.applthermaleng.2019.113788.
296. Zhao W, Liang J, Sun M, Wang Z. Investigation on the effect of convective outflow boundary condition on the bubbles growth, rising and breakup dynamics of nucleate boiling. Int J Therm Sci. 2021;167:106877. https://doi.org/10.1016/j.ijthermalsci.2021.106877.
297. Murallidharan J, Giustini G, Sato Y, Niceno B, Badalassi V, Walker SP. Computational Fluid Dynamic Simulation of Single Bubble Growth under High-Pressure Pool Boiling Conditions. Nucl Eng Tech. 2016;48:859–69. https://doi.org/10.1016/j.net.2016.06.004.
298. Sakashita H. Bubble growth rates and nucleation site densities in saturated pool boiling of water at high pressures. J Nucl Sci Technol. 2011;48:734–43. https://doi.org/10.1080/18811248.2011.9711756.
299. Sielaff A, Dietl J, Herbert S, Stephan P. The Influence of System Pressure on Bubble Coalescence in Nucleate Boiling. Heat Transfer Eng. 2014;35:420–9. https://doi.org/10.1080/01457632.2013.830917.
300. Hardt S, Wondra F. Evaporation Model for Interfacial Flows Based on a Continuum-Field Representation of the Source Terms. J Comput Phys. 2008;227:5871–95. https://doi.org/10.1016/j.jcp.2008.02.020.
301. Ren S, Zhou WZ. Numerical investigation of nucleate pool boiling outside a vertical tube under sub-atmospheric pressures. Int Commun Heat Mass Transf. 2020;116:104662. https://doi.org/10.1016/j.icheatmasstransfer.2020.104662.
302. Hristov Y, Zhao D, Kenning DBR, Sefiane K, Karayiannis TG. A study of nucleate boiling and critical heat flux with EHD enhancement. Heat Mass Transf. 2009;45:999–1017. https://doi.org/10.1007/s00231-007-0286-z.
303. Feng Y, Li HX, Guo KK, Lei XL, Zhao JF. Numerical study on saturated pool boiling heat transfer in presence of a uniform electric field using lattice Boltzmann method. Int J Heat Mass Transf. 2019;135:885–96. https://doi.org/10.1016/j.ijheatmasstransfer.2019.01.119.
304. Feng Y, Li HX, Guo KK, Lei XL, Zhao JF. Numerical investigation on bubble dynamics during pool nucleate boiling in presence of a non-uniform electric field by LBM. Appl Therm Eng. 2019;155:637–49. https://doi.org/10.1016/j.applthermaleng.2019.04.110.
305. Yao JD, Luo K, Wu J, Yi HL. Electrohydrodynamic effects on bubble dynamics during nucleate pool boiling under the leaky dielectric assumption. Phys Fluids. 2022;34:013606. https://doi.org/10.1063/5.0077313.
306. Li W, Li Q, Chang H, Yu Y, Tang S. Electric field enhancement of pool boiling of dielectric fluids on pillar-structured surfaces: A lattice Boltzmann study. Phys Fluids. 2022;34:123327. https://doi.org/10.1063/5.0122145.
307. Tondro AAA, Maddahian R, Arefmanesh A. Assessment of the inclination surface on the microlayer behavior during nucleate boiling, a numerical study. Heat Mass Transf. 2019;55:2103–16. https://doi.org/10.1007/s00231-019-02566-5.
308. Tondro AAA, Maddahian R, Arefmanesh A. Effect of heated surface inclination on the growth dynamics and detachment of a vapor bubble, a numerical study. Heat Mass Transf. 2021;57:205–22. https://doi.org/10.1007/s00231-020-02937-3.
309. Sun T, Li WZ, Dong B. Numerical simulation of vapor bubble growth on a vertical superheated wall using lattice Boltzmann method. Int J Numer Method Heat Fluid Flow. 2015;25:1214–30. https://doi.org/10.1108/HFF-08-2013-0263.
310. Dong B, Zhang YJ, Zhou X, Chen C, Li WZ. Numerical Simulation of Bubble Dynamics in Subcooled Boiling Along Inclined Structured Surface. J Thermophys Heat Transf. 2020;35:16–27. https://doi.org/10.2514/1.T5906.
311. Chen Z, Wu F, Utaka Y. Numerical simulation of thermal property effect of heat transfer plate on bubble growth with microlayer evaporation during nucleate pool boiling. Int J Heat Mass Transf. 2018;118:989–96. https://doi.org/10.1016/j.ijheatmasstransfer.2017.11.083.
312. Diaz R, Guo Z. Enhanced conduction and pool boiling heat transfer on single-layer graphene-coated substrates. J Enhanc Heat Transf. 2019;26:127–43. https://doi.org/10.1615/JEnhHeatTransf.2018028488.
313. Sattari E, Delavar MA, Fattahi E, Sedighi K. Numerical investigation the effects of working parameters on nucleate pool boiling. Int Commun Heat Mass Transf. 2014;59:106–13. https://doi.org/10.1016/j.icheatmasstransfer.2014.10.004.
314. Shan XP, Guan G, Nie DM. Numerical study on the boiling heat transfer induced by two heated plates. Therm Sci. 2020;24:257–65. https://doi.org/10.2298/TSCI20S1257S.
315. Wei JJ, Yu B, Wang HS. Heat transfer mechanisms in vapor mushroom region of saturated nucleate pool boiling. Int J Heat Fluid Flow. 2003;24:210–22. https://doi.org/10.1016/S0142-727X(02)00244-8.
316. Gaertner RF. Photographic study of nucleate pool boiling on a horizontal surface. J Heat Trans-T ASME. 1965;87:17–29. https://doi.org/10.1115/1.3689038.
317. Katto Y, Yokoya S. Behavior of a vapor mass in saturated nucleate and transition pool boiling. Trans JSME. 1975;41:294–305.
318. Ghoshdastidar PS, Kabelac S, Mohanty A. Numerical Modelling of Atmospheric Pool Boiling by the Coupled Map Lattice Method. P I Mech Eng C-J Mec. 2004;218:195–205. https://doi.org/10.1243/095440604322886496.
319. Sadhu S, Ghoshdastidar PS. Heat Flux Controlled Pool Boiling of Zirconia-Water and Silver-Water Nanofluids on a Flat Plate: A Coupled Map Lattice Simulation. J Heat Trans-T ASME. 2015;137:021503. https://doi.org/10.1115/1.4028974.
320. Son G, Dhir VK. Numerical simulation of nucleate boiling on a horizontal surface at high heat fluxes. Int J Heat Mass Transf. 2008;51:2566–82. https://doi.org/10.1016/j.ijheatmasstransfer.2007.07.046.
321. Stephan K, Abdelsalam M. Heat transfer correlation for natural convection boiling. Int J Heat Mass Transfer. 1980;23:73–87. https://doi.org/10.1016/0017-9310(80)90140-4.
322. Garg D, Dhir VK. A Unified Three-Dimensional Numerical Model for Boiling Curve in a Temperature Controlled Model. J Heat Trans-T ASME. 2019;141(1):011504. https://doi.org/10.1115/1.4041798.

323. Berenson PJ. Film Boiling Heat Transfer From a Horizontal Surface. J Heat Trans-T ASME. 1961;83(3):351–6. https://doi.org/10.1115/1.3682280.
324. Wang JS, Diao MZ, Liu XL. Numerical simulation of pool boiling with special heated surfaces. Int J Heat Mass Transf. 2019;130:460–8. https://doi.org/10.1016/j.ijheatmasstransfer.2018.10.120.
325. Liu Y, Olewski T, Véchot LN. Modeling of a cryogenic liquid pool boiling by CFD simulation. J Loss Prevent Proc. 2015;35:125–34. https://doi.org/10.1016/j.jlp.2015.04.006.
326. Kim SJ, Bang IC, Buongiorno J, Hu LW. Surface wettability change during pool boiling of nanofluids and its effect on critical heat flux. Int J Heat Mass Transf. 2007;50:4105–16. https://doi.org/10.1016/j.ijheatmasstransfer.2007.02.002.
327. Kim HD, Kim MH. Effect of nanoparticle deposition on capillary wicking that influences the critical heat flux in nanofluids. Appl Phys Lett. 2007;91:014104. https://doi.org/10.1063/1.2754644.
328. Ahn HS, Lee C, Kim J, Kim MH. The effect of capillary wicking action of micro/nano structures on pool boiling critical heat flux. Int J Heat Mass Transf. 2012;55:89–92. https://doi.org/10.1016/j.ijheatmasstransfer.2011.08.044.
329. McGillis WR, Carey VP, Fitch JS, Hamburgen WR. Pool boiling enhanc-ement techniques for water at low pressure. In: Proceedings, Seventh IEEE Semiconductor Thermal Measurement and Management Symposium. 1991;64–72. https://doi.org/10.1109/STHERM.1991.152914.
330. Márkus A, Házi G. On pool boiling at microscale level: The effect of a cavity and heat conduction in the heated wall. Nucl Eng Des. 2012;248:238–47. https://doi.org/10.1016/j.nucengdes.2012.03.027.
331. Ma XJ, Cheng P. Numerical Simulation of Complete Pool Boiling Curves: From Nucleation to Critical Heat Flux Through Transition Boiling to Film Boiling. J Nucl Sci Technol. 2018;193:1–13. https://doi.org/10.1080/00295639.2018.1504566.
332. Gong S, Zhang L, Cheng P, Wang EN. Understanding triggering mechanisms for critical heat flux in pool boiling based on direct numerical simulations. Int J Heat Mass Transf. 2020;163:120546. https://doi.org/10.1016/j.ijheatmasstransfer.2020.120546.
333. Quan X, Wang D, Cheng P. An experimental investigation on wettability effects of nanoparticles in pool boiling of a nanofluid. Int J Heat Mass Transf. 2017;108:32–40.
334. Sajjad U, Hussain I, Hamid K, Bhat SA, Ali HM, Wang CC. A deep learning method for estimating the boiling heat transfer coefficient of porous surfaces. J Therm Anal Calorim. 2021;145:1911–23. https://doi.org/10.1007/s10973-021-10606-8.